

ANL-6034

15085

ANL-6034

Public Reading Room
U. S. Department of Energy
Idaho Operations Office

Argonne National Laboratory

DESIGN SUMMARY REPORT ON THE TRANSIENT REACTOR TEST FACILITY TREAT

by

G. A. Freund, P. Elias,
D. R. MacFarlane, J. D. Geier,
and J.F. Boland

Our supply of this report is
limited. When you no longer
need it please return to:

REPORT UNIT
D2 G129
TPD

LEGAL NOTICE

This report was prepared as an account of Government sponsored work. Neither the United States, nor the Commission, nor any person acting on behalf of the Commission

- A. Makes any warranty of representation, expressed or implied, with respect to the accuracy, completeness, or usefulness of the information contained in this report, or that the use of any information, apparatus, method, or process disclosed in this report may not infringe privately owned rights; or*
- B. Assumes any liabilities with respect to the use of, or for damages resulting from the use of any information, apparatus, method, or process disclosed in this report.*

As used in the above, "person acting on behalf of the Commission" includes any employee or contractor of the Commission, or employee of such contractor, to the extent that such employee or contractor of the Commission, or employee of such contractor prepares, disseminates, or provides access to, any information pursuant to his employment or contract with the Commission, or his employment with such contractor.

ANL-6034
Reactors - General
(TID-4500, 15th Ed.)
AEC Research and
Development Report

ARGONNE NATIONAL LABORATORY
9700 South Cass Avenue
Argonne, Illinois

DESIGN SUMMARY REPORT
ON
THE TRANSIENT REACTOR TEST FACILITY (TREAT)

by

G. A. Freund P. Elias
D. R. MacFarlane J. D. Geier

Reactor Engineering Division

and

J. F. Boland
Idaho Division

Report Compiled by D. R. MacFarlane

Written: February, 1960

Published: June, 1960

Operated by The University of Chicago
under
Contract W-31-109-eng-38

TABLE OF CONTENTS

| | <u>Page</u> |
|---|-------------|
| I. INTRODUCTION. | 5 |
| II. DESIGN SUMMARY. | 9 |
| A. Site and Buildings. | 9 |
| 1. Reactor Building | 10 |
| 2. Control Building. | 10 |
| B. Reactor. | 13 |
| 1. Core | 13 |
| 2. Control Rods and Drive Mechanisms | 14 |
| 3. Shielding and Experimental Facilities | 15 |
| C. Plant Parameters. | 16 |
| D. Control. | 16 |
| E. Costs | 16 |
| III. COMPONENT DESCRIPTION | 20 |
| A. Core Assembly | 20 |
| 1. Standard Fuel Assembly | 20 |
| 2. Fuel Fabrication | 22 |
| 3. Special-purpose Fuel Assemblies | 23 |
| B. Core Support and Alignment. | 28 |
| 1. Grid Plate. | 28 |
| 2. Control Rod Guide Thimbles. | 31 |
| 3. Control Rod Guide Tubes and Bearings. | 33 |
| 4. Core Clamping Bars | 34 |
| C. Permanent Reflector and Thermal Column | 36 |
| 1. Permanent Reflector. | 36 |
| 2. Thermal Column | 38 |
| D. Control Rods | 39 |
| 1. Design and Development | 39 |
| 2. Components. | 41 |
| a. Poison Section | 41 |
| b. Zircaloy-2 Follower | 43 |
| c. Steel Follower | 43 |

TABLE OF CONTENTS

| | <u>Page</u> |
|--|-------------|
| E. Control Rod Drives | 44 |
| 1. Mechanical Description | 44 |
| a. Pneumatic Actuator | 44 |
| b. Dashpot | 46 |
| c. Positioning Mechanism | 47 |
| d. Latch | 47 |
| e. Knuckle Joints | 49 |
| f. Drive Position Indicators | 49 |
| 2. Control Rod Drive Pressurization Systems | 49 |
| a. Shutdown Drive System | 49 |
| b. Transient Drive System | 50 |
| 3. Installation of Control Rod Drives | 50 |
| F. Shielding | 51 |
| 1. Permanent Shield | 51 |
| 2. Experimental Access Openings | 53 |
| G. Fuel-transfer System | 54 |
| 1. Rotating Shield Plug and Indexing System | 55 |
| 2. Coffin-locating Carriage | 56 |
| 3. Rotating Shield Plug Bearing and Drive Motor | 57 |
| 4. Fuel-transfer Coffin | 58 |
| a. Coffin-body (Shield) Assembly | 59 |
| b. Fuel Assembly-transfer Mechanism | 59 |
| c. Electrical System | 63 |
| 5. Periscope | 64 |
| 6. Manual Fuel-handling Tools | 64 |
| 7. Fuel-storage Area | 67 |
| H. Reactor Cooling and Building Ventilation System | 68 |

TABLE OF CONTENTS

| | <u>Page</u> |
|---|-------------|
| I. Control and Instrumentation | 69 |
| 1. Nuclear Instrumentation | 71 |
| a. Steady-state Operation | 71 |
| b. Transient Operation | 73 |
| 2. Rod Drive Control Systems | 74 |
| 3. Shutdown and Alarm System | 76 |
| 4. Transient Control System | 78 |
| 5. Radiation-monitoring System | 81 |
| 6. Nonnuclear Instrumentation | 82 |
| 7. Emergency Power | 83 |
| APPENDICES | |
| A. Evaluation of Fuel and Structural Materials | 85 |
| B. Heat Transfer | 87 |
| C. Control Rod Drive Calculations | 102 |
| D. Shield Design Calculations | 113 |
| E. Coolant System Pressure Drop and Flow Distribution | 121 |
| F. Initial Fuel Loading and Startup | 123 |

DESIGN SUMMARY REPORT ON THE TRANSIENT REACTOR TEST FACILITY (TREAT)

by

G. A. Freund, P. Elias, D. R. MacFarlane,
J. D. Geier, and J. F. Boland

I. INTRODUCTION

The Transient Reactor Test Facility (Fig. 1) is an air-cooled, thermal, heterogeneous system designed to evaluate reactor fuels and structural materials under conditions simulating various types of nuclear excursions. The immediate objective of TREAT is to provide quantitative data and visual information on the mechanism of melting of fast reactor fuel elements by nuclear heating analogous to a power excursion in a fast reactor core. Initial meltdown studies will be made on single, EBR-II-type fuel pins encapsulated in an inert gas atmosphere and positioned in a vertical thimble at the core center. The tests may be extended to a 19-pin cluster, or perhaps to a full-scale, 91-pin EBR-II subassembly in flowing sodium.

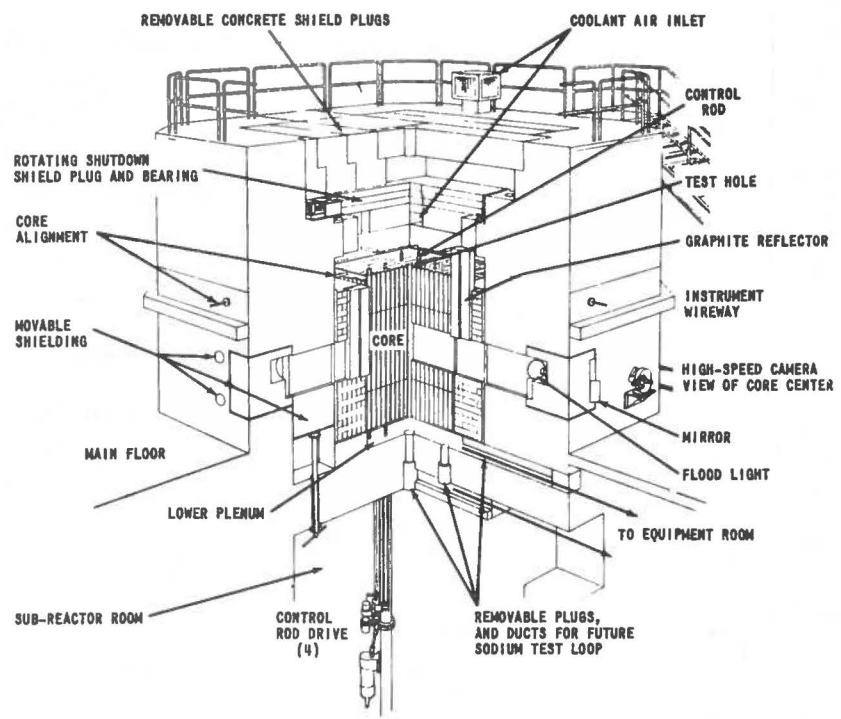


FIG. 1
TREAT PERSPECTIVE

The experimental facilities of TREAT are not limited to meltdown studies. Plans are under way to conduct a program of metal-water reaction experiments involving: (1) rate measurements of hydrogen evolution from fuel and cladding materials in dynamic, low-pressure steam during a transient; and (2) similar measurements in an autoclave containing static water at high pressure. Studies on transient behavior of ceramic fuels for high-temperature systems are also under consideration.

Thus TREAT represents a twofold contribution to the advancement of fast reactor safety technology and design: (1) it will provide basic data for predicting the severity of potential incidents; and (2) it will serve as a proving ground for fuel concepts designed to reduce or preclude the consequent hazards.

TREAT is located on Site 16 at the National Reactor Testing Station, Idaho (Fig. 2). Construction by the Teller Construction Co., Portland, Oregon, was started in February, 1958 and completed in early November, 1958. The reactor first achieved criticality on February 23, 1959.

As of this writing, the physics of the reactor at low power has been investigated thoroughly. Transients in response to reactivity inputs ranging from $0.002 \Delta k/k$ (≈ 36 Mw-sec) to $1.9 \Delta k/k$ (≈ 445 Mw-sec) have been run successfully.

The design, construction, and startup of TREAT were the joint responsibilities of the Reactor Engineering, Idaho, and Metallurgy Divisions, with contributions by the Central Shops, Electronics, and Plant Engineering Divisions at Argonne. Specific credit is due to the following personnel for their substantial contributions and assistance during the course of the project:

| | |
|------------------|----------------|
| R. V. Batch | E. W. Landow |
| W. K. Brookshier | Harry Lawroski |
| R. N. Curran | W. W. Managan |
| A. A. Denst | C. M. Putness |
| G. J. Easter | R. E. Rice |
| R. D. Ivany | D. F. Spencer |
| M. J. Janicke | D. C. Thompson |
| L. E. Wright | |

Two other phases of the project are being reported separately: Physics Calculations¹⁻⁴ and Fuel Element Fabrication.^{5,6} The entire project was carried out as part of the Argonne Fast Reactor Safety Program headed by David Okrent, whose overall guidance is gratefully acknowledged.

¹ Haig P. Iskenderian, Physics Analyses of the TREAT Reactor Design, ANL-6025 (August 1959).

² Haig P. Iskenderian, Post Criticality Studies on the TREAT Reactor, ANL-6115 (February 1960).

³ F. Kirn, Physics Measurements in TREAT, ANL-6173 (to be published).

⁴ D. Okrent et al., Kinetics of TREAT, ANL-6174 (to be published).

⁵ J. H. Handwerk and R. C. Lied, Manufacture of Graphite-Urania Fuel Matrix for TREAT, ANL-5963 (January 1960).

⁶ C. H. Bean and F. D. McCuaig, Manufacture of Zircaloy-3 and Aluminum-jacketed Graphite-Urania Fuel and Graphite Reflector Elements for TREAT, ANL-6013 (to be published).

II. DESIGN SUMMARY

A. Site and Buildings

The TREAT complex comprises a reactor building and a control building located on Site 16 about 4250 ft and 1750 ft, respectively, northwest of the EBR-II containment vessel (Fig. 3). The topography permits an unobstructed view between the two buildings.

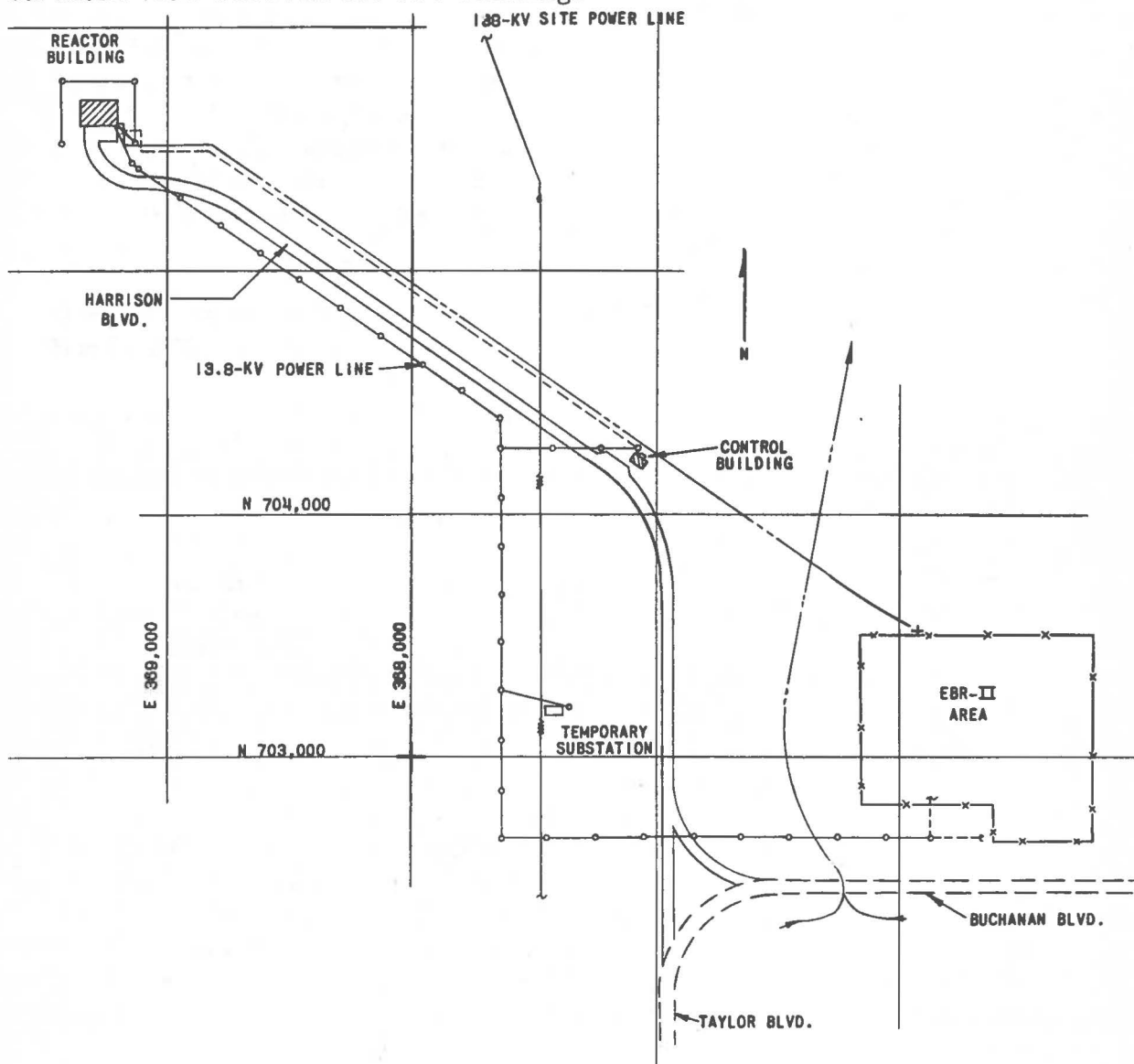


FIG. 3
SITE 16 SHOWING TREAT INSTALLATION

Certain building services and utilities are interconnected with the EBR-II service system. Water is supplied from the EBR-II fire loop by a $4\frac{1}{2}$ -inch, cement mortar-lined steel pipe. Power is supplied by a 13.8-kv electrical transmission line and underground cables leading from the EBR-II substation.

1. Reactor Building

The Reactor Building (Fig. 4) is an aluminum-sided steel frame structure which features a high bay section and adjacent service wing. The high bay section (35-foot ceiling) contains the reactor, fuel storage pit, instrument room, and basement sub-reactor and equipment rooms. The control rod drive mechanisms are located in the subreactor room, which measures 16 ft square by 13½ ft high. The adjacent equipment room (18 ft by 20 ft by 18 ft high) will house auxiliary apparatus, i.e., pumps, storage tanks, piping, etc., required for future experiments with flowing sodium. Access to both rooms is by a stairway from the main floor into the equipment room, and through a door into the adjacent subreactor room. In addition, there is an escape ladder leading from the subreactor room to the main floor. Provision has been made for ventilating both rooms with the reactor cooling blowers in the event exceptional air changes are required.

The entire high bay area, including the top and three faces of the reactor shield, is serviced by a 10-ton bridge crane. The specifications of the crane are as follows:

| | |
|----------|-----------------|
| Hoist: | 2 or 8 ft/min. |
| Trolley: | 5 or 20 ft/min. |
| Bridge: | 5 or 20 ft/min. |

The crane has a maximum lift distance of 26½ ft from the main floor, and 14½ ft from the top of the reactor rotating shield plug. The crane can be used to service the equipment room through a hatchway (7½ ft by 5½ ft) in the main floor.

The service wing (13½ ft high) contains the reactor air coolant turbocompressors and the building services. The building is heated by an oil-fired steam boiler (1,750,000 Btu/hr) and an air-steam heat exchanger unit which supplies 7,500 cfm of heated air. The air is exhausted by a ceiling fan (6,000 cfm) in the high bay area. During hot weather, the reactor instrument room is cooled by a 2-ton air-conditioning unit. Electric power is supplied by three 75-kva transformers. Compressed air at 100 psi is supplied by an air compressor in the utility room.

2. Control Building

The Control Building (Fig. 5) is a single-story, concrete block structure which contains the control panels and instrumentation for remote-controlled operation of the reactor. The building is heated by a forced-draft, oil-fired space heater, and cooled by a 3-ton air-conditioning unit. Electric power is supplied by a 10 kva transformer.

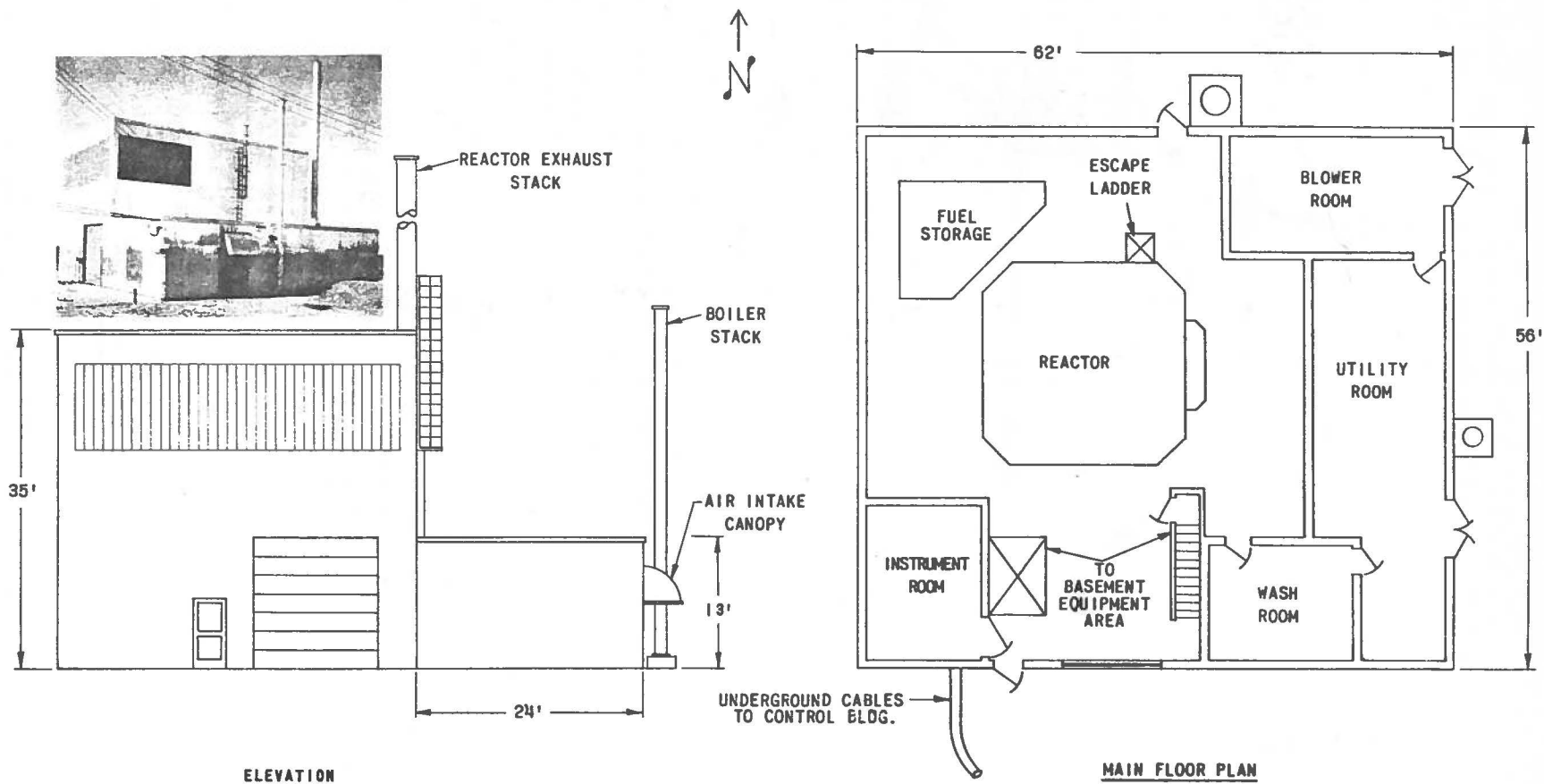


FIG. 4
REACTOR BUILDING ELEVATION AND FLOOR PLAN

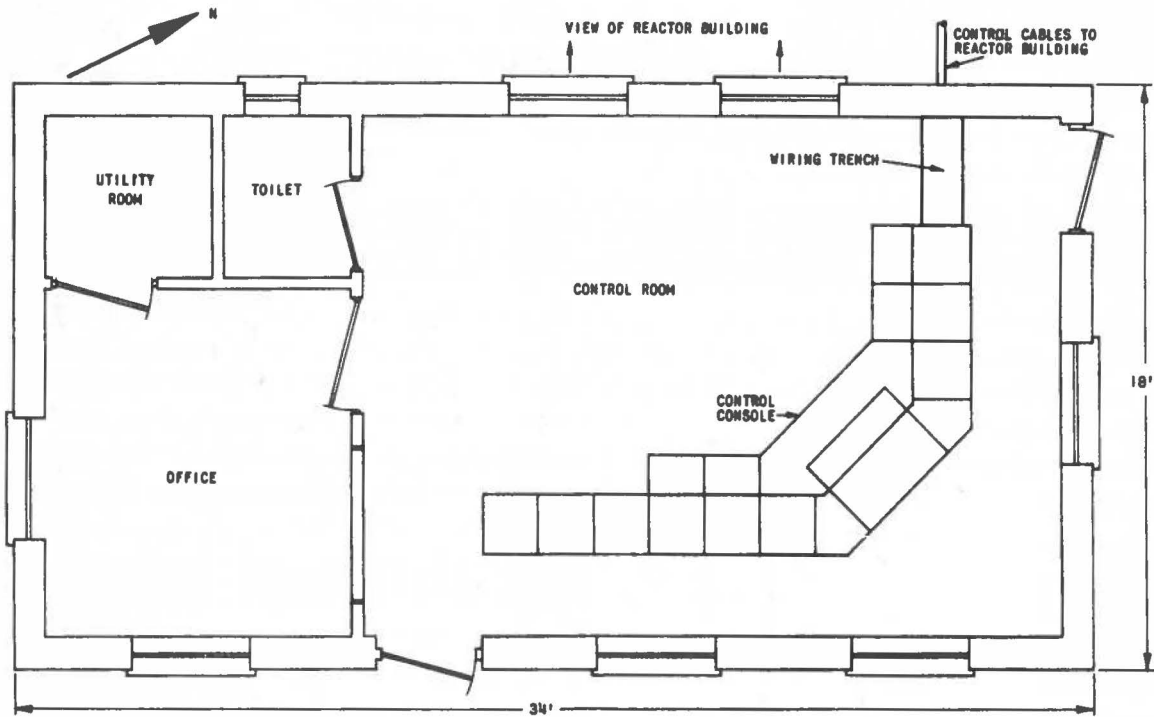
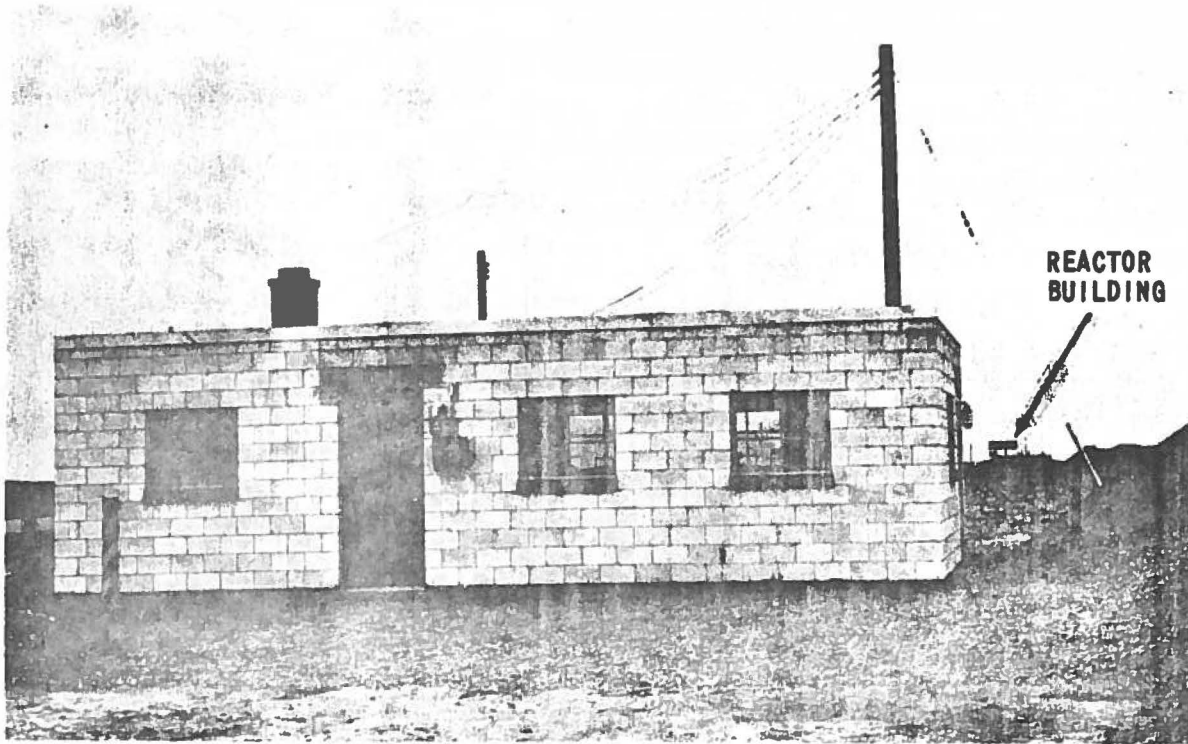


FIG. 5
CONTROL BUILDING

B. Reactor

The major features unique to TREAT are: large flux integral absorption without dependence on cooling systems, due to the high heat capacity of the core; inherent, essentially instantaneous, temperature-dependent shutdown mechanism; rapid control rod motion; and visual access to the core center.

1. Core

The fuel is composed of graphite-urania blocks contained in thin-walled Zircaloy cans. Aluminum-canned graphite reflector sections are riveted to the top and the bottom of the fuel section to form a standard fuel assembly. The completed assembly (with riveted aluminum end fittings) measures slightly under 9 ft long, with a nominal cross section of 3.960 in. square, and weighs ~ 95 lb.

The core complement features variations of the standard fuel assembly. These include slotted assemblies that are aligned to permit visual access to the core center; control rod fuel assemblies machined to accommodate control rod guide tubes; aluminum-canned graphite dummy fuel assemblies to occupy vacant fuel positions in the desired lattice; Zircaloy-canned graphite dummy assemblies that serve as a heat barrier between the aluminum dummies and the active fuel assemblies; thermocouple assemblies that monitor temperatures of the fuel and reflector; and steel assemblies containing lead shot for shielding the viewing slots during installation of experimental equipment.

All assemblies are supported at the bottom by a steel grid plate which can accommodate 361 assemblies arranged on a 4-in. square lattice (maximum core size: 6 ft 4 in. square). The grid plate, in turn, is supported by the control rod thimbles and a concrete ledge which forms the lower plenum chamber. The top ends of the assemblies are aligned and clamped by four horizontal clamping bars to form a rigid "bundle." The core is surrounded (radially) by a permanent graphite reflector. One face of this reflector extends into the concrete biological shield to form a thermal column 7 ft thick.

The reference core of 225 standard fuel assemblies (nominal core size: 5 ft x 5 ft x 4 ft high) is designed to sustain transient thermal flux integrals of 3.5×10^{15} nvt, each corresponding to a total energy release of 1,000 Mw-sec. Such a transient can be generated by an initial reactivity addition of $\sim 0.0325 \Delta k/k$ above delayed critical, resulting in an initial prompt period of ~ 35 milliseconds. The final graphite hot-spot temperature is 413°C . The final graphite average temperature is 273°C .

The core is cooled by a "once-through," induced-draft, air-cooling system. Two turbocompressors draw 6,000 cfm (max.) of air through the reactor. The air is filtered as it enters at the top of the reactor shield. The flow continues downward through square coolant passages formed by chamfered corners of adjacent fuel elements, and around the permanent graphite reflector, into the lower plenum. The coolant is drawn from the plenum by the blowers, passed through AEC absolute filters, and discharged up the 60-ft stack to the atmosphere. The cooling system permits steady-state operation at 100 kw, and cools the reactor in a matter of several hours after an experiment (depending upon the severity of the transient).

Fuel-exchange operations are performed at the top of the reactor with the aid of a lead-shielded coffin and the overhead bridge crane. The top concrete shielding plugs are removed to expose the large (10 ft 10in. diameter) steel rotating shield and indexing plug. The plug features a radial slot containing boron-steel blocks that can be moved to provide access through the plug over the assembly to be removed. The coffin is positioned above the discharge opening and, with the aid of a periscope, the fuel grapple is lowered to engage and withdraw the fuel assembly. The loaded coffin is transferred to the concrete fuel-storage area and the assembly is lowered into a storage hole in the floor and released. The coffin is powered by an electric motor and operated with a pushbutton pendant.

2. Control Rods and Drive Mechanisms

The present control system features eight tubular control rods actuated by four drive mechanisms located in the subreactor room. Provision has been made in the core structure for installation of 32 control rods.

Each control rod comprises a poison section which contains compacted boron carbide powder, a Zircaloy follower, a two-piece steel follower, and a handling attachment to form a long, tubular assembly (1.75 in. OD by 17 ft 6½ in. long), weighing 65 lb. Threaded connections are installed at the ends of each section. Thus, the function of each control rod can be changed from a normal shutdown rod to a transient rod, by interchanging the top poison section and the Zircaloy follower. The length of the poison section (5 ft) is equal to the stroke of the control rod drive mechanism.

The control rod drive is a pneumatic accelerating device with an integral air-hydraulic dashpot, and a motor-driven lead screw mechanism for recocking and intermediate positioning of the rod. Each drive mechanism actuates two control rod assemblies via knuckles that compensate for any misalignment between the rods and the drive mechanism.

The design criteria for the rod drive is to complete the central four feet of the 5-ft stroke in 80 msec. The high speed, combined with the weight of the moving components (270 lb) and the tendency of the slender rods to buckle, led to the selection of the integral air-hydraulic dashpot design. A prototype drive has accomplished the four feet of travel in 80 msec with a cylinder pressure of 450 psi.

The lead screw and motor-driven intermediate positioning mechanism travel at a speed of 6 in./min for fine reactivity control required during steady-state operation (100 kw). This corresponds to a maximum rate of reactivity addition of $\sim 0.0005 (\Delta k/k)/\text{sec}$.

3. Shielding and Experimental Facilities

The shielding is designed (1) to permit personnel access around and atop the reactor during steady-state operation at 100 kw, and (2) to shield experimental equipment against excessive integrated exposure during transients. Access to the subreactor room is controlled during steady-state operation. Prior to transient operations, the building is evacuated of all personnel. Access to the subreactor room is controlled for periods of several hours or more after each transient, depending upon the severity of the transient.

The reactor is shielded radially by high-density concrete, 5 ft thick. The shielding below the reactor is reinforced high-density concrete (3 ft thick) which forms a portion of the ceiling of the subreactor room. Above the reactor, the shielding consists of a laminated steel and boral rotating shield plug (1 ft thick) and removable high-density concrete blocks, 3 ft thick.

Stepped concrete blocks and plugs are used to shield experimental access openings. There are three horizontal access slots which converge on the core center. The openings through the face of the shield can be offset (4 in. wide by 24 in. high) to facilitate high-speed photography; or expanded (2 ft square, stepping out to 3 ft square) to accommodate bulky experimental equipment. There are 14 instrument thimbles (6 in. OD): two thimbles are adjacent to each of the three horizontal access slots and penetrate the permanent reflector; and two thimbles at each corner of the reactor which penetrate the radial shield only. The closure plugs are of high-density concrete and contain holes for instrument leads. The graphite thermal column (5 ft square) is located in the east face of the radial shield. The opening is shielded with a high-density concrete door 33 in. thick. The inner surface of the door is clad with boral $\frac{1}{2}$ in. thick. The door has a 12-in. square opening through which the central thermal column stringers can be removed.

The principal experimental test facilities are two vertical through holes. One hole extends through the geometric center of the core; the other is offset 32 in. south of the central hole. The cross section of the central grid plate hole can be increased from 3.5 in. dia. to 11.25 in. square by removing an insert in the core grid plate and the appropriate number of fuel assemblies. Spacers of equivalent cross section are installed in the vacated fuel positions at the top of the core to maintain rigidity of the clamped core assembly. The second hole is made in similar fashion to align with a 3.5-in. diameter opening in the core grid plate. Either hole can be used to accommodate future installation of a sodium loop for melt-down studies involving pin-type fuel elements ranging from single pins up to a full-scale, EBR-II-type fuel assembly. Extensions of both holes through the bottom shielding are closed with removable concrete plugs.

C. Plant Parameters

The major design features and operating characteristics of TREAT are summarized in Table I.

D. Control

The reactor is operated from the Control Building located one-half mile from the Reactor Building. Neutron chamber signals are amplified in the Reactor Building and transmitted, via underground cables, to the Control Building. Control signals from the control console are returned via underground cables. Scram signals bypass the control console and operate trip relays in the Reactor Building. The cause of the scram is indicated on the control console annunciator panel.

Local control of the reactor is limited to three scram buttons located at various positions in the Reactor Building. Personnel are alerted to the beginning of reactor operations by an audible alarm and flashing warning light which are actuated simultaneously when the control rod drive latches are energized. Personnel are evacuated to the control building during transient operations. The warning light flashes continuously during reactor operation.

E. Costs

The costs of the TREAT Project are summarized in Table II. These include direct costs of engineering design, construction, fabrication, and assembly of site facilities, buildings, reactor and core, as described in this report. In addition to the present control scheme of four complete control rod drives and eight control rods, the costs include 10 additional control rods (18 total), and sufficient zirconium plus some component parts for a total of 32 rods.

Table I

DESIGN PARAMETERS FOR TREAT REACTOR

| | |
|--|--|
| Core | |
| Nominal size (225 fuel assemblies) | 5 ft square x 4 ft high |
| Maximum size (361 fuel assemblies) | 6 ft 4 in. square x 4 ft high |
| Fuel Assemblies | |
| Overall dimensions | 3.960 in. square x 8.94 ft long, with 0.625-in. chamfered corners |
| Fuel Section | |
| Configuration | 6 graphite-urania blocks clad with Zircaloy 3, 25 mils thick |
| Block dimensions | 3.800 in. square x 8 in. long |
| U ₃ O ₈ content | 0.248 wt-% |
| Carbon-U ²³⁵ atomic ratio | 10,000:1 |
| U ²³⁵ enrichment | 93.1% |
| Dispersion | -325 mesh (44 μ, max) |
| Boron content | ~6 ppm |
| Iron content | 0.1% max |
| Reflector (Top and Bottom) | |
| Composition | Graphite |
| Length | 2 ft |
| Cladding | 6063 aluminum, 50 mils thick |
| Assembly | Riveted to ends of fuel section |
| Permanent reflector | Graphite (2 ft thick, min) |
| U ²³⁵ loading (nominal core) | 8.44 kg |
| Excess reactivity (above cold, clean critical) | ~ 19% Δk/k |
| Coolant | Air at atmospheric pressure |
| Control Rods | |
| Configuration | Tubular (1.75 in. OD) |
| Absorber | Carbon steel tube packed with B ₄ C powder |
| Absorber length | 5 ft |
| Zircaloy follower material | Zircaloy tube filled with graphite |
| Zircaloy follower length | 5 ft; interchangeable with absorber section |
| Steel follower material | Steel tube filled with graphite |
| Steel follower length (2 sections) | 7 ft 5 in. |
| Weight of assembled control rod | 65 lb |
| Number of rods (max) | 32 |
| Worth of 24 rods (above cold, clean critical) | ~32% Δk/k |

Table I (Continued)

| | |
|---|--|
| Control Rod Drives | Compressed gas-actuated scram, with lead screw-driven mechanical latch for intermediate positioning and relatching. Integral pneumatic-hydraulic dashpot |
| Number of drives (max) | 16 (2 rods per drive) |
| Regulating speed | 6 in./min |
| Scram time | Ranges from free fall to ~80 msec for central 4 ft of total 5-ft stroke |
| Thermal Data | |
| Steady-state (180 fuel assemblies) | |
| Design power | 100 kw |
| Heat flux | |
| Average | 1940 Btu/(hr)(ft ²)(°F) |
| Maximum | 2940 Btu/(hr)(ft ²)(°F) |
| Hot-spot temperature | |
| Zircaloy cladding | 380°F |
| Fuel | 510°F |
| Coolant air velocity (6500 cfm) | 80 ft/sec |
| Bulk air temperature rise (6500 cfm) | 68°F |
| Transient (Nominal core size; 225 fuel assemblies) | |
| Design energy release | 1000 Mw-sec |
| Time-integrated thermal flux (average over core) | 3.5×10^{15} nvt |
| Fuel temperature at termination of transient | |
| Average | 523°F (273°C) |
| Maximum | 775°F (413°C) |
| Corresponding $\Delta k/k$ in temperature coefficient | 5.5% |
| Minimum reactor period (self-limiting) | 35 msec |
| Prompt neutron lifetime | 8.8×10^{-4} sec |
| Peak thermal flux (for minimum period) | 3×10^{16} nv |
| Coolant outlet temperature | Limited to 250°F by coolant bypass valve |
| Time to cool hot spot after transient | ~5 hr |

Table II

COST SUMMARY - TREAT

| | | | |
|--|-----------------|------------|--------------|
| Engineering Design and Inspection | | | |
| Site and Buildings | | | |
| Title I and II (A-E) | \$ 24,900 | | |
| Title III (A-E and Inspection) | 17,500 | | |
| Site Expenses (Surveys, soil boring, etc.) | <u>27,200</u> | \$ 69,600 | |
| Reactor and Core | | | |
| Design Drafting | 25,400 | | |
| Engineering | 41,000 | | |
| Indirect and Administration Costs | <u>61,000</u> | \$ 127,900 | |
| | <u>Subtotal</u> | | \$ 197,500 |
| Construction, Fabrication, and Assembly | | | |
| Site and Buildings | | | |
| Reactor Building | \$ 253,900 | | |
| Control Building | 18,700 | | |
| Water Line | 16,100 | | |
| Electrical Distribution System | 30,900 | | |
| Access Road | <u>52,100</u> | \$ 371,700 | |
| Reactor Components | | | |
| Core Support and Alignment Structure | \$ 9,600 | | |
| Reflector and Thermal Column | 12,400 | | |
| Source | 3,400 | | |
| Control Rods and Guides* | 19,700 | | |
| Control Rod Drives (including air supply and handling) | 31,700 | | |
| Shutdown Top Plug | 28,900 | | |
| Shielding Gates and Blocks | 12,200 | | |
| Fuel-handling System and Tools | 28,600 | | |
| Instrumentation and Cable | 79,000 | | |
| Miscellaneous | <u>4,000</u> | \$ 229,500 | |
| Core Fabrication | | \$ 429,100 | |
| ANL-incurred Costs | | | |
| Engineering | | | |
| Building and Reactor | \$ 34,000 | | |
| Core | 22,000 | | |
| Technical Labor | | | |
| Component Assembly | 14,000 | | |
| Core | 7,000 | | |
| Indirect and Administration Costs | | | |
| Building and Reactor | 72,000 | | |
| Core | 43,500 | | |
| Building Occupancy Costs | 13,400 | | |
| Reactor Modifications | <u>30,000</u> | \$ 235,900 | |
| | <u>Subtotal</u> | | \$ 1,266,200 |
| TOTAL PROJECT COST (including core) | | | \$ 1,463,700 |
| TOTAL PROJECT COST (excluding core) | | | \$ 962,100 |

* Zircaloy for control rods included in core costs.

Also included are indirect costs incurred by the Laboratory in connection with the above design and construction activities. The summary does not include costs pertinent to physics design and preliminary analyses, development work, and fissionable material in the fuel.

On this basis, the overall cost of the TREAT project is \$ 1,463,700; of this, the core fabrication represents \$ 501,600.

III. COMPONENT DESCRIPTION

A. Core Assembly

The reactor cavity is designed to accommodate a total of 361 assemblies arranged on a 4-inch square lattice, or a maximum core size of 6 ft 4 in. square by 4 ft high. The types of assemblies consist of standard fuel assemblies, and special-purpose assemblies designed to effect access slots through the core; accommodate control rods and thermocouple installations; provide shielding and thermal barriers; and dummy counterparts of the foregoing assemblies as required to complete the desired core configuration.

1. Standard Fuel Assembly

The standard fuel assembly (Fig. 6) comprises an upper and lower graphite reflector section, each canned in Type 6063 aluminum and riveted to a central fuel section. An aluminum gripping fixture is riveted to the upper reflector can, and an aluminum support and alignment pin is riveted to the lower reflector can to complete the fuel assembly. The completed assembly is slightly under 9 ft long, with a nominal cross section of 3.960 in. square, and weighs ~95 lb. The wide chamfers at the corners of the assembly combine with those of adjacent assemblies to form 0.625-in. square coolant passages through the assembled core.

The fuel section comprises six 8-in. long fuel blocks, and two zirconium spacers contained in a Zircaloy can. Each block is a homogeneous, relatively dilute dispersion of uranium dioxide in a carbon-graphite moderator. The graphite-urania fuel was selected because of the following inherent advantages afforded in a reactor designed to absorb large thermal neutron flux integrals applied over very short periods of time:

- (1) High heat-absorbing capability of the graphite moderator provides an effective heat sink for transient-generated heat without dependence on coolant during the transient.
- (2) Homogeneity of fuel and moderator gives an essentially instantaneously acting, large, negative temperature coefficient and, hence, self-limiting transients.
- (3) Excellent thermal shock resistance of graphite will sustain the high rates of heat input of the transient.

The zirconium spacers above and below the fuel blocks serve to delay heat transfer from the fuel to the reflector sections and, thus, to protect the aluminum cans during severe transients. The fuel section is canned in Zircaloy-3 for protection against oxidation and for retention of fission products.

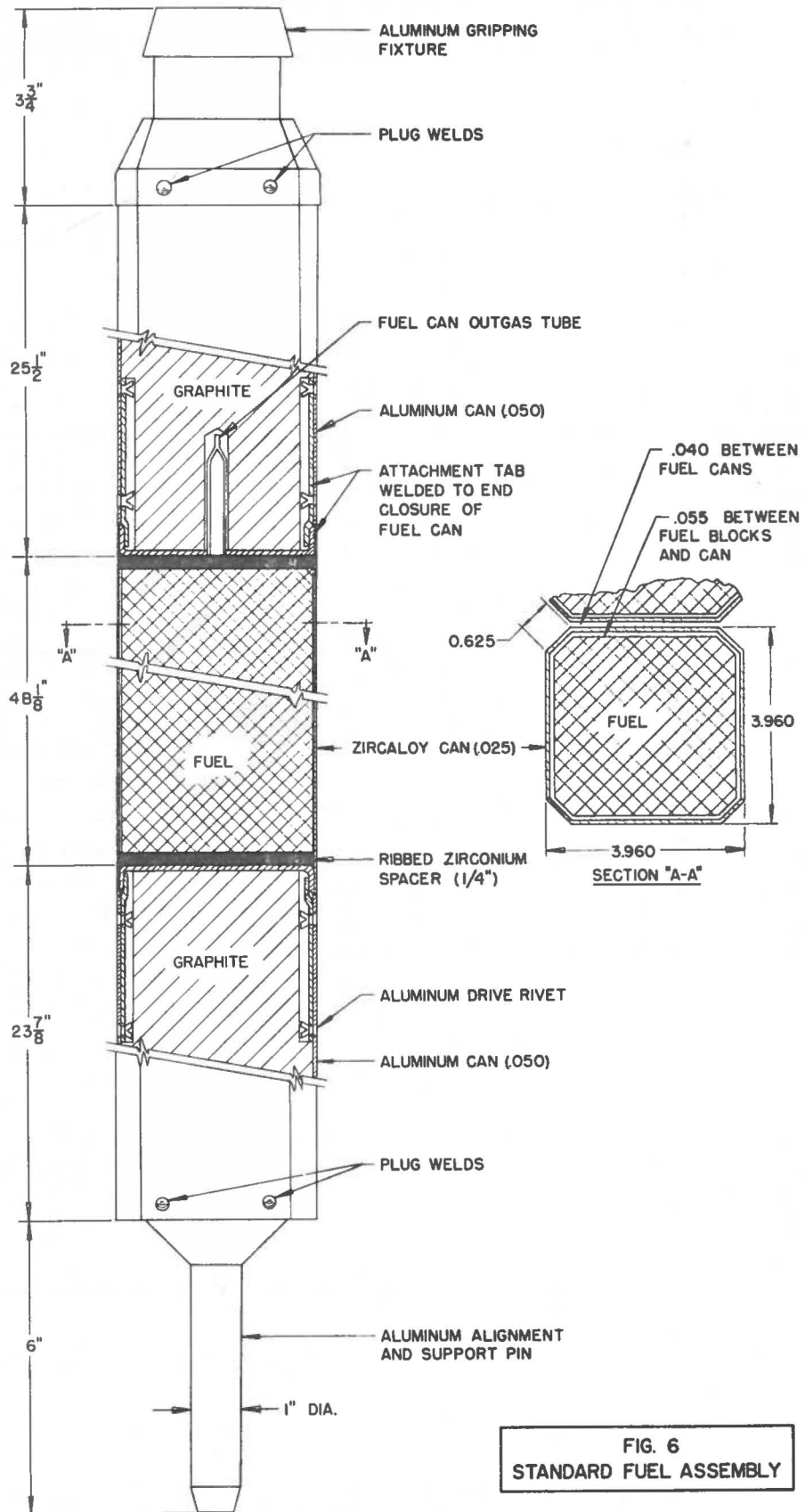


FIG. 6
STANDARD FUEL ASSEMBLY

2. Fuel Fabrication

The graphite-urania fuel blocks were made by a direct fabrication process developed by the Great Lakes Carbon Co., Morton Grove, Illinois. A detailed description of the process has been published as ANL-5963.⁵ In brief, the process consists of blending and grinding uranium oxide (U_3O_8) with graphite flour and pitch. The plastic mixture is die pressed at 5,000 psi and $\sim 100^\circ C$ essentially to finish size. The green blocks are then baked in stainless steel containers at $950^\circ C$ for a cycle lasting about two weeks. During the baking period, the pitch is transformed to carbon and the U_3O_8 is reduced to UO_2 , resulting in a graphite- UO_2 matrix cemented together by carbon.

The baking containers are divided into quadrants by 1% boron-stainless steel plates ($\frac{1}{4}$ in. thick) to reduce the criticality hazard. As a consequence of the unexpected diffusion of boron into the graphite during the baking cycle, the boron content of the fuel blocks varied considerably from the originally specified concentration of 1 ppm. The average boron content was 6 ppm. The foregoing process limits the machining requirements to trimming certain blocks to obtain the desired overall length of the block assembly for canning.

The cans for the fuel section are made from ingots of Zircaloy-3 sponge, forged and bloomed into billets, hot rolled to a thickness of 0.090 in., cold rolled to final thickness of 0.025 in., and heliarc welded in a fixture to form a rectangular can. The end caps are hot formed from Zircaloy sheet, $\frac{3}{32}$ in. thick. The bottom cap is welded to the fuel can, and the fuel blocks and zirconium spacers are loaded.

Prior to loading, the fuel blocks are outgassed to reduce pressure buildup during subsequent outgassing during reactor operation. The outgassing cycle consists of heating for 12 hr at $900^\circ C$ and a pressure of 25μ or less, followed by cooling for 30 hr at 25μ or less. The outgassed blocks are loaded immediately into the can and the top end cap is welded in place. A small tube is attached to the end cap to facilitate subsequent evacuation, leak testing, and sealing of the can under vacuum.

The graphite reflector sections are canned separately in one-piece Type 6063 aluminum extrusions. (The reflector material was machined from graphite used originally in the CP-2 reactor.) The assembled reflector sections are riveted to triangular Zircaloy tabs which, in turn, are resistance welded to the fuel section. The sides of the aluminum cans in the welded region are slotted to compensate for the large difference in thermal expansion coefficient between the dissimilar metals. Cast aluminum fittings for handling and alignment are riveted at the top and bottom to complete the fuel assembly.

3. Special-purpose Fuel Assemblies

In addition to the standard fuel assembly, the core lattice is composed of special-purpose fuel assemblies. They are similar in geometry to the standard fuel assembly but differ in structural design and composition in accordance with their function in the core assembly.

Four of the special-purpose fuel assemblies are shown in Fig. 7. The center of the Control Rod Fuel Assembly [Fig. 7 (B)] is machined to accommodate a Zircaloy-2 guide tube ($2\frac{1}{4}$ in. OD x $\frac{1}{8}$ in. wall thickness) and a bearing for support of a control rod. The bearing is attached to a removable aluminum tube so that it may be replaced, if necessary (see Control Rod Guide Tubes and Bearing, p. 33).

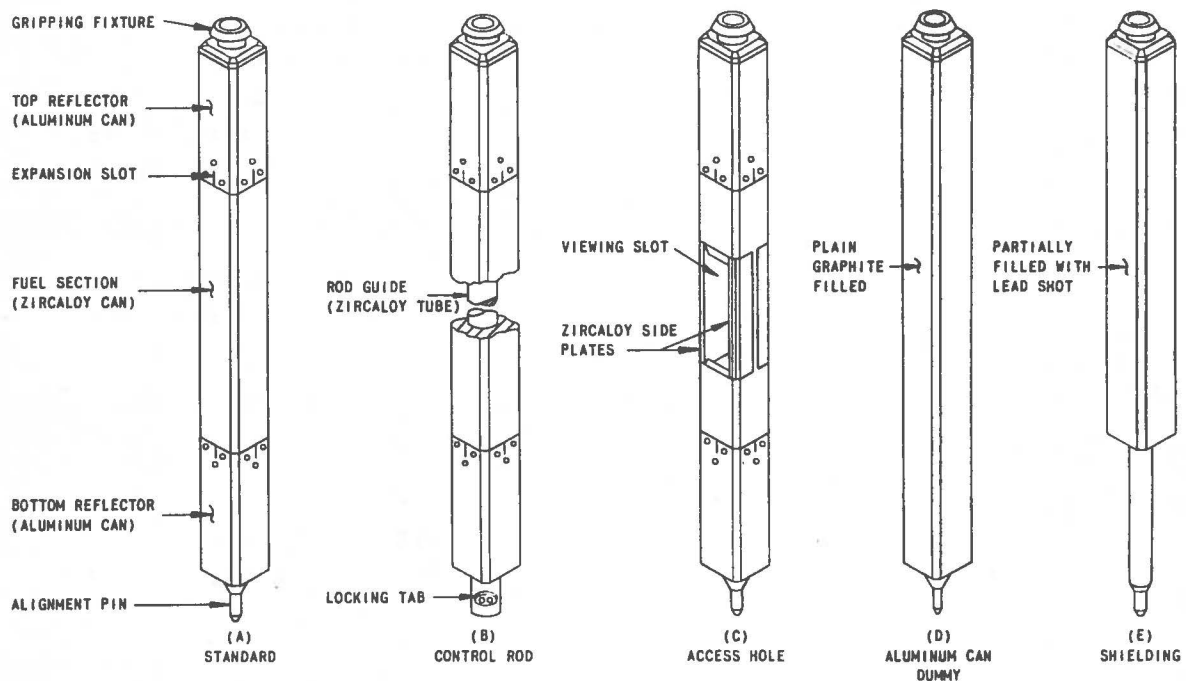


FIG. 7
STANDARD AND SPECIAL-PURPOSE FUEL ASSEMBLIES

The Access Hole Fuel Assembly [Fig. 7 (C)] is designed to provide an opening, $3\frac{1}{2}$ in. wide by $21\frac{3}{4}$ in. high, through the assembly. The opening is accomplished by removing the central two feet of the 4-ft long fuel section and interconnecting the remaining 1-ft fuel sections with two Zircaloy side plates, 0.060 in. thick. These assemblies are aligned in the active core region wherever a viewing slot is required.

The Aluminum Can Dummy Fuel Assembly [Fig. 7 (D)] consists of plain graphite blocks assembled in a single aluminum can. These assemblies are installed in vacant grid plate positions between the active fuel assemblies and the permanent reflector.

Not shown in Fig. 7 is a Zircaloy Can Dummy Fuel Assembly which is identical to the standard fuel assembly but contains plain graphite. These assemblies are installed in fuel positions immediately adjacent to the active core, and serve as a heat barrier to protect the aluminum dummy assemblies from excessive core heating.

Also not shown is an Access Hole Dummy Fuel Assembly. These assemblies contain plain graphite in lieu of the fuel-bearing graphite in their active assembly counterparts. They are aligned to permit extension of the viewing slots through the ring of dummy fuel assemblies.

The Shielding Assembly [Fig. 7 (E)] is a steel box of $3\frac{7}{8}$ in. square cross section, partially filled with lead shot. These assemblies are installed at the edge of the core grid plate to provide shielding as needed for access to the horizontal viewing slots in the face of the biological shield during reactor shutdown.

Thermocouple fuel assemblies are used to monitor temperatures at various points of interest in the fuel and reflector sections. Owing to the limited number of thermocouples that may be installed in a single fuel assembly, five types of thermocouple assemblies and three types of thermocouple installation are employed (see Table III).

With reference to Table III, thermocouple Type A is chromel-alumel couple sheathed in Type 304 stainless steel (0.062 in. dia) and insulated with MgO. The method of installation is shown in Fig. 8. Type B is a chromel-alumel couple using 28-gauge wire with asbestos-glass insulation. Type C is a fast response chromel-alumel couple with 28-gauge wires attached individually to the fuel blocks by means of small conical wedges. Figure 9 shows a Type C couple installation.

The thermocouples are attached to an 8-pin chromel-alumel Amphenol connector located in the upper end fitting of the fuel assembly. Lead wires (chromel-alumel) are attached by means of an aluminum holder which contains the male half of the Amphenol plug (see Fig. 10). A special shielded tool is used to connect and to disconnect the Amphenol plug assembly. The lead wires extend through the reactor coolant inlet ducts and terminate at a junction panel mounted on the outer surface of the concrete shield.

Table III

CHARACTERISTICS OF THERMOCOUPLE FUEL ASSEMBLIES

| <u>Series</u> | <u>Type of Thermo-couple</u> | <u>Temperature Monitored</u> | <u>Location, in. from top of Zr Can</u> | <u>Amphenol Connector Pins</u> |
|----------------------|------------------------------|------------------------------|---|--------------------------------|
| 500-503; 506-519* | A | Fuel | 42 | AB |
| | A | Fuel | 30 | CD |
| | A | Fuel | 18 | EF |
| | A | Fuel | 6 | GH |
| 504-505 | A | Fuel | 6 | AB |
| | A | Fuel | 1 $\frac{1}{2}$ | CD |
| | A | Reflector | 1 $\frac{1}{2}$ | EF |
| | A | Reflector | 6 | GH |
| 520-549 | B | Reflector | $\frac{7}{8}$ | AB |
| | A | Fuel | 24 | CD |
| | B | Zircaloy skin | 24 (corner) | EF |
| | B | Reflector | $\frac{9}{16}$ (from bottom) | GH |
| 550-579 | C | Fuel | 24 | AB |
| | B | Aluminum skin | 1 (corner) | CD |
| 620-621 | A | Fuel | 8 | AB |
| | B | Zircaloy skin | 8 (corner) | CD |
| | A | Fuel | 4 | EF |
| | B | Zircaloy skin | 4 (corner) | GH |

*Several Zircaloy-clad reflector assemblies are of this type.

In order that the various types of fuel assemblies can be readily identified, the respective aluminum gripping fixtures are stamped with a serial number and color coded by anodizing, as shown in Table IV.

Table IV

FUEL ASSEMBLY CODING SYSTEM

| <u>Series</u> | <u>Type of Fuel Assembly</u> | <u>U²³⁵ Weight, gm</u> | <u>Color</u> |
|------------------|------------------------------|-----------------------------------|--------------|
| 100, 200, 300 | Standard | 37.5 | Red |
| 500 | Thermocouple | 37.0 | Red |
| 600 | Access Hole | 18.4 | Yellow |
| 700 | Control Rod | 26.0 | Green |
| 0-1 to 0... | Zircaloy Dummy | - | Black |
| A-1 to A... | Access Hole Dummy | - | Blue |
| X-1 to X... | Aluminum | - | Silver |

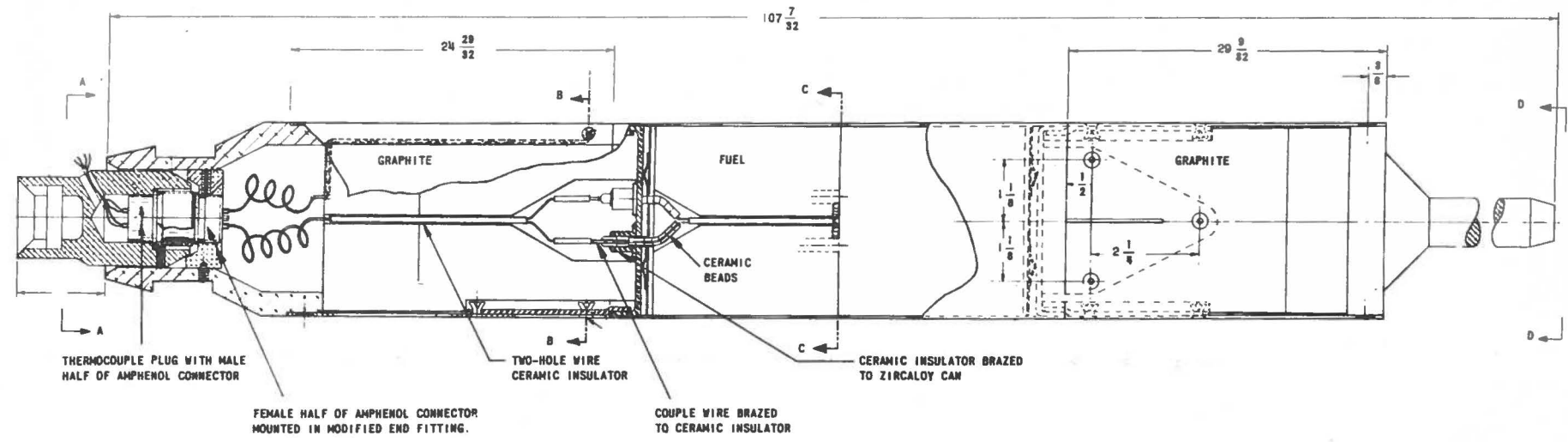
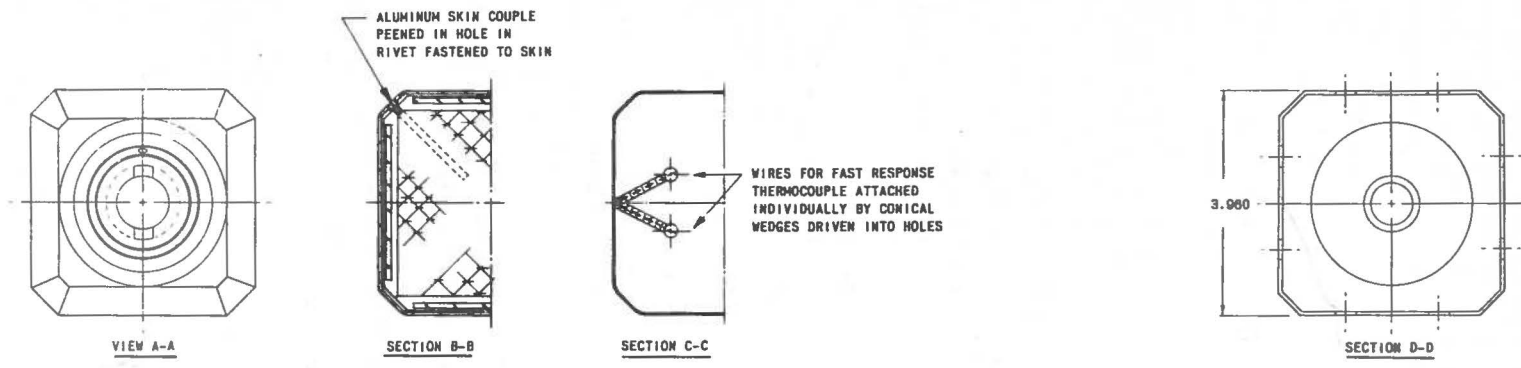


FIG. 9
TYPE C FAST RESPONSE THERMOCOUPLE INSTALLATION

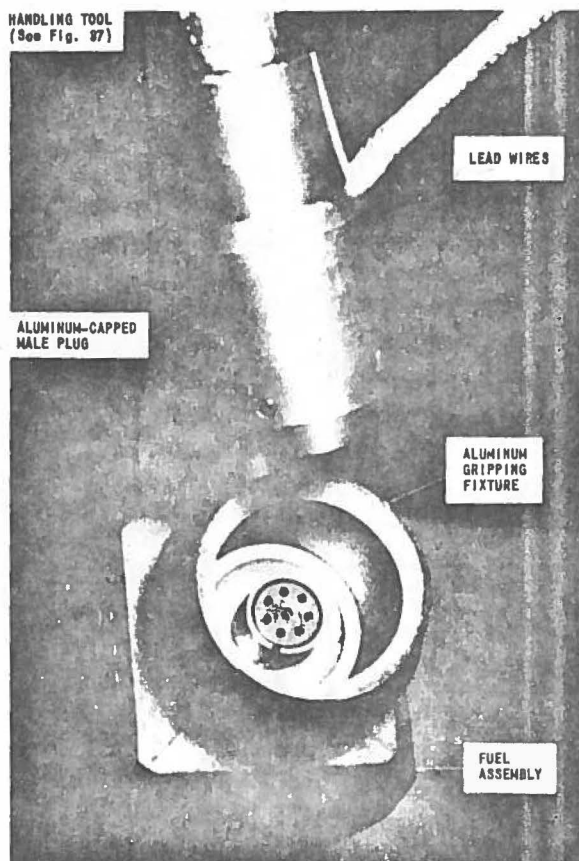


FIG. 10
THERMOCOUPLE LEAD WIRE CONNECTOR PLUG INSTALLED
IN GRIPPING FIXTURE OF THERMOCOUPLE FUEL ASSEMBLY.

Certain of the foregoing fuel assemblies have been modified further, and are identified as follows. The Source Fuel Assembly is a Zircaloy Can Dummy Assembly with a tubular penetration which extends from the top end to the midpoint for installation of the neutron source. The Source Fuel Assembly is identified by a solid top end fitting.

The Control Rod Dummy Fuel Assembly is a Control Rod Fuel Assembly with the fuel-bearing graphite replaced with plain graphite. It is used to provide a core through hole in the temporary reflector at a control rod position. The Control Rod Dummy Fuel Assembly is identified by a black end fitting with four notches 90° apart.

The Vertical Access Hole Fuel Assembly is a Control Rod Fuel Assembly with the rod guide bushing removed, and the lower end of the guide tube cut short and replaced with a standard element align-

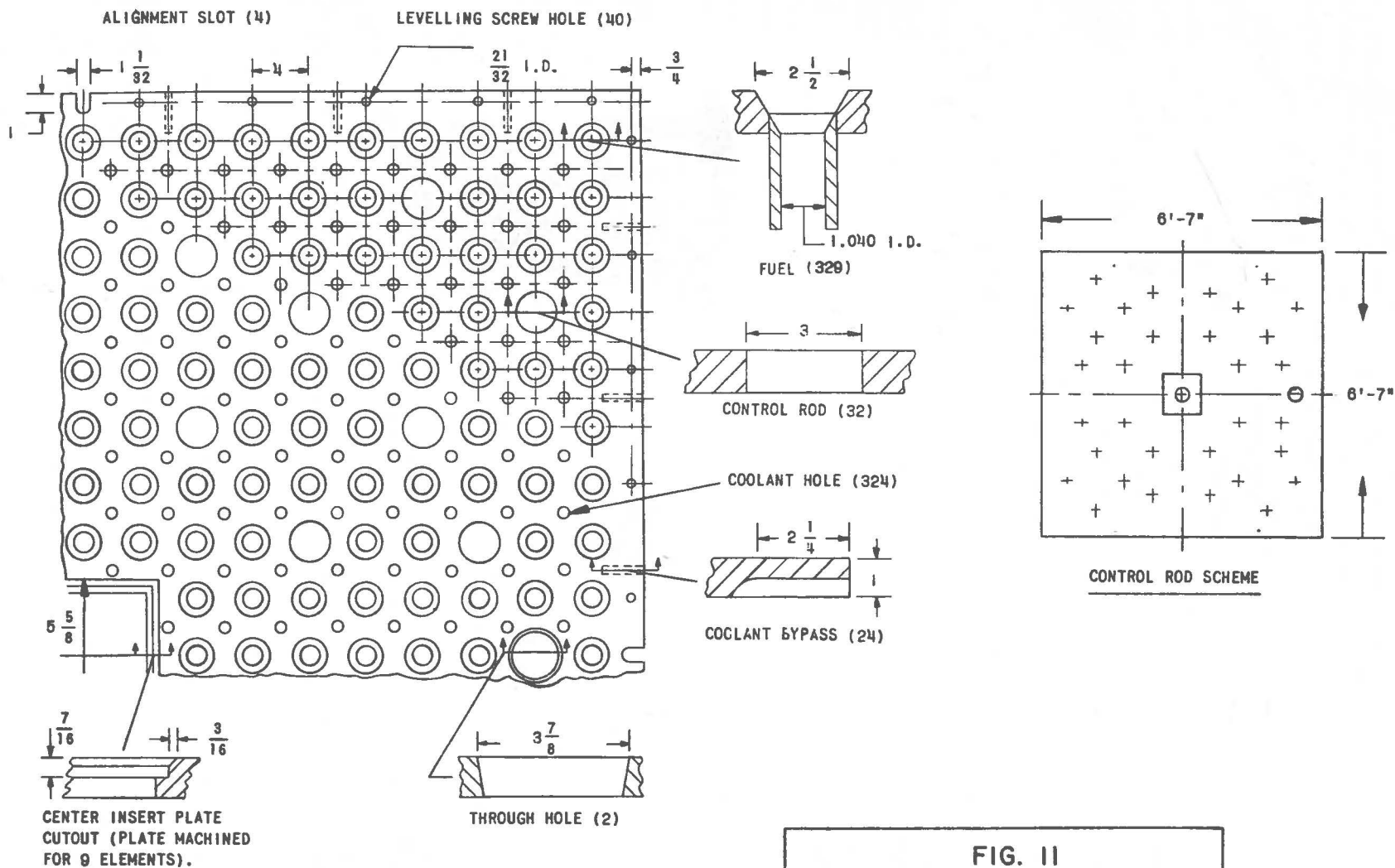
ment pin. The assembly is used to provide a vertical access hole in the core. It is identified by a magenta-colored end fitting stamped "X-725."

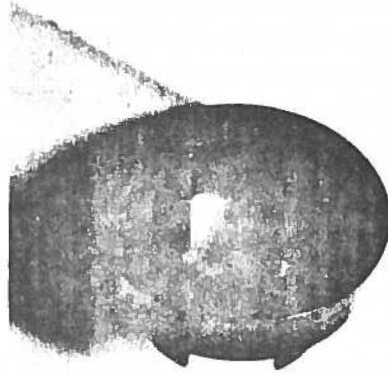
The Vertical Access Hole Dummy Fuel Assembly contains plain graphite. As in the case of its fuel-bearing counterpart, the dummy fuel assembly can be installed at any location in the core. It is identified by a magenta-colored end fitting.

B. Core Support and Alignment

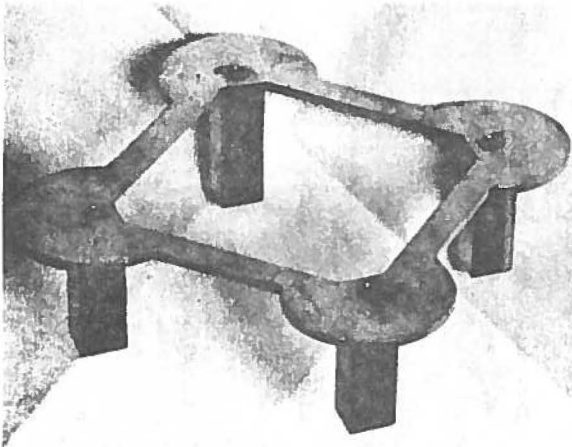
1. Grid Plate

The total weight of the core (~34,000 lb) is supported on a hot-rolled mild steel grid plate, 6 ft 7 in. square and 1 in. thick, shown schematically in Fig. 11. The grid plate is machined to accommodate 329 regular fuel assemblies (1.040 dia. opening) and 32 control rods (3 in. dia. opening). If desired, the control rod openings can be used as fuel positions by attaching special adapters (Fig. 12) to the regular fuel

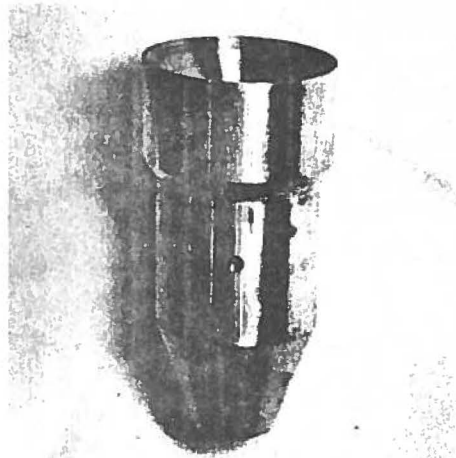




ADAPTERS FOR STANDARD FUEL ASSEMBLY (LEFT) AND CONTROL ROD FUEL ASSEMBLY (RIGHT) INSTALLATION IN THROUGH HOLE IN GRID PLATE.



SPACER FOR VACATED FUEL POSITION.



ADAPTER FOR CONTROL ROD POSITION

FIG. 12

ADAPTERS AND CORE SPACER USED TO ACCOMMODATE FUEL ASSEMBLIES IN SPECIAL GRID PLATE POSITIONS AND TO MAINTAIN CORE ALIGNMENT IN VACATED FUEL POSITIONS.

assemblies. Openings (3.5 in. dia.) are provided for future installation of a test loop: one at the center of the grid plate, and one offset 32 in. from the center. For additional flexibility, the center portion of the grid plate can be lifted out to provide an opening $11\frac{1}{4}$ in. square.

All of the fuel position openings are countersunk and threaded to aid leading in of the fuel element alignment pin and to accommodate short guide tubes (1.040 in. ID) on the underside for additional support.

Other openings ($\frac{7}{8}$ in. dia.) are provided at the corners of each fuel cell. These openings are aligned with the air-coolant passages formed by the chamfered corners of adjacent fuel assemblies. Approximately 10% of the coolant flow is bypassed to cool the inside surfaces of the shield and the permanent graphite reflector. This is accomplished by 24 slots spaced around the underside edges of the grid plate.

The edges of the grid plate are supported by the concrete ledge of the shield cavity which forms the coolant plenum chamber. The central area of the plate is supported by, but not affixed to, the 32 control rod thimbles. Alignment of the plate in the shield cavity is accomplished with four pins embedded in the concrete. Each pin engages with an elongated slot machined at the midpoint along each edge of the grid plate. This method of support and alignment permits free movement of the grid plate on thermal expansion.

The grid plate was within $\frac{1}{16}$ in. of flat prior to machining operations. However, when the fuel element guides were screwed in, the plate became slightly concave, with a maximum deviation of $\frac{1}{8}$ in. from perfectly flat. This is attributed to stresses induced by tightening the multiplicity of guides, and the absence of metal due to the large countersunk areas on the upper side. However, this amount of bowing does not interfere with the function of the grid plate.

2. Control Rod Guide Thimbles

The 32 control rod guide thimbles extend through the bottom concrete shield into the subreactor room. The thimbles are steel tubes (with a $\frac{3}{16}$ -in. wall) which step from $3\frac{5}{8}$ in. OD at the top (grid plate) to $5\frac{3}{4}$ in. OD at the bottom.

In order to ensure accurate alignment of the thimbles and the steel tubes for the central and the offset through holes with corresponding openings in the grid plate, the entire unit was bolted between two steel plates and then cast into the concrete shield. Figure 13 shows the control rod guide assembly prior to installation in the core cavity. The steel plate ($\frac{3}{8}$ in. thick)

at the top served as a dummy grid plate. The lower steel plate ($\frac{3}{4}$ in. thick) subsequently formed a portion of the subreactor room ceiling.

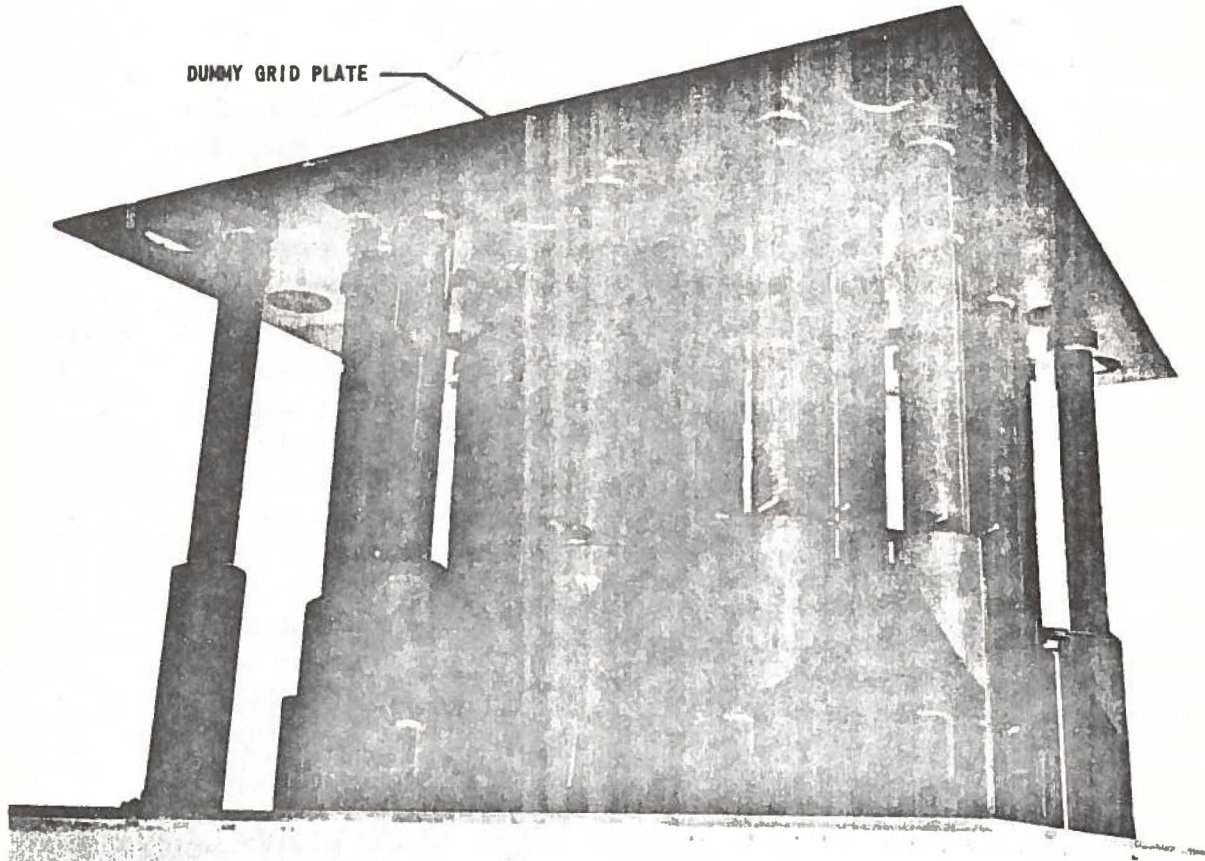


FIG. 13
CONTROL ROD GUIDE THIMBLE ASSEMBLY
PRIOR TO INSTALLATION IN CORE CAVITY.

In the actual installation, the assembly was braced up from the bottom with steel struts flush with the adjacent wood forming and leveled with a precision level by driving steel wedges under the supporting struts. The steel skirts which form the walls of the coolant plenum, and the coolant outlet ducts, were welded in place. The concrete was then poured. Figure 14 shows the control rod guide thimbles (dummy grid plate removed) protruding from the concrete surface of the lower coolant plenum.

In general, the results were satisfactory except that a number of tubes in the north half of the assembly were found to be misaligned as much as $\frac{3}{64}$ in. on installation of the actual grid plate. It was also noticed that the north side of the angle iron frame which forms the

support for the edge of the grid plate had been bowed about $\frac{1}{4}$ in. due to the cutting into and welding of the coolant ducts into the steel skirt. Since this necessarily distorted the dummy grid plate by the same amount, it is believed that this contributed to the misalignment of the thimbles. The condition was rectified by machining out some of the control rod guides to produce a correspondingly larger clearance between the guide and the control rod fuel element.

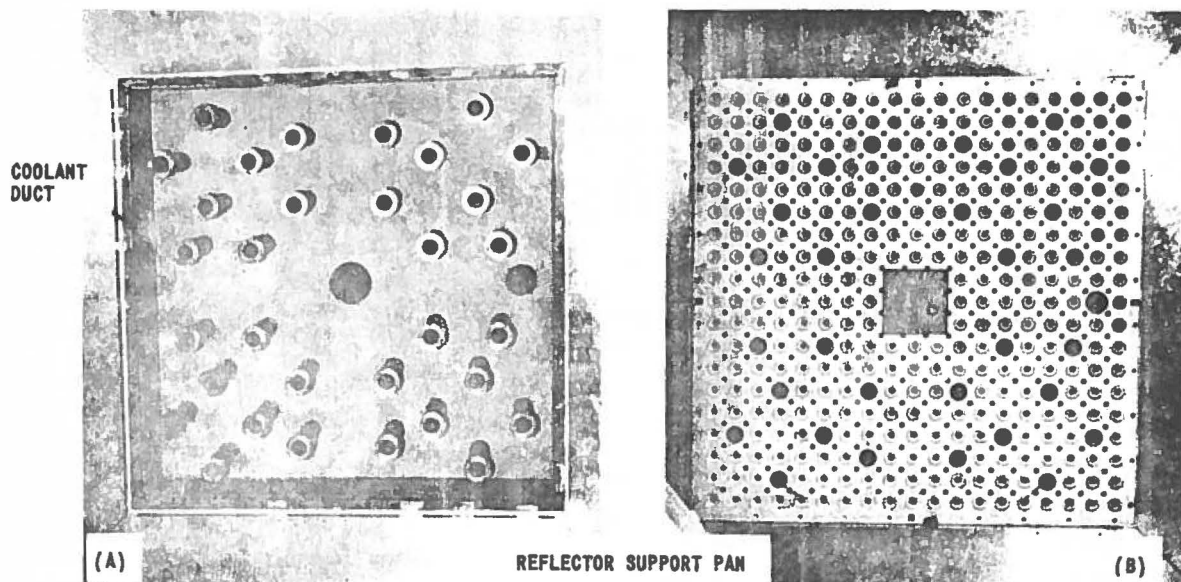


FIG. 14
 PLAN VIEWS OF (A) LOWER PLENUM CHAMBER IN CORE CAVITY
 AND (B) CORE GRID PLATE INSTALLED.

3. Control Rod Guide Tubes and Bearings

Each control rod thimble (Fig. 15) houses a mild steel guide tube, two graphitar bearings, and a shield plug. The guide tube ($2\frac{7}{8}$ in. OD x 4 ft long x $\frac{1}{2}$ in. wall thickness) is interlocked by an ear and slot arrangement with the guide tube in the control rod fuel assembly. The control rod fuel assemblies lock into the upper end of the guide tube by an ear and slot arrangement that necessitates rotating the control rod 90 degrees.

The ID of the thimble guide tube is machined to accommodate two graphitar bearings spaced 40 in. apart. A third graphitar bearing is located in the control rod fuel assembly approximately 80 in.

above the upper bearing in the thimble guide tube. The nominal ID of the bearings (1.775 ± 0.005 in.) provides a minimum diametral clearance of 0.020 in. between the rod and the bearings. The length of unsupported rod between the subreactor room ceiling and the rod drive knuckle when the oil dashpot starts to operate is $6\text{ ft } 3\frac{1}{3}\text{ in.}$

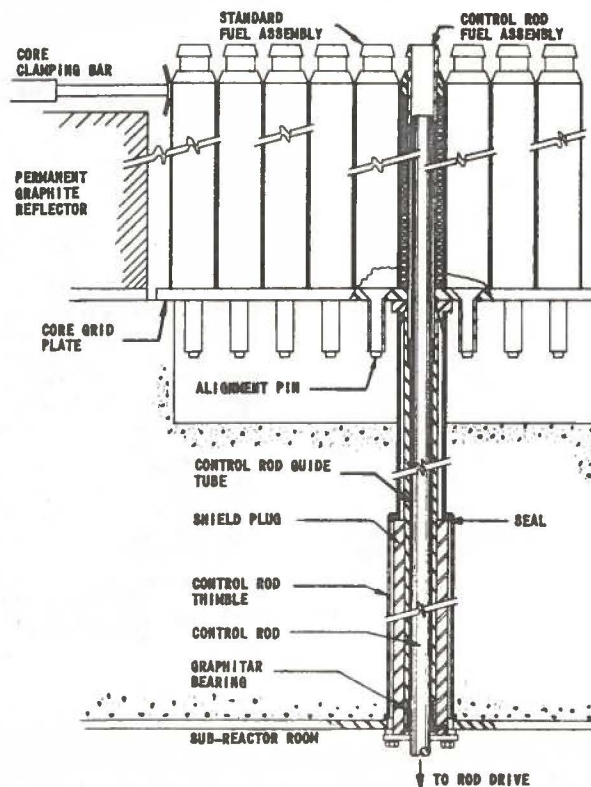


FIG. 15
CONTROL ROD THIMBLE AND GUIDE TUBE INSTALLATION.

The shield plug is a carbon steel tube, $4\frac{3}{4}$ in. OD, 19 in. long, with a 1-in. wall thickness. The shield plug and the guide tube can be removed into the subreactor room for inspection or replacement of the guide bearings.

4. Core Clamping Bars

The core assembly is aligned vertically by four horizontal clamping bars which apply pressure to the tops of the outermost row of assemblies on each side of the core. Each clamping bar (Fig. 16) is actuated by two push rods which operate through horizontal penetrations in the concrete shield. The push rods on the north and east sides of the core are flanged and bolted in position, while those on the south and west

sides are spring loaded with a total spring force of about 1000 lb per bar. The spring loading ensures a uniform clamping force and permits thermal expansion of the core and the push rods.

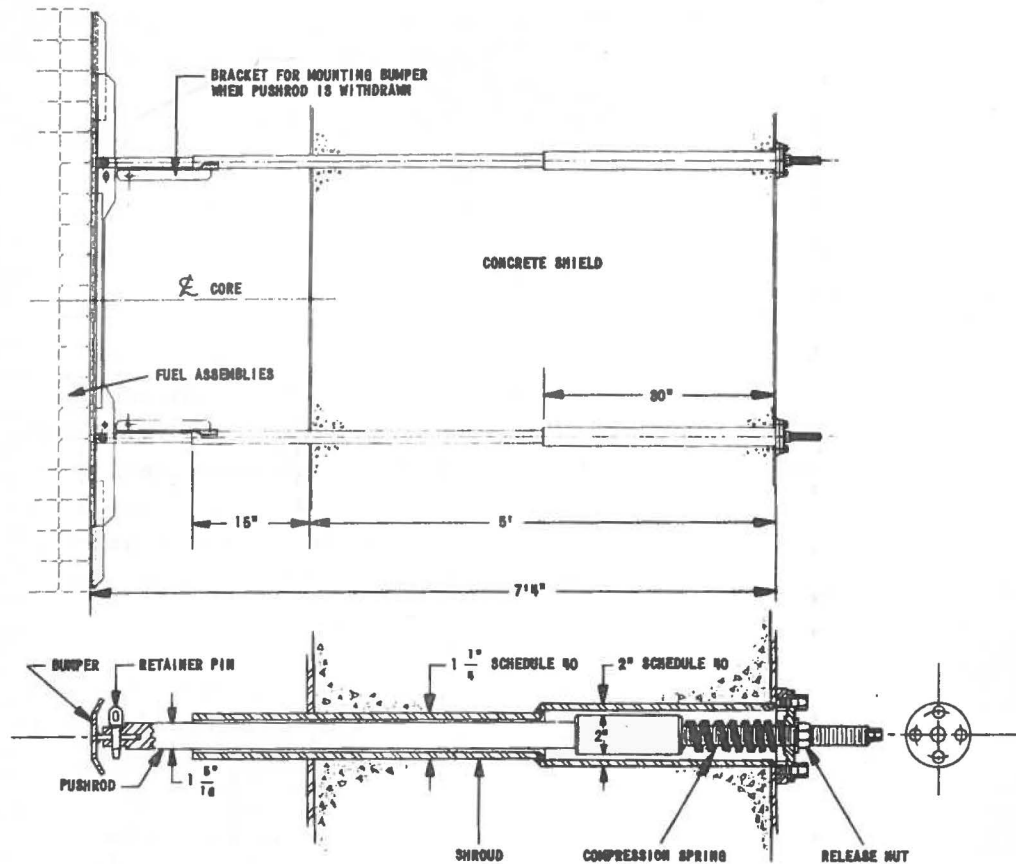


FIG. 16
CORE CLAMPING BARS INSTALLED IN FACES OF CONCRETE SHIELD.

Normally, the bars clamp a fully loaded core, 6 ft 4 in. square. However, by adding spacers of the proper length (at the outside face of the shield) the push rods can be repositioned to clamp a core as small as 5 ft square.

Preparatory to fuel-handling operations, the springs are compressed by tightening up retaining nuts on the push rods, thus withdrawing the clamping bar. The fixed bars are moved back by loosening bolts on the retaining flange which holds them in position.

To remove the push rods for maintenance, the rods are withdrawn until the bumpers engage holding brackets attached to the inside surface of the shielding. Holding pins which attach to bars to the

push rods are removed and used to position the bars in the clips. The detached push rod is then withdrawn through the shielding.

C. Permanent Reflector and Thermal Column

1. Permanent Reflector

The permanent reflector (see Fig. 1) is constructed of 4-in. square stringers of graphite stacked 7 ft 8 in. high and 2 ft thick along the four inside walls of the shield cavity. The graphite was used previously in the CP-2 reactor.

Large, movable blocks of graphite (~ 275 lb) are installed in regions which face viewing slots in the core. These blocks move vertically, and are supported in the "open" position by an aluminum lifting bracket mounted on the ledge of the concrete shield above the reflector. There is one movable block each in the south and west sides, which provides a slot $4\frac{1}{4} \times 24$ in. through the reflector. There are three movable blocks in the north side: the central block can be lifted to provide a slot 4×32 in., or all three blocks can be removed (through the shutdown shield plug) to provide an opening $14\frac{1}{4} \times 32$ in.

There are two horizontal holes (6 in. dia.) in each of the north, south, and west faces to accommodate installation of fast-response instruments close to the core.

There are 48 asbestos-glass-insulated, chromel-alumel thermocouples (20 gauge): six couples are located at each inside (core) face of the reflector (1 in. from the aluminum liner), and six couples are brazed to inside steel liner of the reactor shield (see Fig. 17). The thermocouple leads are brought out through the reactor air intake ducts and terminate at junction boards mounted on the face of the concrete shield.

The permanent reflector is supported by angle iron spacers and sheet metal framework which is anchored to the steel liner of the concrete shield cavity. This is best seen in the series of photos taken during assembly of the reflector. Type 1100 (2S) aluminum is used for the components as noted.

Figure 18 shows the inside of the shield with the aluminum support pans ($\frac{1}{8}$ in. thick) and the vertical angle iron spacers installed. The support pans rest on aluminum bars ($\frac{7}{8}$ in. thick) which are shimmed up from the concrete to level the pans. The angle irons are pinned to clips which, in turn, are welded to the steel liner. The holes in the clips are elongated to compensate for irregularities in the shield. Steel liner sheets ($\frac{1}{16}$ in. thick) are tack welded to the angle irons to provide vertical support for the graphite blocks. The gap formed by the angle iron spacers and the aluminum bars beneath the support pans provides a passage for coolant flow between the reflector and the concrete shield.

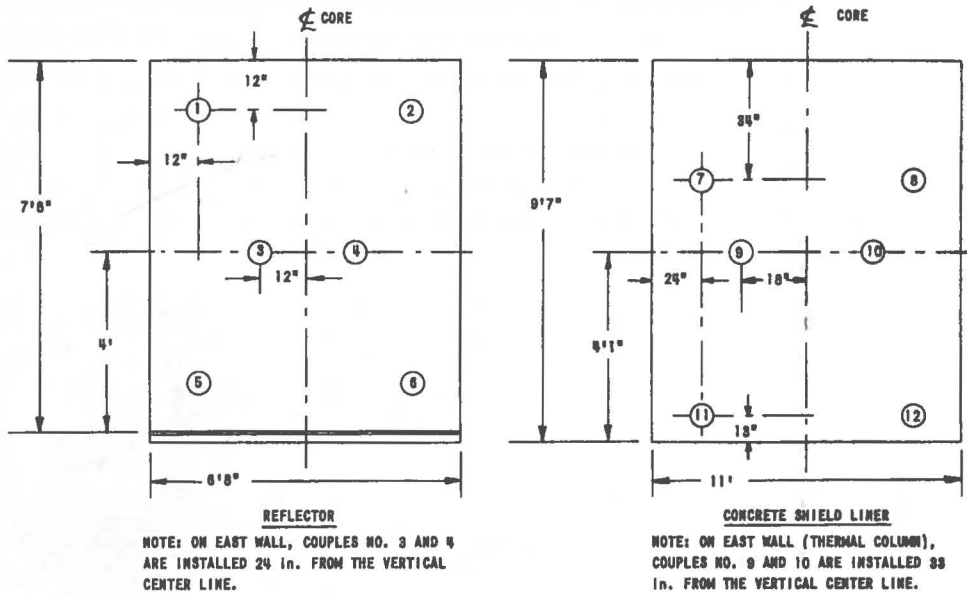


FIG. 17
 TYPICAL THERMOCOUPLE INSTALLATION ON INSIDE WALLS OF PERMANENT GRAPHITE REFLECTOR AND CONCRETE SHIELD LINER. NORTH WALLS SHOWN.

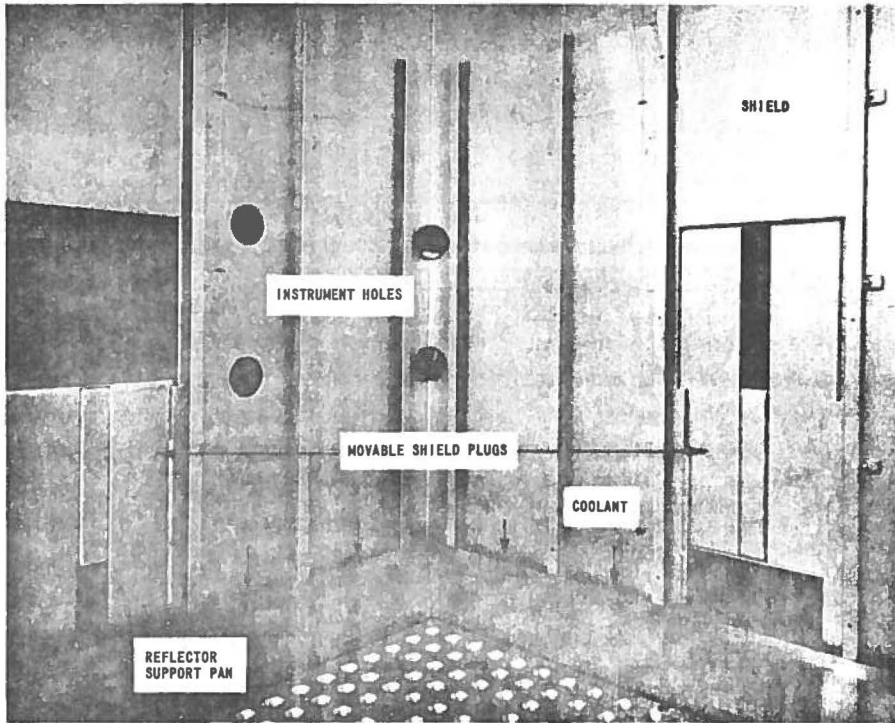


FIG. 18
 REACTOR SHIELD CAVITY WITH GRAPHITE REFLECTOR SUPPORT PANS, VERTICAL ANGLE IRON SPACERS, AND MOVABLE SHIELD ACCESS HOLE BLOCKS INSTALLED.

Figure 19 shows the graphite reflector with one of the inner aluminum retaining sheets ($\frac{1}{8}$ in. thick) and one aluminum cover sheet ($\frac{1}{16}$ in. thick) installed. The retaining sheets are held in place by aluminum tie bolts which extend through the graphite stringers and are fastened to the vertical angle iron spacers. The retaining sheets are drilled and the graphite stringers are recessed to accommodate cupped washers for the holddown nuts. The top cover sheets are attached with sheet metal screws.

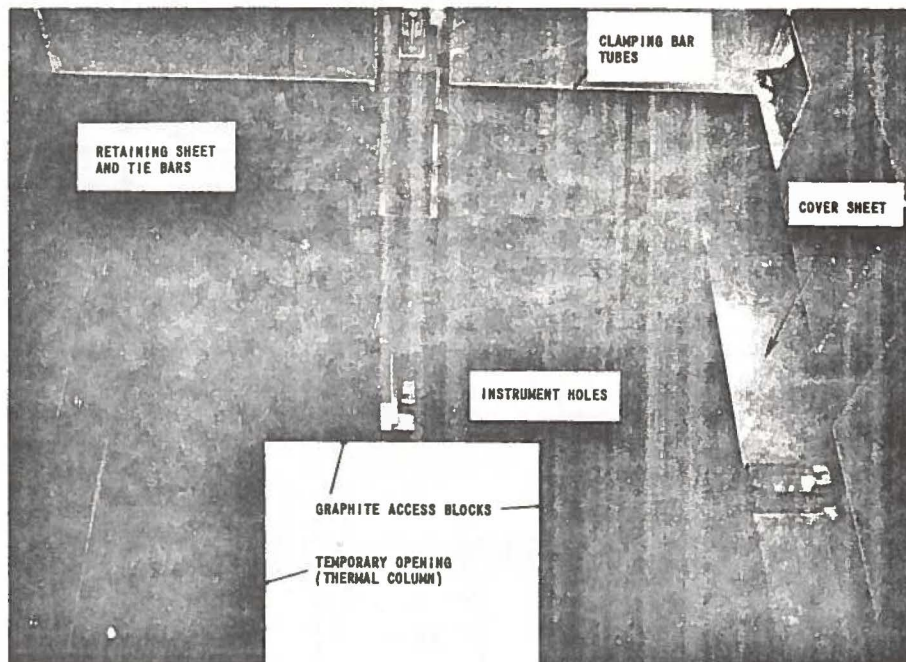


FIG. 19
PERMANENT GRAPHITE REFLECTOR PREPARATORY TO INSTALLATION OF RETAINING SHEETS AND COVER SHEETS.

Also visible in Fig. 19 are two of the movable graphite blocks installed in their respective aluminum sheet ($\frac{1}{16}$ in. thick) guides, and two horizontal instrument holes. The holes are formed by machining a quarter circle from four stringers, and are supported by aluminum tubes (6 in. dia., $\frac{1}{8}$ in. wall) which extend into the concrete shield.

Figure 20 is a plan view of the completed reflector and the core partially loaded with dummy fuel assemblies.

2. Thermal Column

The thermal column is essentially an extension of an area of the east face of the permanent reflector into the concrete shield. It is constructed of 4-in. square stringers of CP-2 graphite stacked 5 ft square in cross section, stepping out to 5 ft 8 in. square halfway through the

concrete shield. The central 9 stringers (12 in. square) are machined to a nominal 3.99-in. square cross section to facilitate ease of removal. Other openings include three vertical access holes ($2\frac{1}{2}$ in. dia.) which extend from the top of the concrete shield and terminate 10 in. above the horizontal center line of the thermal column.

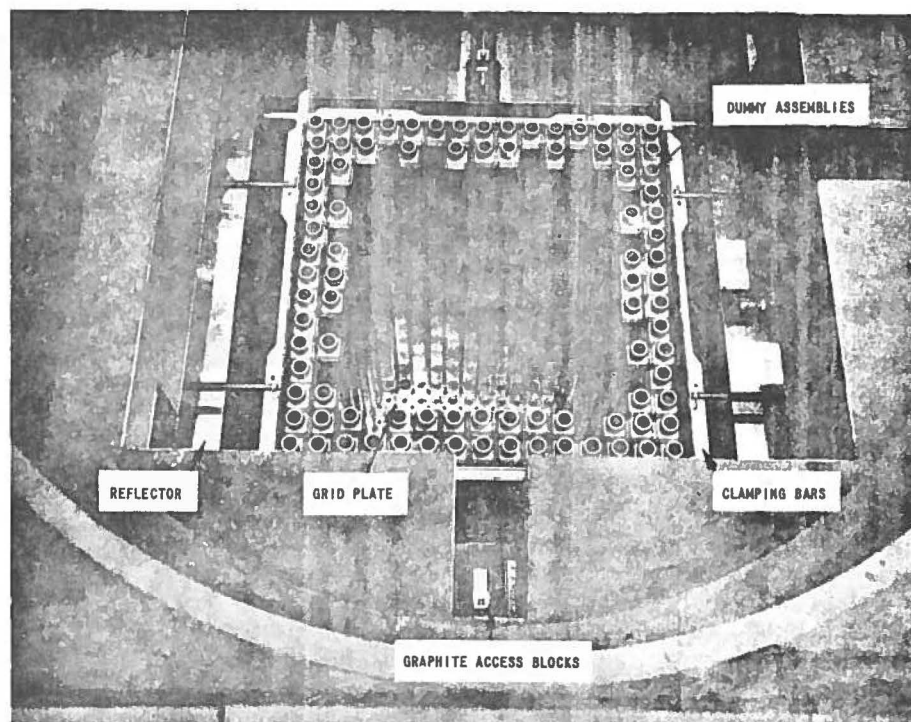


FIG. 20
COMPLETED REFLECTOR AND PARTIALLY LOADED CORE ASSEMBLY

The outer face of the thermal column is shielded by a magnetite concrete door (33 in. thick); the inner surface of the door is clad with boral sheet ($\frac{1}{4}$ in. thick). Figure 21 shows the outer face of the thermal column with the shielding door moved aside.

D. Control Rods

1. Design and Development

For reasons of simplicity of operation and maximum reliability with a minimum requirement of engineering development work, a more or less conventional control system consisting of poison rods driven by a mechanical actuator or control rod drive was established as the reference system early in the reactor design stage. The physical size of the core and, hence, required stroke of travel for complete poison

removal or insertion, dictated a long slender control rod. The problem then resolved into one of designing a suitable rod and a control rod drive capable of moving the rods very rapidly (4 ft in \sim 80 msec) and then decelerating them to a complete stop in a short distance (6 in.) without excessively loading and hence bending them.

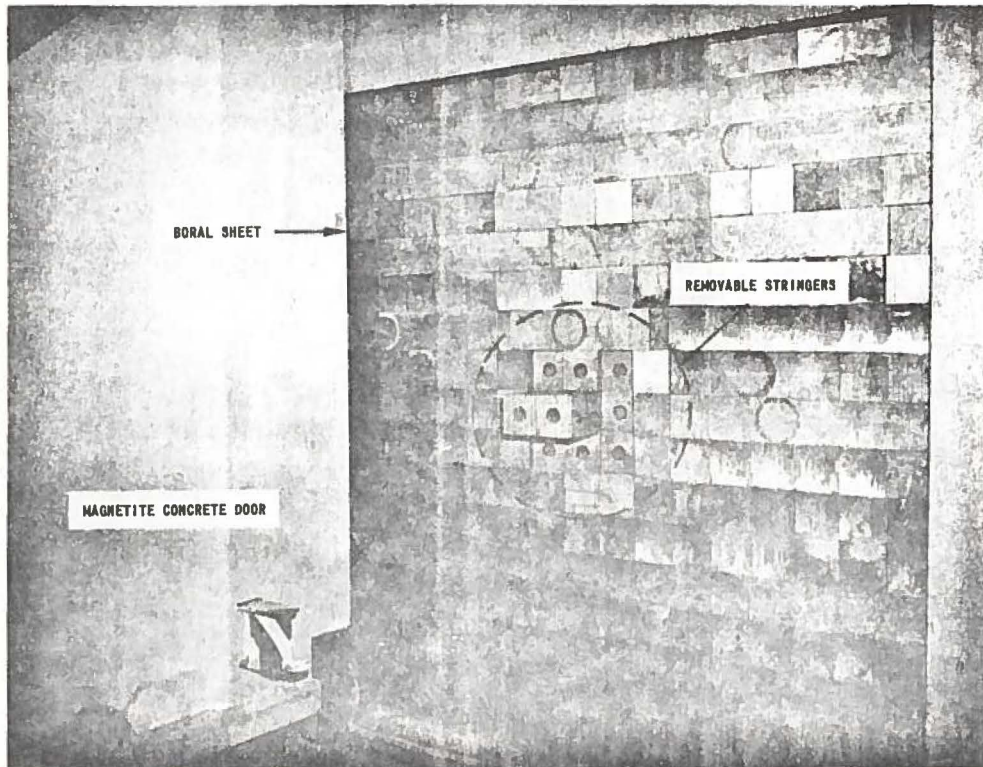


FIG. 21
THERMAL COLUMN AND SHIELDING DOOR IN EAST FACE OF CONCRETE SHIELD.

A study of the buckling tendency of slender columns and the rod drive pneumatic pressures required to accelerate a given mass indicated that a tubular control rod with a $1\frac{3}{4}$ in. OD in a $\frac{1}{8}$ in. wall thickness would be sufficiently rigid and yet not excessively heavy so as to require extreme rod drive pressures (see Appendix C). Accordingly, initial efforts were directed toward procurement of 2% boron-Type 304 stainless steel tubes of the above diameter and wall thickness, as this appeared to be the simplest approach. However, existing methods proved inadequate to the task of fabricating 2% boron-stainless steel tubes with satisfactory dimensional tolerance (straightness and roundness). Consequently, the alternate scheme of packing boron carbide into steel tubes was adopted. This scheme offers an additional advantage in that the worth of rods may be varied, if desired, by diluting the boron carbide powder.

The complete control rod assembly shown in Fig. 22 consists of a poison section, a Zircaloy follower, a two-piece steel follower, and a handling attachment. The length of the poison section (5 ft) is equal to the stroke of the control rod drive. In the fully inserted position, the poison section overlaps the top and bottom of the core by giving the following reactivity-distance relationship:

- a. Release rod: Start of travel.
- b. First 6 in.: Acceleration (negligible change in reactivity); lower end of rod flush with top of core at end of this increment.
- c. Second 4 ft: Rod moving into core (reactivity changing). Rod flush with bottom of core upon completion of this travel increment.
- d. Last 6 in.: Dashpot deceleration (negligible change in reactivity).

In order to accomplish the reactivity insertions and removals with a control rod drive firing in one direction, the poison and Zircaloy follower sections are merely interchanged. Figure 22 shows the normal shutdown control rod with the poison section at the upper end. Conversion to a transient rod is accomplished by interchanging the poison section and the Zircaloy follower. The handling attachment is then replaced at the top end of the rod on the Zircaloy follower to complete the conversion.

2. Components

a. Poison Section

The poison section is a cold-drawn carbon steel seamless tube (1.750 in. OD x 5 ft long x $\frac{1}{8}$ in. wall) packed with boron carbide powder compacted to a minimum density of 1.6 gm/cc. Male and female threaded end plugs and alignment stubs are welded at opposite ends of the tube for interconnection with other components of the rod assembly. Other fittings include a small fillister head-locking bolt at each threaded joint, and small holes to accommodate spanner wrenches during assembly and disassembly.

All welds were leak tested to ensure against leakage of radioactive products during reactor operations. X-ray films taken before and after a large number of scram cycles revealed no compacting of the boron carbide powder. Nuclear burnup of the powder and consequent release of helium gas does not pose a problem, since the integrated doses received by the rods are very low.

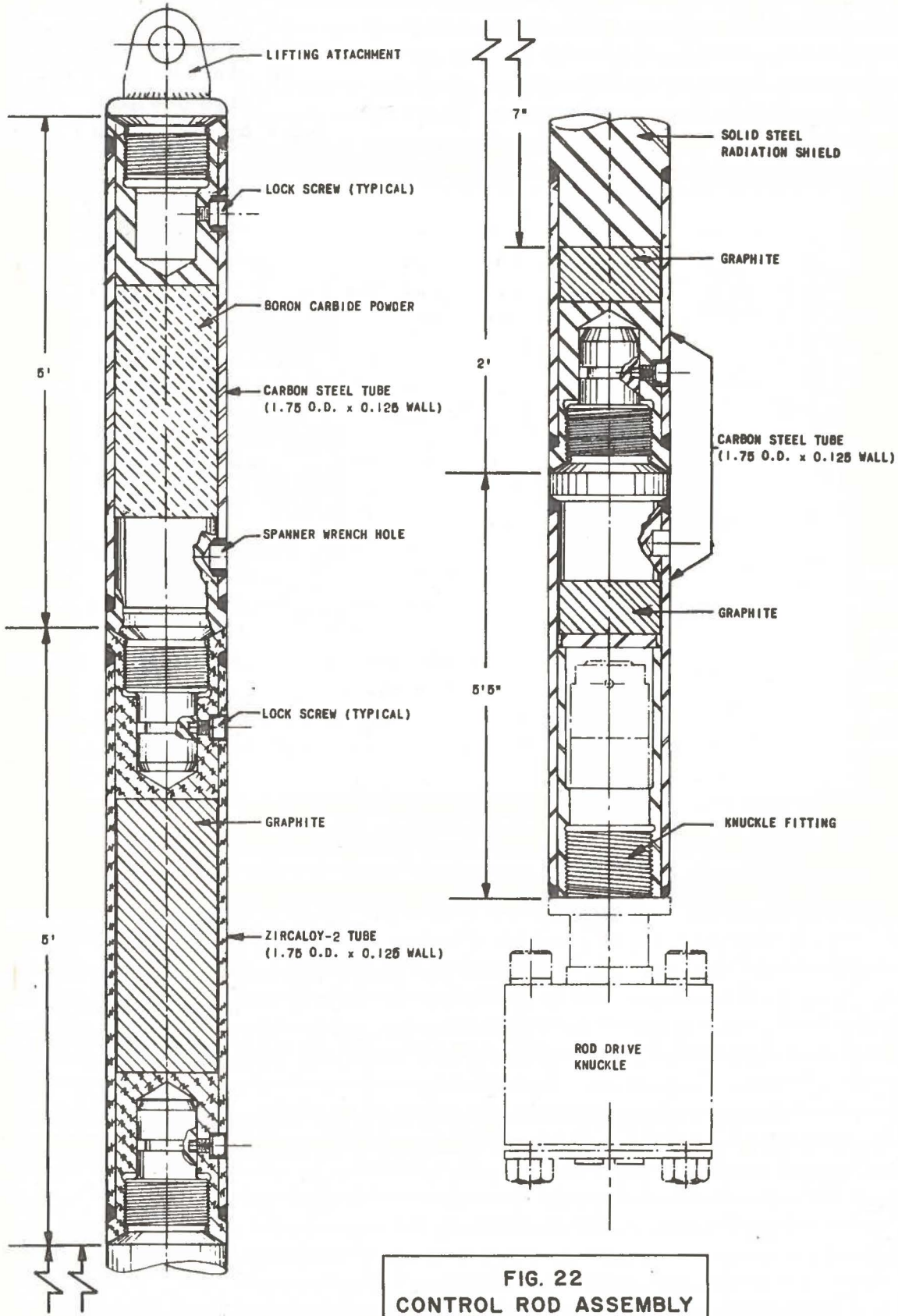


FIG. 22
CONTROL ROD ASSEMBLY

The completed poison section is Kannigen nickel plated (2 mils thick) for protection against corrosion by air at elevated temperatures in the reactor.

b. Zircaloy-2 Follower

The Zircaloy-2 follower section is a tube (1.750 in. OD x 5 ft long x $\frac{1}{8}$ in. wall) filled with graphite rods. Threaded end plugs with drilled holes for the alignment stubs are welded at each end of the section in close contact with the graphite filler rods. Both end plugs have female threads which tighten on heating, due to the lower coefficient of thermal expansion of the Zircaloy tube relative to the steel poison tube and steel follower section which it interconnects.

c. Steel Follower

In the preliminary design, fully annealed Type 304 stainless steel tubing was selected for the steel followers. However, subsequent performance tests revealed a permanent set of $\frac{1}{4}$ in. at the lower 3-ft length after 200 firings on the prototype control rod drive. Carbon steel tubing was substituted and produced a follower with physical and mechanical properties sufficient to withstand the deceleration impact load.

The steel follower is a carbon steel seamless tube (1.750 in. OD x 7 ft-5 in. long x $\frac{1}{8}$ in. wall) comprised of two sections. The upper section (2 ft long) features an extra long threaded male fitting which provides about 10 in. of steel shielding in the control rod thimble when the rod drive is in the "shutdown" position. The balance of the upper fitting is filled with graphite and sealed with a female threaded end plug which interconnects with the lower steel follower section. The latter section (5 ft 5 in. long) is filled with graphite, and the end plug is threaded to receive the control rod drive knuckle fitting. Both sections are Kannigen nickel plated (2 mils thick) for protection against atmospheric corrosion.

For purposes of inspection and/or replacement, the radioactive control rod is withdrawn in two sections. The lower section of the steel follower is detached and withdrawn into the subreactor room. The upper portion of the rod is withdrawn above the reactor and stored temporarily in one of the sodium-loop holes in the concrete shield.

At this writing, some difficulty has been experienced with the Kannigen nickel plating on the steel follower sections. Longitudinal score marks have been observed on certain sections after a considerable number of scrams. The scorings which have resulted in gouging of the lower graphitar bearing are attributed to poor mechanical wear properties of the Kannigen plating. Additional steel followers and poison sections (in fabrication) will be chrome plated in an effort to remedy the situation.

E. Control Rod Drives

The four control rod drives in TREAT are the product of an early design and development program. They were installed as a temporary measure to permit preliminary reactor operations while a final design could be evolved and tested. (Note: At this writing, the final design is undergoing prototype fabrication and tests, with installation in TREAT scheduled for early 1960.)

The design of the control rod drives conforms with the following basic specifications:

- (1) Normal regulation with continuous fine position indication and a regulating speed of 6 in./min.
- (2) Scram from any position. Scramming speed to range from free fall to approximately 80 msec for central 4 ft of the total 5-ft stroke.
- (3) Remote actuation and positioning against full scram air pressure.
- (4) Fail-safe operation, i.e., reactivity removal on loss of power.
- (5) Two control rods per drive (weight, 130 lb).
- (6) Essentially complete exchangeability. The same basic control rod drive unit is to be used for actuation and for shutdown of a transient.

Item (6) is made possible by interchange of control rod components as described earlier.

Other governing factors included space limitations, i.e., 13- $\frac{1}{2}$ ft height of subreactor room, and a maximum cross-sectional area dictated by the control rod scheme (see Fig. 11).

1. Mechanical Description

The basic fast scram control rod drive (Fig. 23) is a pneumatic-accelerated device with an integral air-hydraulic dashpot, and a motor-driven lead screw mechanism for recocking and intermediate positioning.

a. Pneumatic Actuator

The pneumatic actuator comprises three cylinders fabricated from mild steel. The inner stationary piston (2.875 in. ID, 3.625 in. OD) is the compressed gas accumulator. The gas is supplied

through an air-line fitting at the top of the drive assembly. The outer surface of the piston is grooved for piston rings which provide a dynamic seal against the middle moving cylinder.

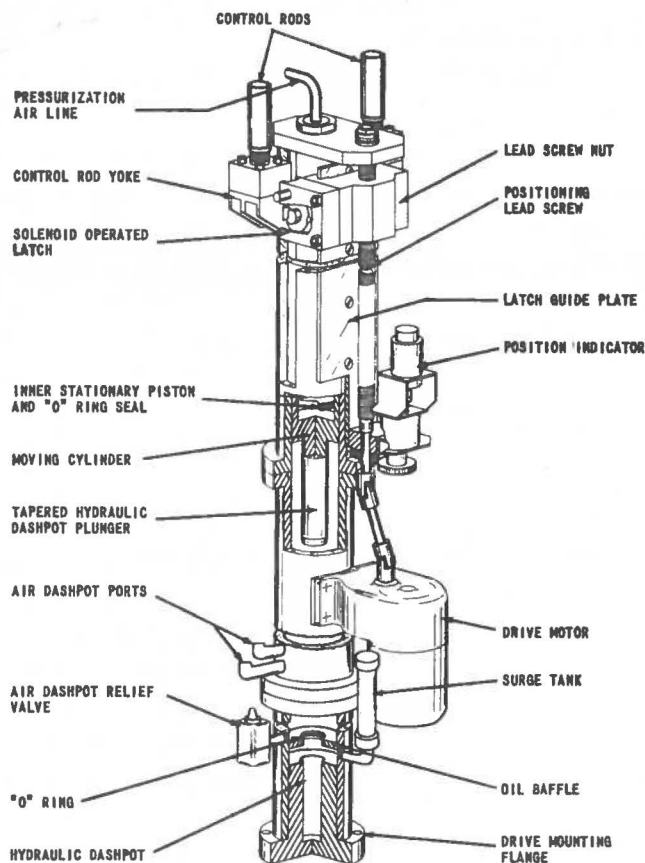


FIG. 23
CONTROL ROD DRIVE

The middle moving cylinder (3.624 in. ID, 4.505 in. OD) features an integral yoke with two knuckle joints which interconnect with two control rods at the upper end. A 2 in. OD x 6 in. long plunger is attached to the lower end.

The outer stationary cylinder (4.515 in. ID, 6 in. OD) consists of three flange-connected sections. The upper section is slotted to permit travel of the control rod yoke. The center section is the guide tube for the moving cylinder. The lower section contains the air-hydraulic dashpot.

Initial operations revealed severe galling between the middle and outer cylinders. The problem was resolved satisfactorily in the following manner.

- (1) The three sections were tack welded together and the inside diameter was machined and honed as a unit assembly.
- (2) Bronze wear rings were shrunk fit at the top and bottom of the moving cylinder.
- (3) A leather wiper ring was grooved into the wall of the outer cylinder immediately below the slots in the upper section to prevent entrance of foreign material into the annulus between the two cylinders.

b. Dashpot

The dashpot dissipates the kinetic energy of the moving cylinder and the two control rods, a total mass of about 270 lb, or approximately 20,000 ft-lb based on the acceleration required to attain the design scram time. The tendency of the slender control rods to buckle under dynamic load makes it essential that deceleration be accomplished without impact effects. Calculations pertinent to the strength of the control rods, and the design of the dashpot are described in Appendix C.

The design evolved consists of an air chamber (12 in. long), an oil baffle with an "O" ring seal and a tapered dashpot (6 in. long) filled with a heavy hydraulic oil (Sinclair Duro 900).

Deceleration of the moving cylinder is effected in the following manner. As the plunger enters the air chamber, the air is displaced and exhausted to the atmosphere through four ports in the chamber above the oil baffle. The air confined beneath the moving cylinder exerts a continuously increasing resistance to the cylinder. In order to prevent an abrupt stop and bounceback of the moving cylinder, the confined air is released to the atmosphere through a relief valve set at 450 psi.

The effectiveness of the air chamber was demonstrated by the bounceback of the moving cylinder produced by a diesel effect (bluish exhaust through the air ports) produced between the air and the hydraulic fluid displaced by the plunger upon entry into the tapered dashpot. Consequently a surge tank (3 in. dia. capped pipe, 22 in. long) was added to reduce the compression ratio and, to a certain extent, the effectiveness of the air chamber.

The capacity of the dashpot depends upon the kinetic energy of the moving components and upon the time allowed to dissipate this energy. By neglecting the last portion of the deceleration process and assuming a cutoff point one-hundredth of the maximum velocity, the deceleration time is about 10 msec. The dashpot therefore develops about 2×10^6 ft-lb/sec, or $\sim 4,000$ hp. The temperature rise in the dashpot is negligible (3-4°F).

The hydraulic dashpot is screwed into the bottom of the outer cylinder. The lower portion of the dashpot forms a floor flange for mounting the control rod drive on a $7\frac{1}{8}$ -in. diameter bolt circle.

c. Positioning Mechanism

For controlled reactivity addition or removal, motion is imparted to the moving cylinder (and control rods) by an Acme lead screw (5 threads/inch) which is driven at 30 rpm by a Master Electric Co. $\frac{1}{3}$ -hp electric gear motor. This gives a control rod travel speed of 6 in./min.

Linkage between the drive motor and lead screw consists of a jointed shaft made up with two Boston Gear J-150-B Universal Joints. Linkage between the lead screw and the moving cylinder consists of a mechanical latch bolted to the travelling nut on the lead screw. The latch engages a projection on the control rod yoke which is welded to the moving cylinder.

During the positioning operation, the air pressure in the moving cylinder exerts a downward force of 2,000 lb (for 200 psi pressure on the drive; piston area = 10 sq. in.), producing an overturning moment on the latch. This force is counteracted by two key blocks which are held by the lead screw nut into V-grooves in a latch guide plate. The guide plate (3.9 in. wide) is bolted to a flattened portion of the outer cylinder. The two key blocks are 6 in. long and have a bearing width of 1.06 in. on the two faces of the V-grooves. One of the blocks is tapered longitudinally to permit adjustment of clearance between the blocks and the V-grooves.

The key blocks and guide plates were originally fabricated from Meehanite and mild steel, respectively. However, initial operations revealed gouging of the V-grooves and scoring of the key blocks. Subsequent experimentation led to the selection of tool steel for the guide plate and aluminum-bronze for the key blocks.

The lubricant used is Sinclair Pennant Grease No. 1
E.P.

d. Latch

The solenoid-operated latch (Fig. 24) is engaged with the control rod yoke for fine positioning of the rods, and disengaged to effect rapid insertion of the rods (fully inserted position). Assuming the rods have just been released, re-engagement is accomplished in the following manner.

The lead screw is rotated to lower the latch which is bolted to the lead screw nut. As the latch engages with the projection on the control rod yoke, the latch anchor is rotated to its closed position (release pin in groove), as shown in Fig. 24. The release pin clip is connected to a spring-loaded follower which actuates a microswitch as soon as the release pin enters the groove in the anchor. The microswitch energizes a solenoid which holds the clip in the closed position by rotating the lock pin against the delatching spring. The load (control rod yoke) is lifted by the anchor to the desired rod position.

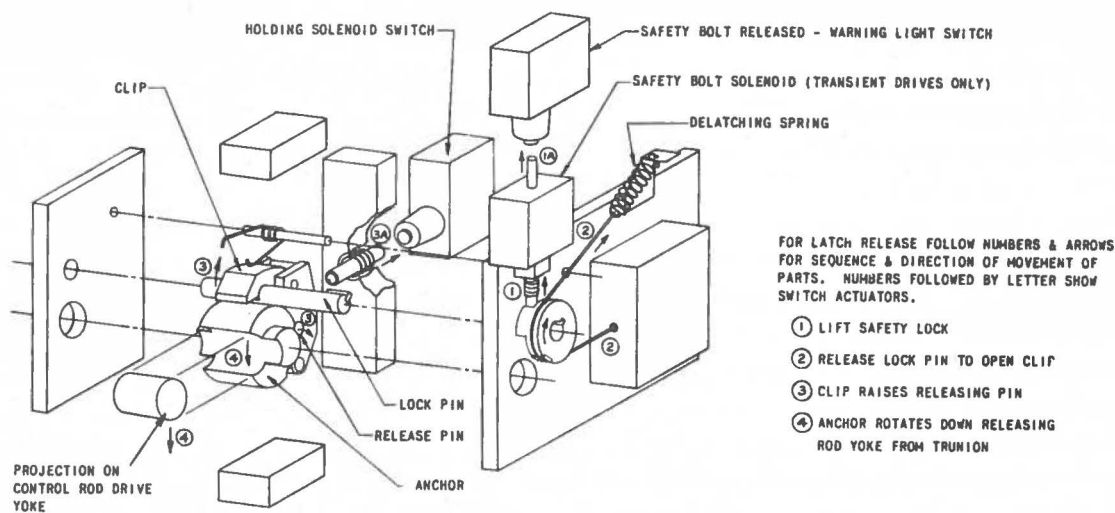


FIG. 24
EXPLODED VIEW OF CONTROL ROD DRIVE LATCH IN LOCKED POSITION
HOLDING PROJECTION ON CONTROL ROD DRIVE YOKE.

The control rod yoke is delatched by de-energizing the holding solenoid. This action releases the delatching spring which, in turn, allows the lock pin to rotate counterclockwise to set the clip free. The loaded anchor rotates down to release the moving cylinder.

When a drive is used in conjunction with rods to initiate a transient, the release pin is locked in the "closed" position by a solenoid-operated safety bolt. This bolt prevents the release of the rod and, hence, unwanted reactivity addition in the event of a power failure. Just prior to start of a transient, the bolt is released by energizing its solenoid. The safety bolt is removed on shutdown drives so that it cannot be inadvertently in place.

e. Knuckle Joints

The control rods are connected to the moving cylinder through self-aligning knuckle joints. Each knuckle joint houses a monoball bearing which allows about $\frac{1}{8}$ -in. lateral movement. Axial shocks are absorbed by Belleville springs. These springs are tightened down almost completely to ensure reproducibility of control rod positioning. The knuckle joints are bolted to the control rod yoke (a double cantilever structure), which, in turn, is welded to the moving cylinder. Since there are two possible spacings of the two control rods, depending upon the location of the drives, the yoke has two sets of bolt holes.

f. Drive Position Indicators

Control rod drives No. 1 and No. 2 are used for fine reactivity control. Accordingly these drives have selsyn position indicators. The remaining drives are equipped with potentiometer position indicators.

All position indicators are attached with a universal bracket to the side of the drive. They are driven by a gear at the lower end of the latch drive lead screw.

2. Control Rod Drive Pressurization Systems

The driving force for the fast scramming action of the shutdown drives and the transient drives is supplied by the respective nitrogen pressurization systems shown schematically in Fig. 25 (A) and (B).

a. Shutdown Drive System

With reference to Fig. 25 (A), gas is admitted to the system by opening valve (A), and the nitrogen regulator is set at the desired pressure. Valve (B) is a bleed-off valve for releasing the gas pressure on the shutdown drives. Low gas pressure warning and scram signals are given by two mercoid switches (C) and (D), respectively. Excess gas pressure is discharged through relief valve (F). The accumulator, consisting of four nitrogen bottles manifolded together, increases the total system gas volume so that momentary pressure loss (when one drive is scrammed) will not initiate a low gas pressure scram of the other drives. Valve (H) isolates the accumulator from the rest of the system. Gages (E) and (G) indicate system pressure; one is on the main floor and one in the subreactor room. Final connection to the drives is made with flexible hoses and Aeroquip quick-disconnect fittings.

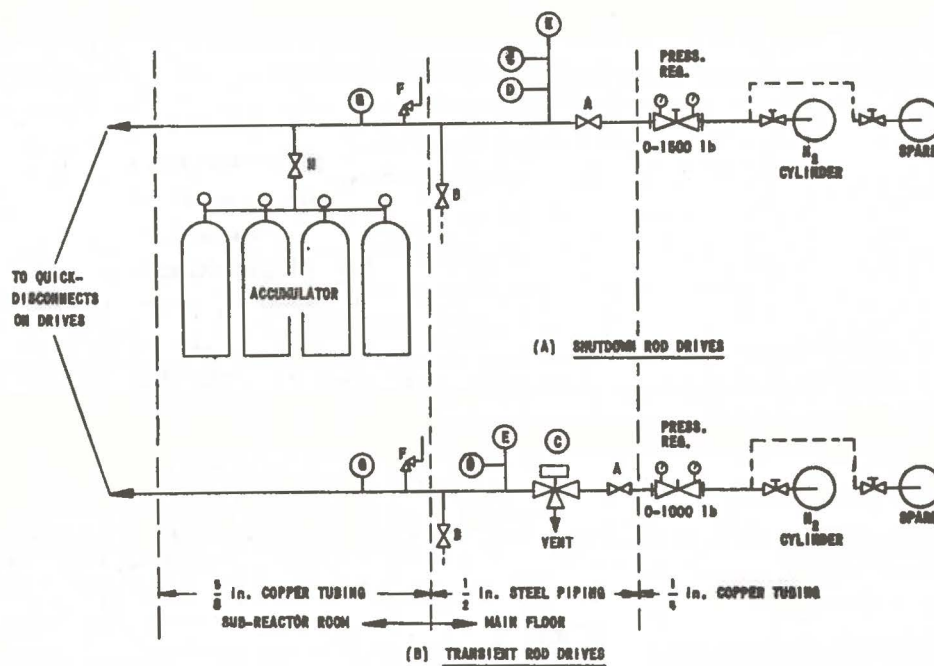


FIG. 25
CONTROL ROD DRIVE PRESSURIZATION SYSTEMS

b. Transient Drive System

The transient drive system [see Fig. 25 (B)] differs from the shutdown drive system in that a three-way solenoid valve (C) is installed to permit remote-controlled pressurization and depressurization of the drives at the start and termination of the transients. The mercoid switch (D) transmits a low system gas pressure signal.

The use of nitrogen gas bottles is a temporary measure, satisfactory for initial reactor operations with only four control drives. Subsequently an air compressor will be installed to service the large-capacity gas pressure system required for the full complement of rod drives. However, the installation of the compressor will not reflect any major changes in the operation of the two systems as outlined above.

3. Installation of Control Rod Drives

The control rod drives are bolted to steel plate (6 ft square x $1\frac{1}{2}$ in. thick) embedded in the concrete floor ($6\frac{1}{2}$ ft thick) of the subreactor room.

Figure 26 is a view of the subreactor room with the four rod drives installed. The drives are serviced by a $\frac{1}{2}$ -ton chain hoist on a monorail mounted on the ceiling. When future maintenance or modifications

dictate their removal, the drives can be lifted with the monorail hoist, transferred to a dolly and wheeled into the sodium-equipment room. Subsequent transfer to the main floor is accomplished with the building overhead crane through the access hatch in the ceiling of the sodium-equipment room.

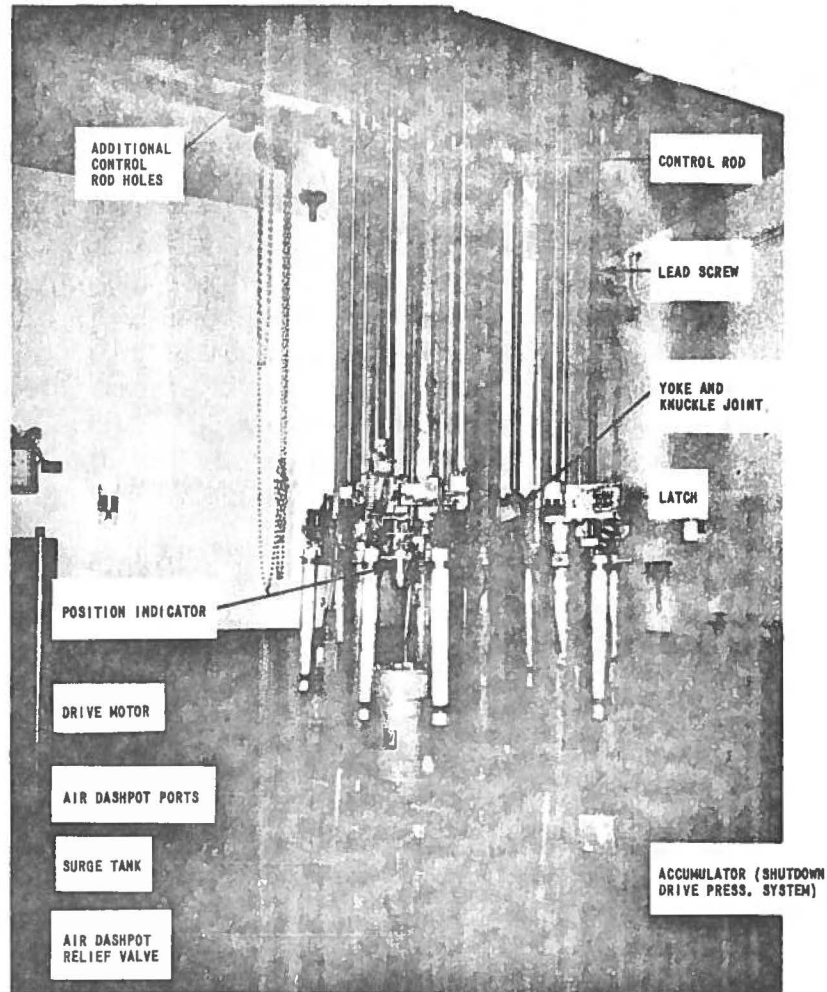


FIG. 26
CONTROL ROD DRIVE INSTALLATION IN SUB-REACTOR ROOM

F. Shielding

1. Permanent Shield (Fig. 27)

The reactor is shielded radially with heavy magnetite and/or hematite concrete (density: 220 lb/ft³), 15 ft high and 5 ft thick. The inside surface of the concrete is faced with permanent forms of steel plate ($\frac{1}{4}$ in. thick) installed prior to pouring of the bulk concrete. On the outside surface, the steel plate extends up to the 8-ft level.

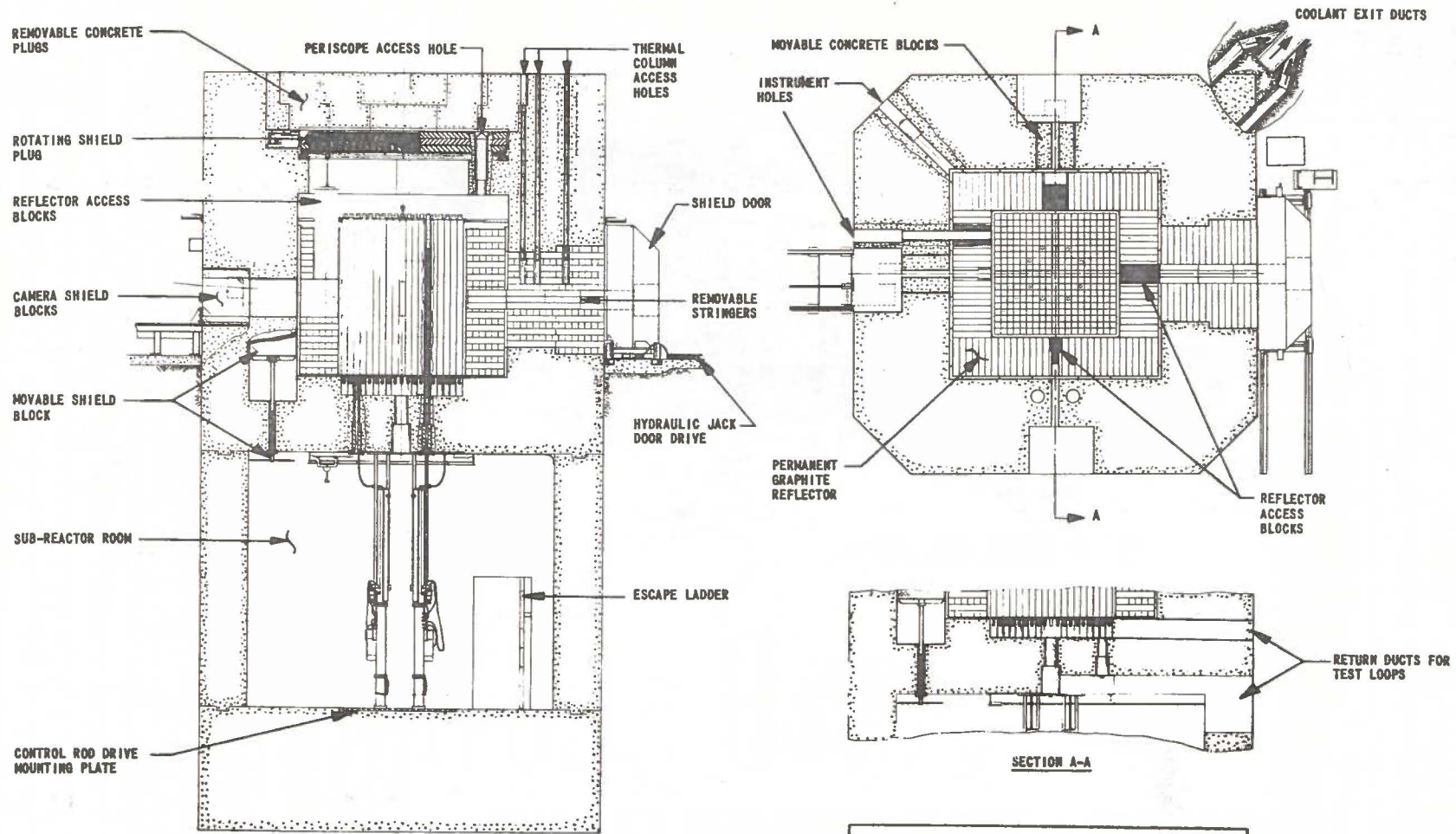


FIG. 27
CROSS-SECTIONAL VIEWS OF REACTOR SHIELDING

The concrete shielding below the reactor is 3 ft thick, faced at the bottom with the steel plate ($\frac{3}{4}$ in. thick) used to pre-assemble the control rod thimbles. The bottom steel plate forms a portion of the sub-reactor room ceiling.

Moving axially upward from the top of the core, the shielding consists of the boral and steel plate rotating plug (1 ft thick), the checker steel floor plate ($\frac{1}{4}$ in. thick) and the heavy concrete blocks (3 ft thick).

The permanent shield is designed to permit personnel access around the sides and on top of the reactor during steady-state operation at 100 kw. The calculated dose rate at the shield exterior is well below 7.5 mr/hr.

The steel shutdown control rod followers, which are in regions of high neutron flux during transients and are then withdrawn into the subreactor room, create a radiation hazard in the room immediately after shutdown. The activity is due almost entirely to 2.5-hr Mn^{56} . Therefore, following transients and short-duration, steady-state power runs, the activity level decays to a negligible value in 24 hr.

The steel and boral rotating shield and the fuel-transfer coffin permit personnel to conduct fuel-exchange operations as early as two hours after a 1000-Mw-sec transient or after 100 hr of operation at 100 kw. The dose rates are less than 7.5 mr/hr at the surface of the fuel coffin (containing a central fuel assembly) and the rotating shield plug.

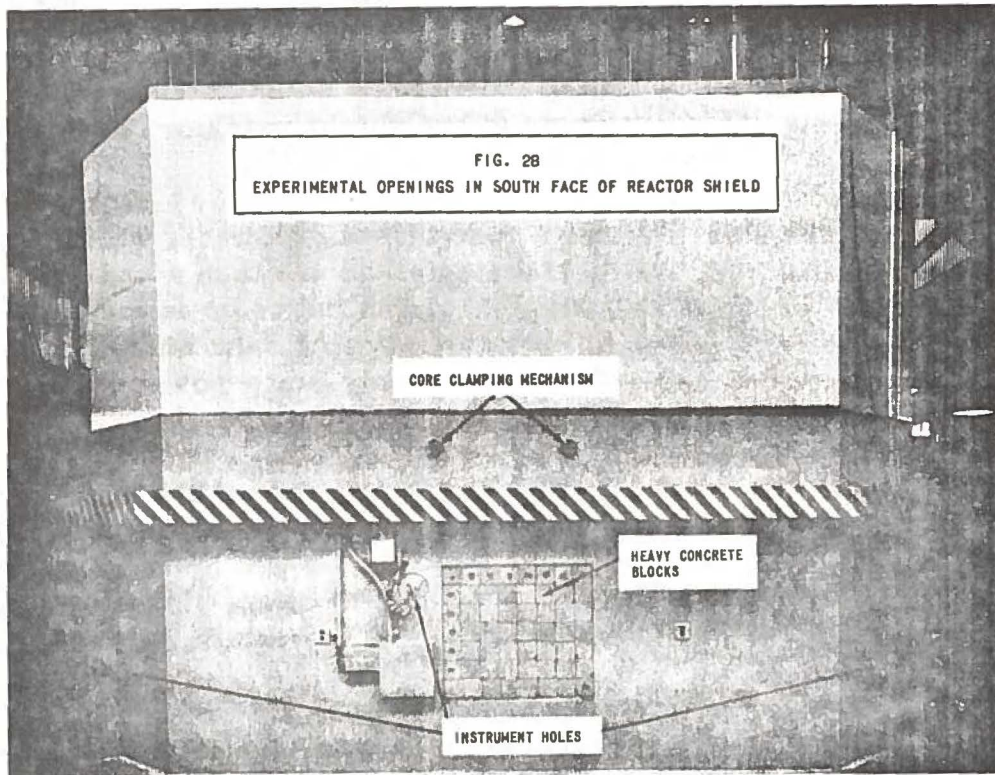
The bulk shielding provides adequate protection for experimental equipment since the integral dose from a 1000-Mw-sec transient is only equal to 2.8 hr exposure at 100 kw steady-state operation.

The calculation methods and constants used for the shielding design are summarized in Appendix D.

2. Experimental Access Openings

Three horizontal access slots converge on the core center. The methods of extending these slots through the permanent reflector and the core have been described earlier. Two of the three openings in the concrete shield are convertible. With the aid of a screw-jack, individual concrete blocks can be moved to provide either a small offset opening (4 in. wide x 24 in. high) for high-speed cameras external to the shield, or a larger opening (2 ft square, stepping out to 3 ft square) for bulky equipment that must be positioned close to the core. Apparatus falling in the latter category would be the gamma pin-hole camera for "photographing" fuel-pin

meltdown experiments contained in opaque capsules. The third opening in the concrete shield provides an offset access slot 4 in. wide by 24 in. high. In all three holes an offset opening can be effected by rolling the camera shield block into the reactor shield by means of a supporting frame which butts against the side of the shield. During startup operations the opening in the shield is filled with high-density concrete blocks, 4 in. square by 15 in. long (Fig. 28).



The thermal column (5 ft square) in the east face of the radial shield is shielded by a magnetite concrete door 33 in. thick. The inside surface is covered with a layer of boral $\frac{1}{4}$ in. thick. The door moves parallel to the reactor face on four wheels and two guide rails embedded in the concrete floor. The door can also be moved (on its axes) perpendicularly in close contact with the opening by a pair of hydraulic jacks which are operated from a single cylinder.

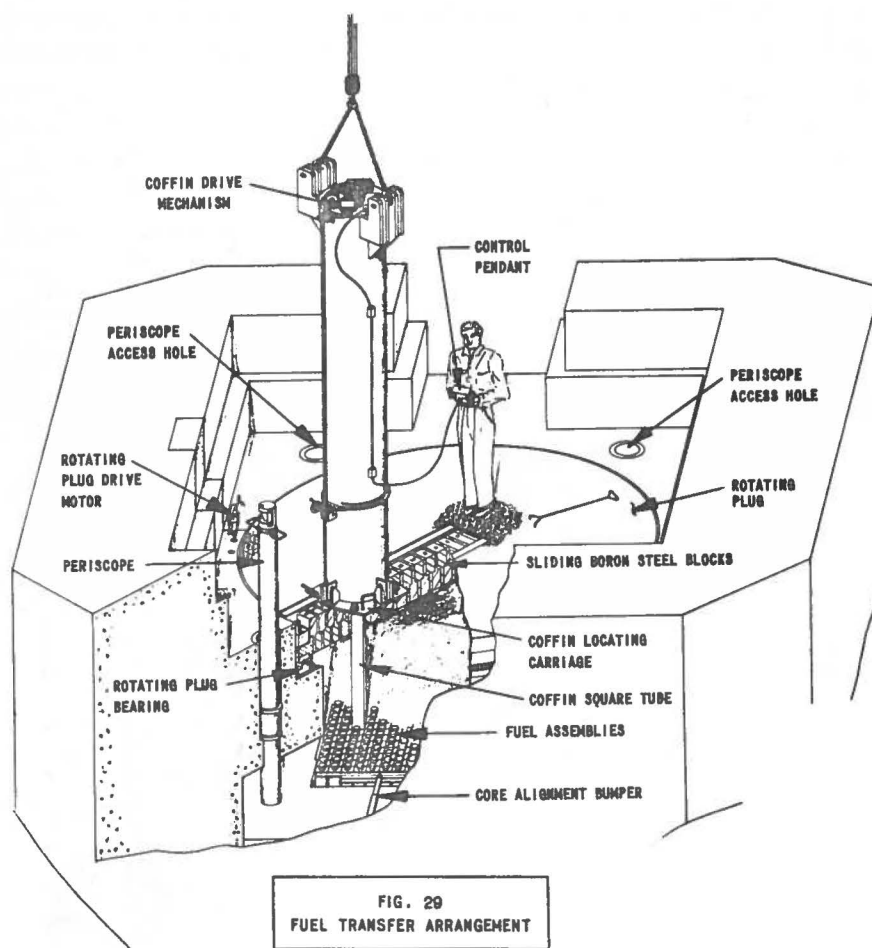
The vertical access openings in the thermal column and the vertical through holes are shielded with stepped plugs of high-density concrete.

G. Fuel-transfer System

The fuel-transfer system consists of a rotating shield plug and indexing system, a fuel-transfer coffin and coffin-locating carriage, and a periscope. Because of the difficulties attendant to the absence of a

transparent liquid shield above the core (as in water-cooled reactors), the indexing system and the fuel coffin are designed for essentially remotely controlled operation (pushbutton pendant). The only visual aid is rendered by the periscope which scans the top of the core to ensure there are no obstructions (i.e., thermocouple wires) which might interfere with the operation of the coffin-transfer mechanism.

Figure 29 is a cutaway drawing of the upper portion of the reactor shield, showing the components of the fuel-transfer system in their relative positions for removal or insertion of a fuel assembly.



1. Rotating Shield Plug and Indexing System

Fuel-transfer operations are performed through the rotating shield plug. The plug consists of three 4-in. thick slabs of steel (10 ft 10 in. dia.) and weighs about 25 tons. The top and bottom surfaces of the plug are coated with a layer of boral ($\frac{1}{4}$ in. thick) for thermal neutron attenuation. The top layer of boral is covered with steel checker plate ($\frac{1}{4}$ in. thick) which serves as a working floor. The plug rotates on a ball bearing which is embedded in the bottom of the plug cavity (11 ft dia.) formed in the top of the concrete shield.

The fuel is transferred through a radial slot in the plug. The slot is stepped, having a minimum width of 8 in., and is filled with 30 interlocking, cast boron-steel ($1-\frac{1}{2}\%$ B) blocks. Two of the blocks (master blocks) are removed from the slot to provide an opening (8 in. x 11 in.) through the plug. The remaining 28 blocks are retained and slide on two rails bolted to the plug so that the opening can be adjusted to any radial position above the core. Angular positioning of the slot to $\pm\frac{1}{16}$ in. over the desired fuel assembly is accomplished by a pointer at the edge of the plug. The pointer is indexed to a steel scale mounted on the upper edge of the plug cavity.

2. Coffin-locating Carriage

The coffin-locating carriage is an all-welded assembly consisting of a steel base plate ($\frac{3}{4}$ in. thick), four spring-loaded balls, three coffin guide lugs and two heavy-duty toggle clamps.

The opening in the plate (11 in. dia.) is positioned ($\pm\frac{1}{16}$ in.) above the unloading port by a steel scale mounted adjacent to one of the retaining rails. The carriage is then clamped to the retaining rails in readiness to receive the fuel-transfer coffin (Fig. 30).

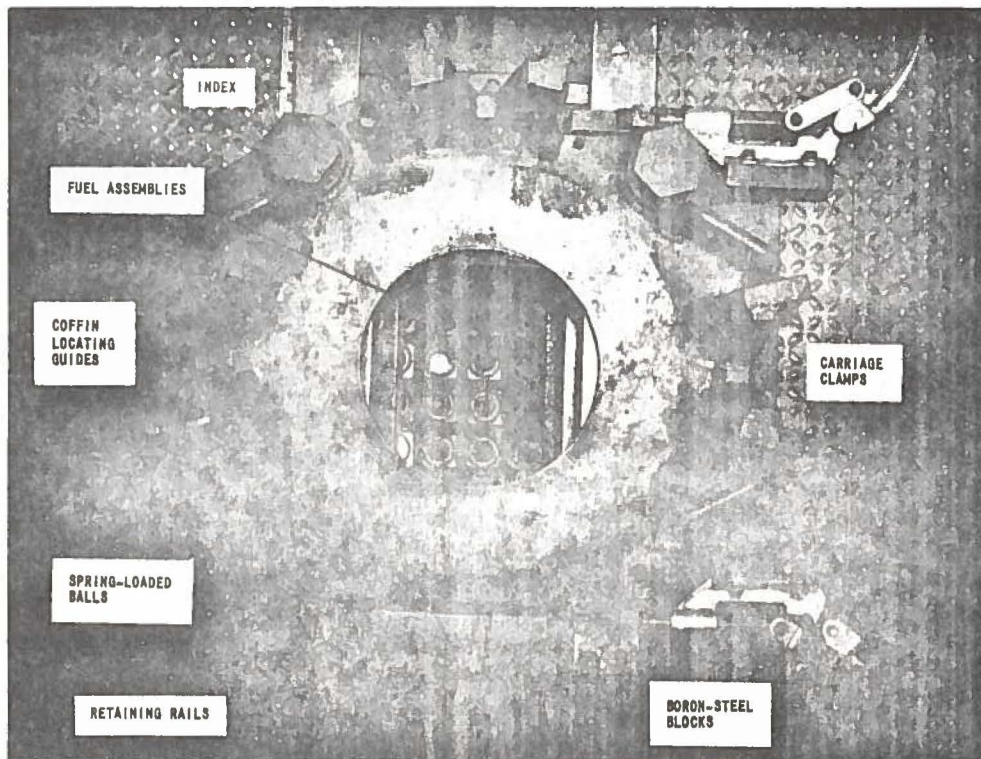


FIG. 30
COFFIN LOCATING CARRIAGE INSTALLED ABOVE OPENING IN ROTATING SHIELD PLUG

3. Rotating Shield Plug Bearing and Drive Motor

The weight of the rotating shield plug (25 tons) and the transfer coffin (5 tons) is carried by an angular contact ball thrust bearing (130 in. dia.) designed and built by the Kaydon Engineering Co., Muskegon, Michigan. The upper race of the bearing is bolted to the bottom steel slab of the plug. The lower race is grouted into the plug cavity in the reactor shield.

Prior to grouting, the lower race was centered over the reactor grid plate and leveled with a Watts Micrometer Water Level in conjunction with a series of leveling bolts that were welded to a steel base plate cast into the reactor shield (see Fig. 31). About 2 in. of Embecco low-shrinkage grout was packed between the race and the shield. This method of leveling and of supporting a large bearing of this type is unique in that it eliminates the heavy, accurately machined, race base plate that is normally used as a reference surface for the leveling operation. Vertical runout on the race was held to 5-mil TIR (Total Indicated Runout), with no slopes greater than 2 mils per 16-in. increment of ball path.

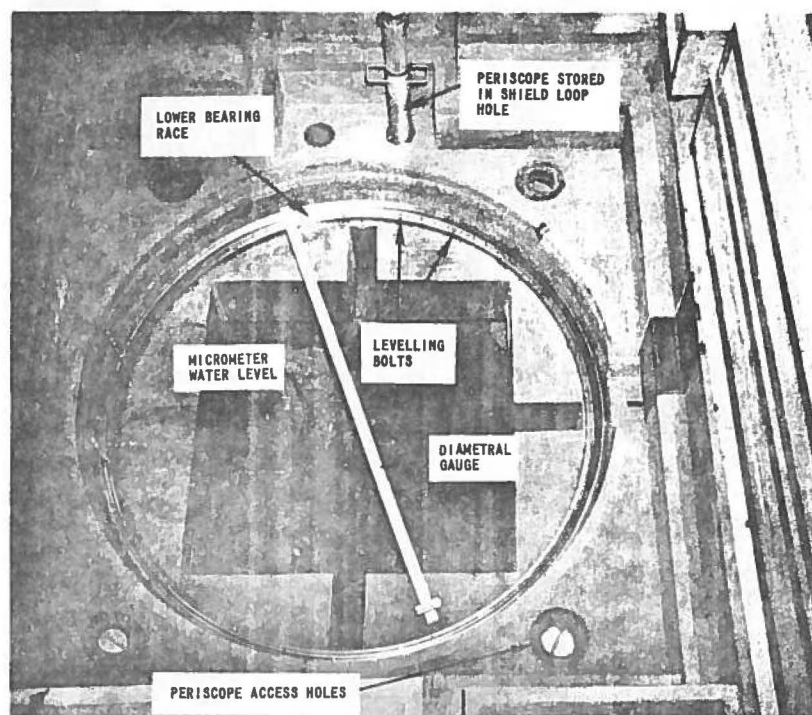
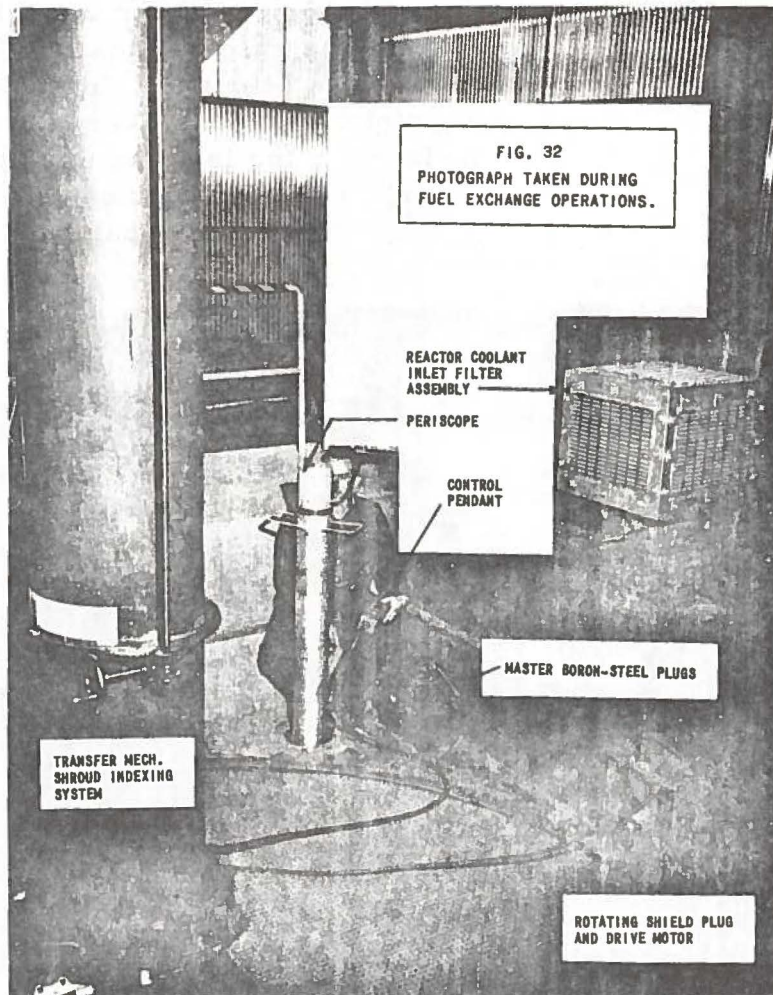


FIG. 31
INSTALLATION OF LOWER BEARING RACE FOR ROTATING SHIELD PLUG.

After grouting, the lower race was packed with an oxidation-resistant grease (Shell Cyprina), the 165 balls and ball cages were installed, and the bottom slab of the plug, carrying the upper race, was set in place.

The middle and upper steel plug slabs were lowered to complete the assembly. Radial runout of the loaded bearing measured 10 mils TIR.

The entire plug assembly is rotated by a $\frac{3}{8}$ -in. electric drill motor and reduction gear box mounted beside the plug in a recess in the concrete shield (see Fig. 32). The output of the gear box is a double sprocket which engages a chain wrapped around and welded to the bottom slab of the plug. The drill speed at full load is 250 rpm; the gear box reduction is 1250 to 1, thus giving the plug a turning speed of $\frac{1}{5}$ rpm. The gear box is equipped with a jaw slip clutch to prevent damage to the reduction gearing by overrun of the massive rotating shield plug.



4. Fuel-transfer Coffin

The fuel-transfer coffin is designed to provide adequate shielding for a fuel assembly removed from the center of the core two hours after shutdown from a 1000-Mw-sec transient. The steel and lead

shield houses a mechanism which is used to transfer a fuel assembly to and from the core. The transfer mechanism is powered by an electric motor atop the coffin. All transfer operations are controlled with a pushbutton pendant at the end of a multiconductor control cable. Figure 32 shows the coffin in position for a fuel transfer. Because of its ungainly proportions (20 in. OD x 10 ft high) and great weight (5 tons), the coffin is attached to the overhead bridge crane during the entire sequence of fuel-transfer operations. When not in use, the coffin is stored in a pit in the main floor.

a. Coffin-body (Shield) Assembly

The coffin body (Fig. 33) is a double-walled structure composed of an outer steel tube (20 in., Schedule 20) and an inner steel tube (8 in., Schedule 40) welded to a steel base plate ($\frac{3}{4}$ in. thick). The intervening annulus (6 in.) is filled with lead shot (density = 75% of solid lead). Two lifting lugs are welded at the top, and three guide lugs are welded at the bottom of the outer tube. The guide lugs engage with the coffin locating carriage. The coffin is shielded at the bottom by a lead-filled drawer, 4 in. thick.

A steel plate ($\frac{5}{8}$ in. thick) is welded to the top of the inner tube to provide a seat for a 12-in. ball thrust bearing which carries the weight of the fuel assembly-transfer mechanism.

b. Fuel Assembly-transfer Mechanism

The Fuel Assembly-transfer Mechanism performs the following functions after the core clamping bars have been released:

- (1) Rotates relative to the coffin body to achieve orientation of the square spreading tube with the desired fuel position in the core. This operation is performed manually by the operator.
- (2) Spreads the upper ends of assemblies adjacent to the reference fuel position.
- (3) Lowers the gripper mechanism to engage the fuel assembly and removes it into the coffin (Fig. 34), or inserts the assembly and disengages the gripper mechanism (Fig. 35).
- (4) Withdraws the square spreading tube to permit re-alignment of the adjacent fuel assemblies.

To accomplish the required angular orientation with the core, the square spreading tube and the fuel assembly gripper are mounted in a shroud. The shroud, in turn, is fastened to the drive unit mounting plate (1 in. thick steel) which rotates on the 12-in. diameter ball thrust bearing at the top of the inner tube.

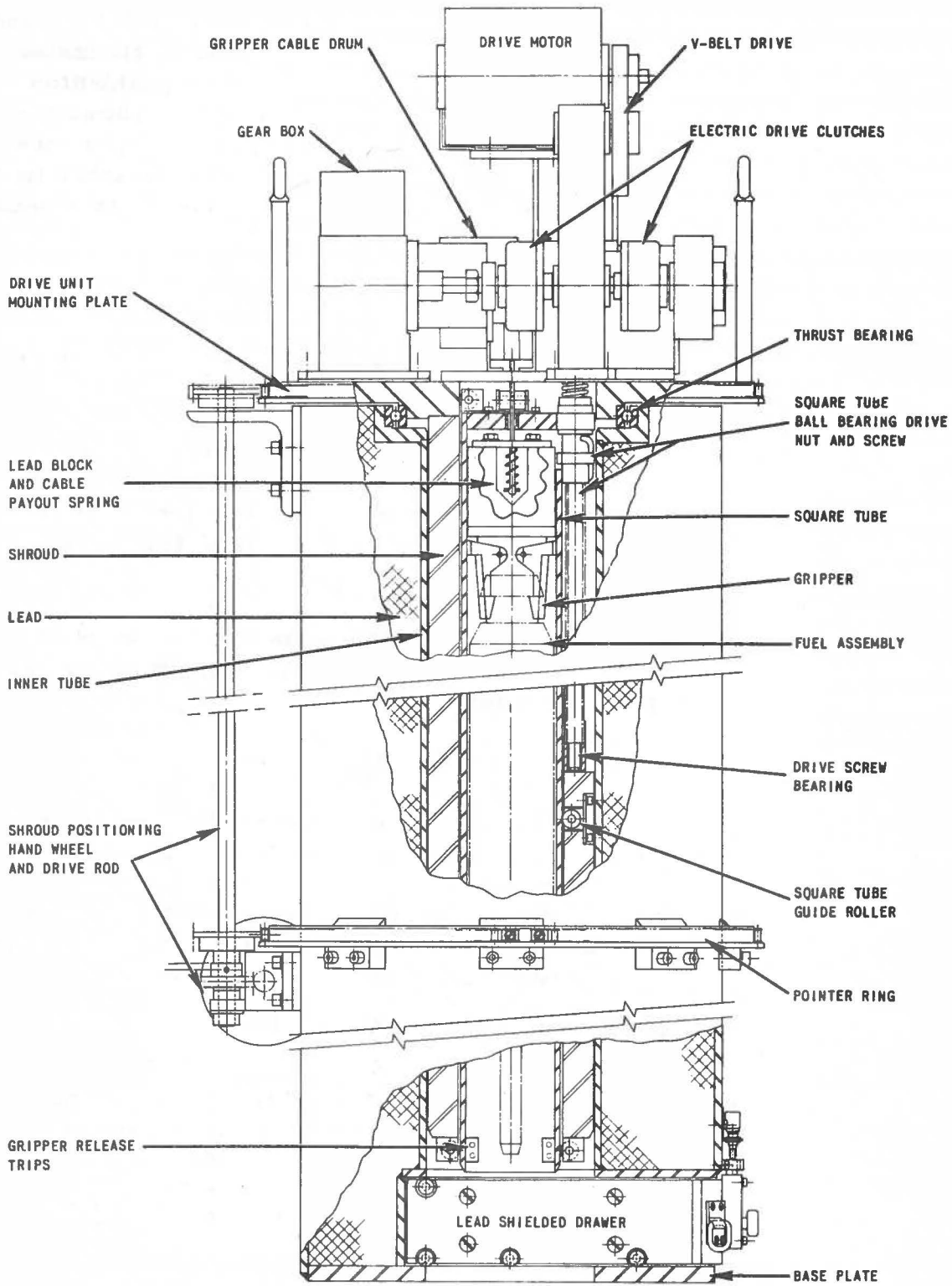


FIG. 33
FUEL TRANSFER COFFIN

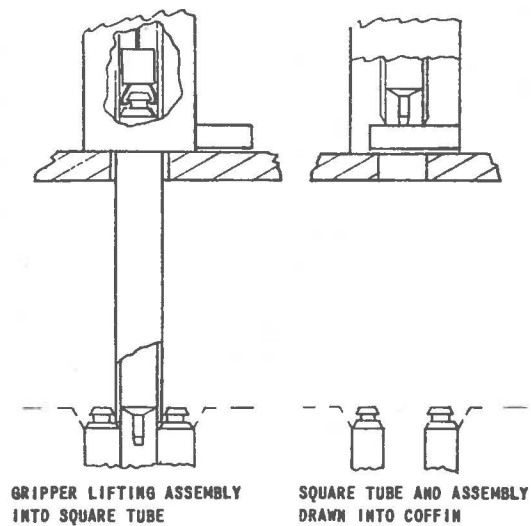
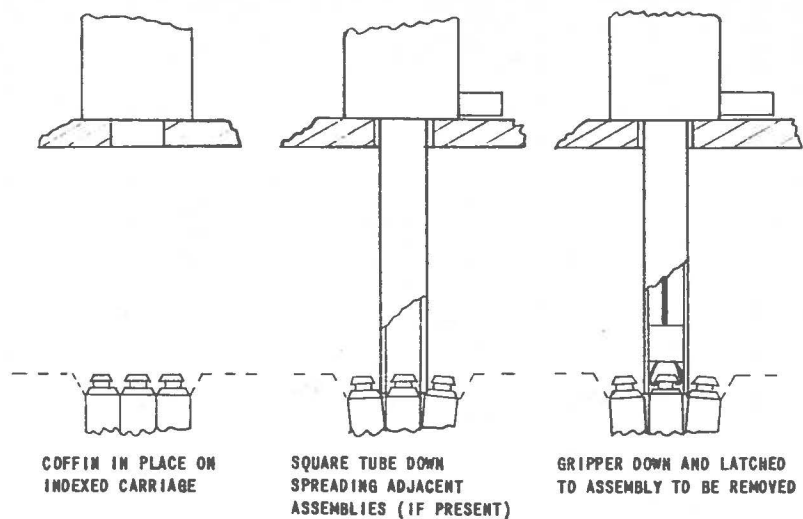


FIG. 34
FUEL ASSEMBLY REMOVAL

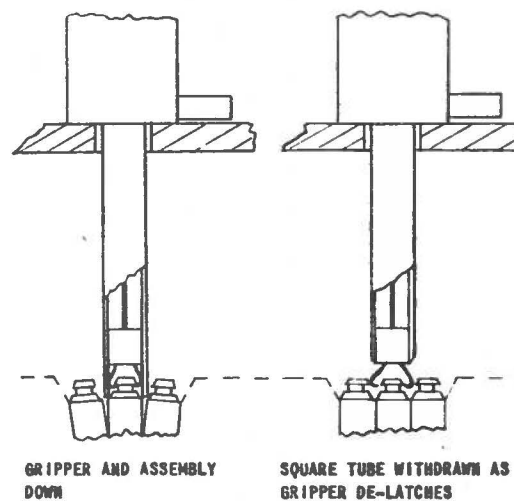
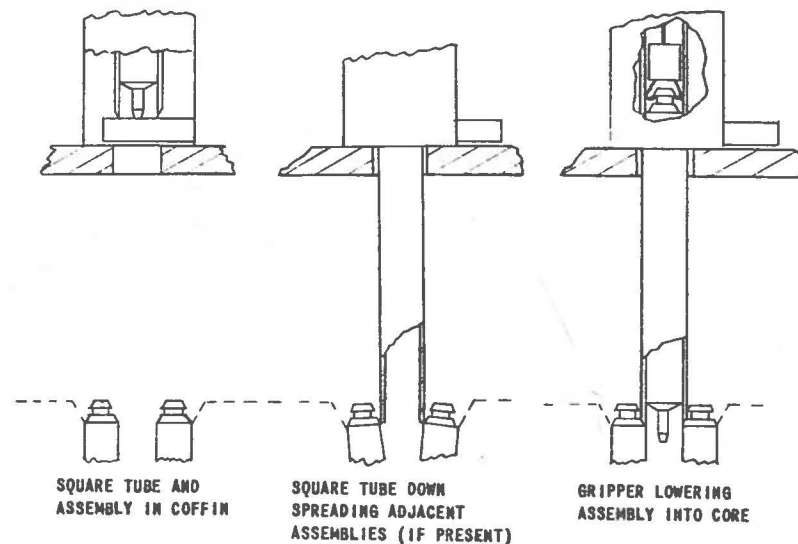


FIG. 35
FUEL ASSEMBLY INSERTION

The shroud is composed of two semicircular steel sections bolted together. A rectangular groove is milled into the mating flat surfaces of each section; hence the shroud is a cylinder with a square hole to accommodate the square spreading tube.

The shroud is positioned relative to the core by a manually operated indexing system mounted on the outer surface of the coffin body. The system consists of a handwheel, a rotating ring and pointer, and a scale. The handwheel is geared to a rod which rotates both the pointer ring and the shroud through two sprocket and chain drives. The scale on the coffin body is calibrated to the scale on the rotating shield plug. Thus, for proper counter rotation of the coffin shroud, the readings are the same on both scales.

The square tube is driven up and down in the shroud by a ball-bearing lead screw mounted in the upper half of one of the shroud sections. The lead screw is turned by the drive motor through an electric clutch and reduction gearing.

The square tube (inside dimension = $4\frac{1}{4}$ in. square) guides the fuel assembly gripper mechanism and spreads the adjacent fuel assemblies. Therefore, in its fully extended position, the tube projects 4 ft from the bottom of the coffin. The tube is guided at the upper end by three adjustable rollers which ride on the inside surface of the shroud. The lower end is guided by four rollers mounted on the end of the shroud. The lower end of the tube is also beveled to mate with the beveled surfaces of the adjacent fuel assemblies.

The total downward force applied against the adjacent assemblies by the tube is determined by the preset compression of a die spring, and ranges from 200 to 700 lb. When the preset force is exceeded, the ball-bearing lead screw "climbs" slightly and activates a switch which de-energizes the electric drive clutch.

The fuel assembly gripper is a four-jawed, spring-loaded latching device which grasps the fuel assembly by the aluminum end fitting. The gripper is raised or lowered by a steel cable ($\frac{1}{4}$ in. dia.) and a grooved, brass drum mounted on a splined shaft. The shaft (and drum) is rotated by the coffin drive motor through a worm drive and electric clutch. As it rotates, the drum is forced along the splined shaft by a fiber rider which rides in the drum grooves. This maintains a 90-degree angle between the drum axis and the cable as it winds and unwinds. A slack detector, consisting of a pulley on a spring-mounted arm connected to a drive motor switch, is installed to prevent the drum from paying out excess cable and overriding the gripper travel.

The gripper is weighted with a 25-pound lead block to maintain cable tension and to aid the delatching operation. The cable is attached to the gripper through a spring in the lead block in such a manner that the spring is compressed as the pull on the gripper is increased. When the gripper reaches the end of its downward travel, the compressed spring expands and takes up about $2\frac{3}{4}$ in. of cable "pay out" before the slack detector switch de-energizes the cable drum drive motor.

At the start of the delatch action the gripper cable and the square tube rise simultaneously. However, because of the spring-loaded "pay out," motion of the gripper is delayed sufficiently to permit small triangular blocks (mounted in each corner of the square tube) to engage with dogs on the gripper jaws and effect their disengagement from the assembly end fitting. The triangular blocks also retain the gripper within the confines of the square tube.

c. Electrical System

The transfer mechanism in the coffin is driven by a reversible, 120-volt, ac, $\frac{1}{3}$ -hp, 1750-rpm capacitor start motor. The magnetic clutches for the square tube and the gripper drives are powered by 90-volt dc supplied by a conventional full-wave bridge rectifier without a ripple filter. Dropping resistors (300 ohm, 10 watt) are used to reduce the voltage from 120 to 90 volts.

The coffin mechanism is operated with a pendant at the end of 8 ft of 10-conductor cable. The pendant displays three lights and three manual holddown push buttons as follows:

| | <u>Color</u> | <u>Action</u> |
|---------|--------------|------------------------------------|
| Lights | Green | Gripper drive clutch energized |
| | Green | Square tube drive clutch energized |
| | Red | Coffin drawer lock bolt not seated |
| Buttons | Black | Gripper up |
| | Black | Gripper down |
| | Red | Gripper delatched |

The buttons operate a series of four Allen-Bradley Type C-200 relays which perform proper switching for the various coffin functions.

Limit switches are provided to prevent overtravel and damage to any of the drive motor components. Main fuses and a plug receptacle are mounted and readily accessible on the side of the coffin below the pendant cable terminal strip. Also mounted on the side of the coffin is a relay box which houses the control relays, motor and clutch fuses, and

the 300-ohm voltage dropping resistors. The dc power supply for the clutches is mounted on top of the relay box. Quick-disconnect plugs are used between the pendant terminal strip on the side of the coffin body and the terminal strip inside the relay box.

5. Periscope

The periscope (Fig. 36) is used to scan the reactor upper plenum to ensure there are no obstructions that will interfere with the operation of the fuel transfer mechanism. The entire assembly, which consists of two telescoping aluminum tubes, is manually installed and operated through one of the four access holes most convenient to the core region being serviced.

The depth of penetration of the periscope into the plenum chamber is controlled by an adjustable flange which encircles the outer tube ($6\frac{1}{2}$ in. OD) and seats on the top of the access hole. The inner upper tube (6 in. OD) can be adjusted to the height of the operator. Radial scanning is performed by rotating the assembly. Axial scanning is performed by tilting the lower mirror with a throttle-type flexible cable.

6. Manual Fuel-handling Tools

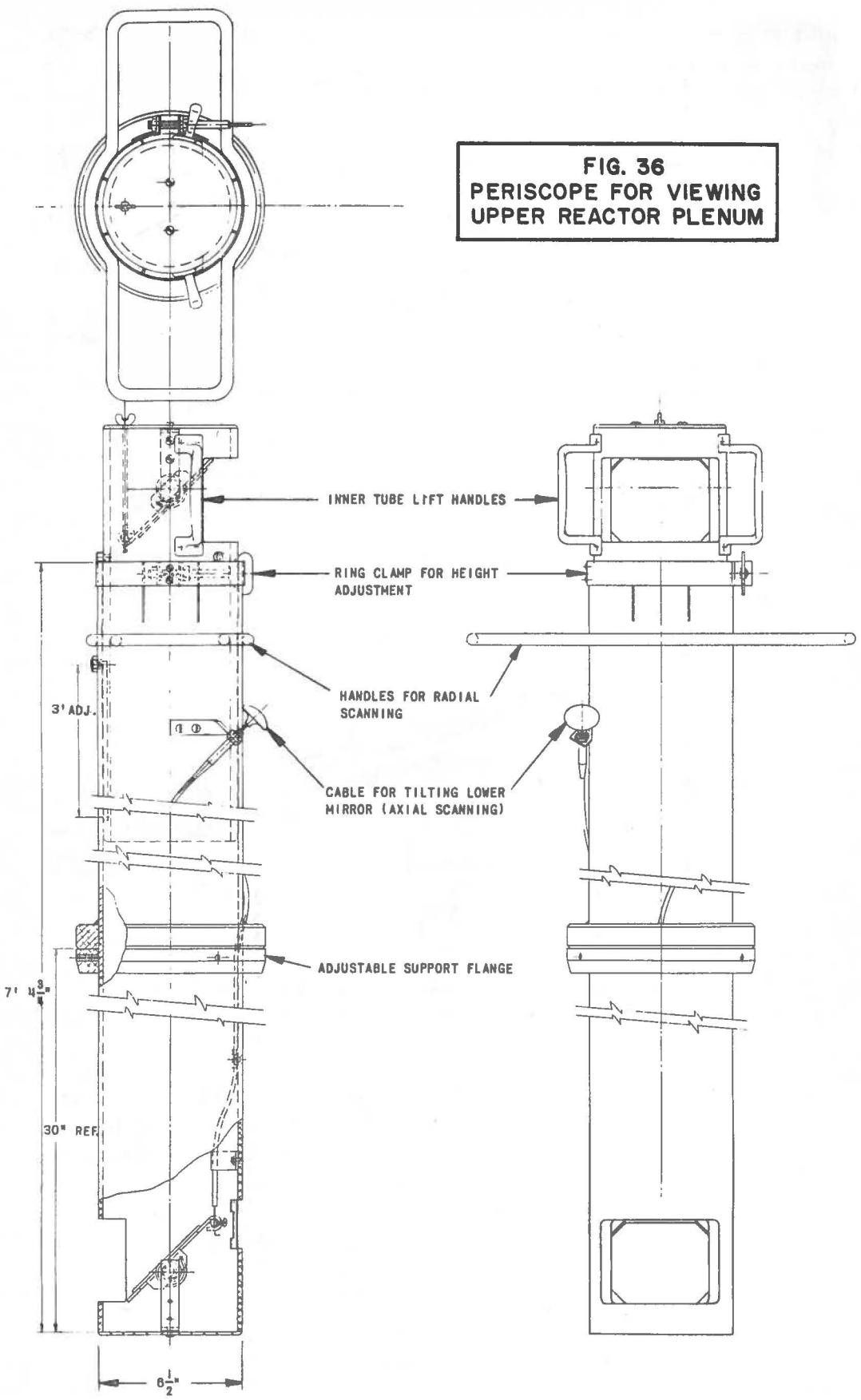
The initial loading of the fuel assemblies and thermocouple attachments was made with the manually operated tools shown in Fig. 37. The spreader performs the same function as the square spreading tube in the coffin. The underside of the four engagement lugs is machined to fit the hollow end fittings of adjacent fuel assemblies. The spreading action is effected by application of a downward force on the linkage and consequent radial outward thrust and movement of the engagement lugs in slots machined in the spreader flange.

The fuel gripper differs in one respect with its counterpart in the transfer coffin: the de-latching is effected by a rod attached to the 5-ft long handle.

The thermocouple plug tool is an aluminum rod (5 ft long) which is rotated within an aluminum tube to effect engagement and disengagement of an end fitting on the rod with the thermocouple plug on the fuel assembly.

Figure 38 shows the shielded tool used for thermocouple installations subsequent to reactor startup. The tool is used in conjunction with a glass shield window, 12 in. thick. Both components are installed in the slot in the rotating shield plug. The thermocouple tool consists of an aluminum tube which is raised or lowered through a steel ball (9 in. dia.).

FIG. 36
PERISCOPE FOR VIEWING
UPPER REACTOR PLENUM



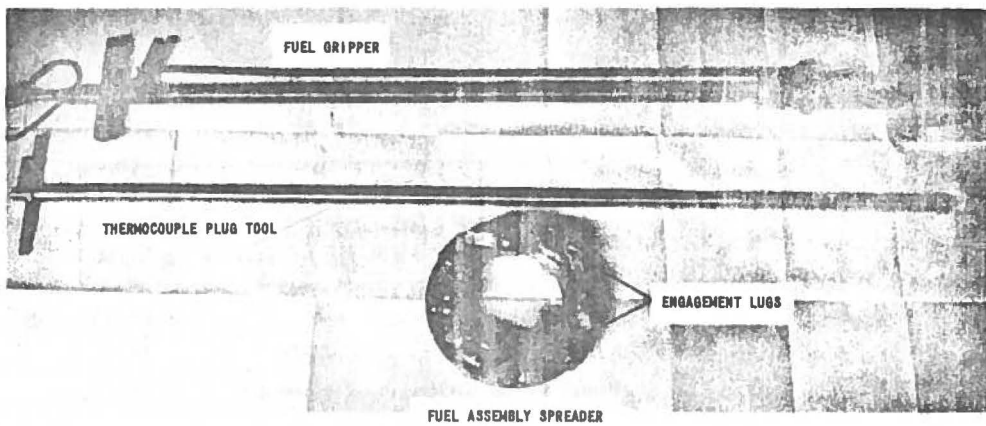


FIG. 37
MANUALLY OPERATED TOOLS USED FOR INITIAL CORE LOADING.

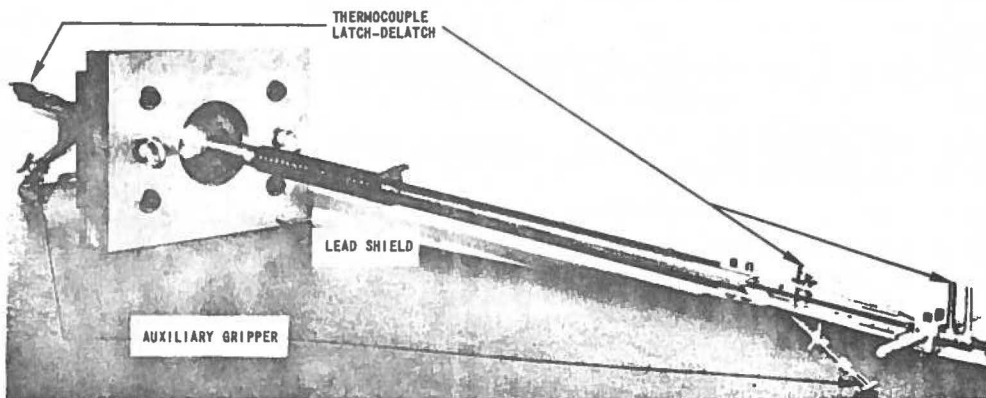


FIG. 38
SHIELDED TOOL USED FOR POST-STARTUP THERMOCOUPLE INSTALLATIONS.

The ball rotates inside the lead and steel shielding. The aluminum tube houses a metal-sheathed flexible shaft and a throttle-type cable which interconnect the manipulators with the thermocouple latch-delatch and the auxiliary gripper mechanisms. The metal sheath on the flexible shaft is used to engage and rotate the thermocouple plug to align the engagement slot. The latching or delatching is effected by rotating a small locking pin mounted on the lower end of the flexible shaft. The auxiliary gripper is used to position the thermocouple wires, and for other operations that may be required at the top of the core.

7. Fuel-storage Area

Irradiated fuel elements are transported in the coffin to the fuel-storage area located at the northwest corner of the reactor building. The storage area consists of 147 steel tubes arranged on 10-in. centers and cast in high-density concrete 11 ft thick. The tubes are stepped from 6-in. Schedule 20 pipe, 10 ft 5 in. long at the lower end, to 8-in. Schedule 20 pipe, 22 in. long at the upper end. The upper section houses a closure plug of high-density concrete. The storage area is secured by seven interlocking, hinged steel doors ($\frac{1}{4}$ in. thick) and a padlock.

Figure 39 shows the transfer coffin being positioned over a storage hole with the aid of the coffin guide insert. The guide insert is a steel plate ($\frac{3}{8}$ in. thick) with three coffin guide lugs welded on the upper



FIG. 39
FUEL TRANSFER COFFIN BEING POSITIONED OVER COFFIN GUIDE INSERT
IN FUEL STORAGE HOLE.

surface. The center of the plate is machined to accommodate a guide tube welded to the underside. A plate with a $4\frac{1}{2}$ in. square opening is welded to the bottom end of the guide tube. The opening is aligned with, and stops the descent of the coffin square tube at the proper height to actuate the delatch mechanism and release the fuel assembly.

H. Reactor Cooling and Building Ventilation System

The reactor is cooled by an induced draft air system, thus keeping the core at a slightly negative pressure. The air flow is controlled by two 40-hp Spencer Turbocompressors operating in parallel. Each turbocompressor is rated at 3,250 cfm against a head of 1 psi at 250°F, with an intake pressure of 25 in. Hg.

The reactor cooling and building ventilation system is shown schematically in Fig. 40. Prefiltered building air enters the upper reactor plenum via two 12-in. square ducts in the reactor shield. Each filter assembly contains five American Air Filters, Type G (16 x 20 x 2 in.). The air flows down through the coolant channels formed by the corners of adjacent fuel assemblies and exits into the lower plenum chamber. Approximately 10% of the flow is diverted to the permanent reflector and shield by orificing at the outer edges of the core grid plate. The air exits from the plenum chamber via two $10\frac{1}{2}$ -in. diameter ducts which lead to the turbocompressor room. These ducts contain resistance thermometers, thermocouples, and pitot tubes for steady-state coolant heat removal measurements. About 13 ft from the plenum, the two ducts and a $9\frac{1}{2}$ -in. diameter bypass line join into a 19-in. diameter line which extends the remaining distance to the exhaust filters in the turbocompressor room.

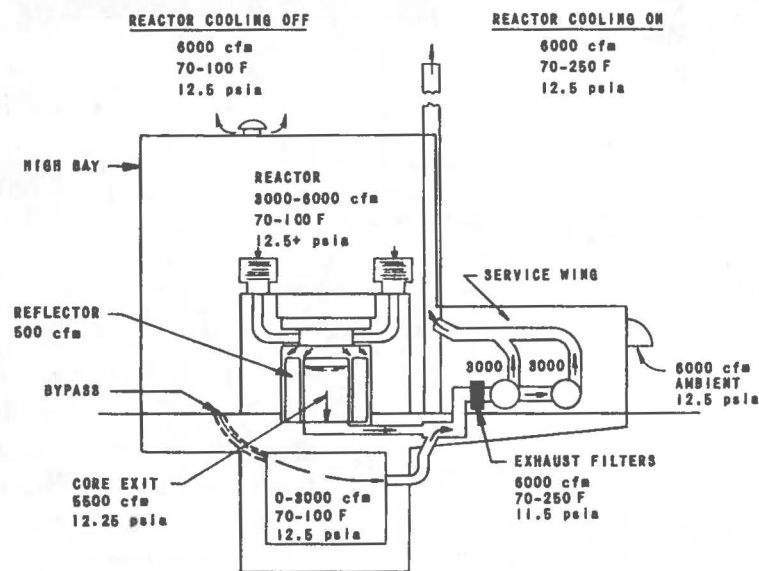


FIG. 40
TREAT COOLING AND VENTILATING SYSTEM

The bypass line serves two purposes. The primary purpose is to subcool the reactor effluent consistent with the temperature limitation of 250°F on the exhaust filters. The bypass line draws subcooling air from the subreactor room, thereby performing a secondary function of ventilating the basement area.

The bypass line features an 8-in. diameter butterfly valve which can be controlled manually, or positioned automatically by a thermostat installed upstream of the exhaust filters. With the valve in the fully open position, the reactor flow is reduced by about $\frac{1}{3}$; however, this ratio may be varied in either direction by closing the valve, or throttling the manually operated damper valves on the reactor intake ducts.

The coolant air from the plenum chamber and the bypass line flows through a bank of six high-efficiency, high-temperature, AEC-type exhaust filters into the turbocompressors and discharges up through a stack (24 in. dia., 60 ft high) to the atmosphere. Figure 41 shows the exhaust filter-turbocompressor arrangement. Air flow is controlled by a pneumatically operated throttle valve in the 19-in. diameter line upstream of the exhaust filters. The valve is positioned by a controller which senses and maintains the turbocompressor motor current at a specified value. Each turbocompressor discharge line is equipped with a butterfly damper valve which opens and closes automatically to isolate the reactor from the exhaust stack when the compressors are not in operation.

During cold weather operation, the reactor coolant is supplied by a bulk air-heating unit rated at 7500 cfm of air. In the event of reactor shutdown, the building is ventilated by an exhaust fan (6000 cfm) installed in the roof.

I. Control and Instrumentation

All control switches, indicators, and recorders required for startup, steady-state, or transient operations are displayed on the control console (Fig. 42) located in the Control Building.

Control at the Reactor Building is limited to manual scram buttons at three locations in the building. The instrument room contains the dc amplifiers, logarithmic amplifiers, and pulse amplifiers required to amplify the various chamber signals to a suitable level for transmission to the control building. The chamber voltage supplies, thermocouple amplifiers and reference junction, and integrated power circuit are also located in the instrument room.

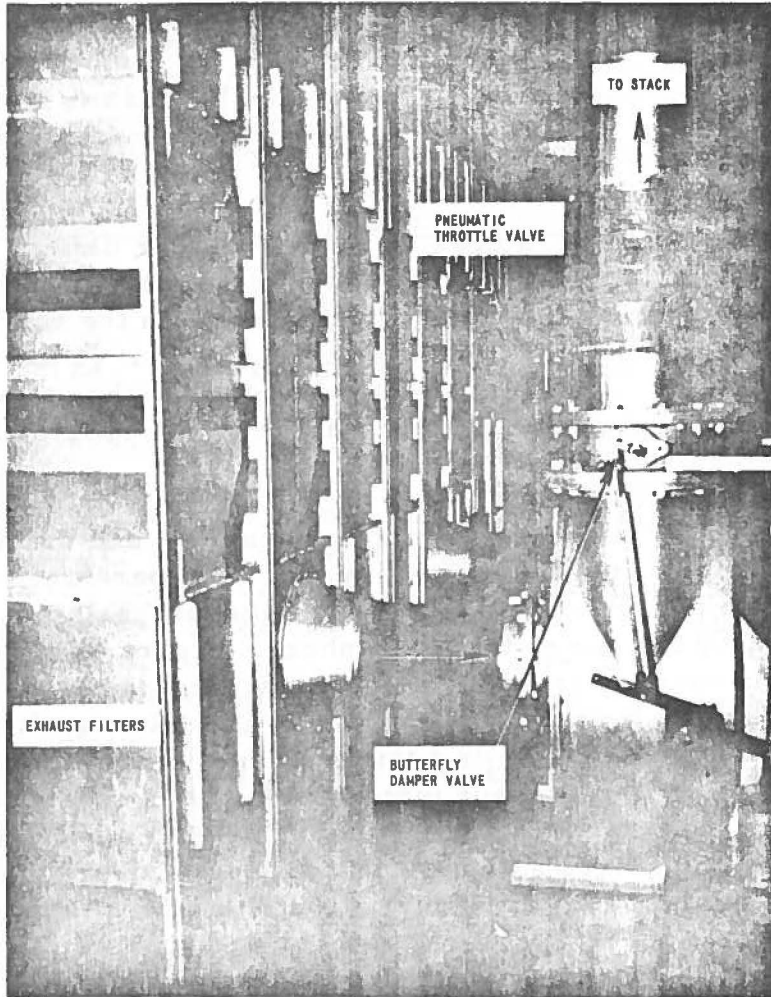
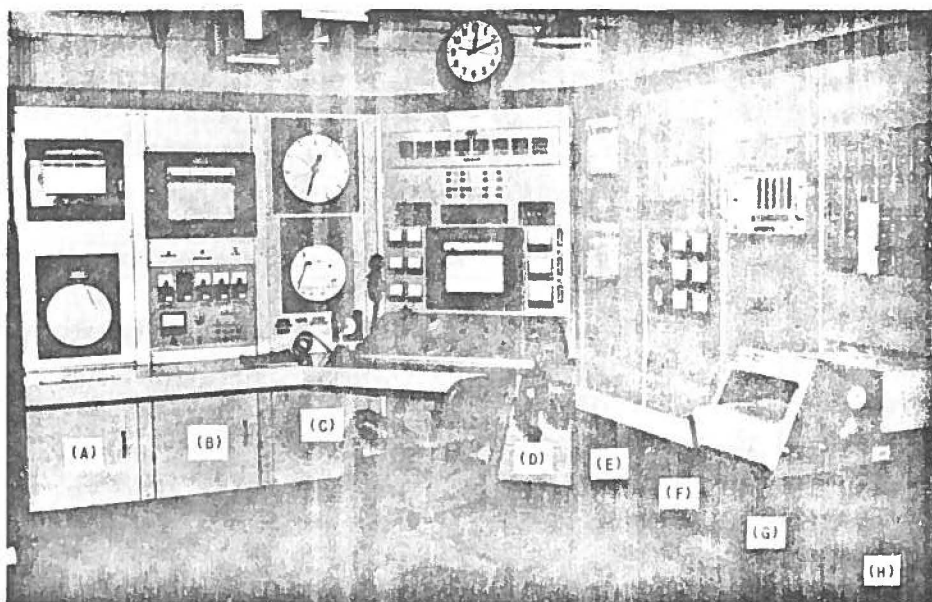


FIG. 41
COOLANT AIR EXHAUST FILTERS
AND TURBOCOMPRESSORS

All instrument and control signals between the two buildings are transmitted via five polyvinyl chloride-jacketed, aluminum-armored, twisted-pair, 19-gauge polyethylene insulated conductor, direct burial-type telephone cables. These include: one 76-pair and one 52-pair cable for control signals; one 26-pair cable for meter signals; one 26-pair cable for transient recorder signals; and one 16-pair cable for use by experimenters. Pulse signals are carried by eight Type RG 11/AV coaxial cables.

The control and instrumentation systems are essentially dual in nature. One group of instruments and controls is required primarily for startup and steady-state power operation. The second group is

required for control and record during transients. In the case of nuclear instruments, the two groups which serve the same functions over different input signal ranges, have been designated as "steady-state," and "transient."



CABINET A.
WIND DIRECTION RECORDER
WIND VELOCITY RECORDER
BAROMETRIC PRESSURE RECORDER

CABINET B.
RADIATION MONITORS

CABINET C.
COOLANT ΔT RECORDER
COOLANT FLOW INDICATOR
COOLANT FLOW CONTROLS

CABINET D.
ANNUNCIATOR PANEL
ROD POSITION INDICATORS
LINEAR FLUX RECORDER
STEADY-STATE SAFETY CIRCUITS
STEADY-STATE LOG POWER AND PERIOD
LOG COUNT RATE AND PERIOD
ROD CONTROL SWITCHES

CABINET E.
12-POINT TEMPERATURE RECORDER
LOG POWER AND PERIOD RECORDER
DUAL SCALER FOR STARTUP COUNTERS

CABINET F.
TRANSIENT SAFETY CIRCUITS
TRANSIENT LOG POWER AND PERIOD METERS
DUAL SCALER FOR ABSOLUTE FISSION COUNTER
TRANSIENT ROD PROGRAMMING AND CONTROL

CABINET G.
TRANSIENT TIMERS

CABINET H.
FAST RECORDER
FAST RECORDER DRIVERS

FIG. 42
CONTROL CONSOLE IN CONTROL BUILDING

1. Nuclear Instrumentation

a. Steady-state Operation

The steady-state instrumentation is conventional and consists of the following units.

(1) Linear Operating Instrument (1 channel)

This unit is an ANL-A125 linear dc amplifier. The amplifier has an input range from 10^{-12} to 10^{-4} amp in decade steps

and provides an output to a remote meter and strip chart recorder [Brown, Model Y 153XII-V-II-(W72)-30-K] at the control console. Range switching is controlled from the control console.

(2) Power Safety Circuit (2 channels)

This unit is an ANL CD161 linear dc amplifier. The amplifier has an input range from 10^{-10} to 10^{-4} amp in decade steps and provides outputs (0-10 volts) to the Shutdown Chassis and to a remote meter on the control console. Range switching is controlled from the control console.

(3) Log Power and Period Safety Circuit (2 channels)

This unit is an ANL-X38 logarithmic amplifier and period circuit. The logarithmic amplifier has a range from 10^{-11} to 10^{-3} amp and provides an output to a meter on the control console. The period circuit has a range of -50 to +5 sec, and provides outputs (0-10 volts) to the Shutdown Chassis and to a remote meter on the control console. Check circuits for the logarithmic amplifier and period circuit are provided in the instrument. The logarithmic amplifier output and the period output of one of the two channels is recorded on a dual-pen strip chart recorder [Brown, Model Y 153X27-VV-II-III-30(v)].

(4) Startup Circuit (2 channels)

The startup circuit consists of an ANL-A61DXX linear pulse amplifier and ANL-A104 pre-amplifier which operate a dual scaler (ANL-59D) and a log count rate and period meter (ANL-CRM12). The log count rate and period circuit has a logarithmic range from 10 to 10^5 counts/sec, and a period range from -50 to +5 sec. It provides outputs to a count rate meter and period meter at the control console.

The pulse pre-amplifier input is provided by a BF_3 proportional counter (Westinghouse WL-6307). The Westinghouse proportional counter is serviced by an ANL-V54 dual high-voltage supply.

(5) Ion Chambers

All ion chambers (steady-state and transient), with the exception of one used by the linear operating instrument, are ANL-IC25 parallel-plate B^{10} -coated and uncompensated. The signal to the linear operating instrument is supplied by an ANL-IC20 parallel plate, B^{10} -compensated ion chamber.

(6) Chamber Voltage Supplies

The chamber voltage supply (ANL-V119) for the uncompensated ion chambers is electronically regulated and provides a positive 750-volt output.

The chamber voltage supply (ANL-V120) for the compensated ion chambers is electronically regulated and provides a positive 750-volt output and a variable 0 to negative 400-volt output.

All chamber voltage supplies provide an output to the Panelite alarm system to indicate failure of the supply.

b. Transient Operation

(1) Transient Power Safety Circuit (2 channels)

This unit is an ANL-CD160 linear dc amplifier with an input range from 10^{-9} to 10^{-3} amp in decade steps. It provides outputs (0-10 volt) to the Shutdown Chassis, a meter at the control console, and the Fast Recorder.

(2) Transient Log Power and Period Safety Circuit (2 channels)

This unit is an ANL-CD166 logarithmic amplifier and period circuit. The logarithmic amplifier has a range from 10^{-11} to 10^{-3} amp. It provides outputs to a meter on the control console and the Fast Recorder. The period circuit has four period ranges: ∞ to 2 sec, ∞ to 0.2 sec, ∞ to 0.02 sec, and ∞ to 0.002 sec. The period circuit provides outputs (0-10 volts) to the Shutdown Chassis and to a meter at the control console. Check circuits for the logarithmic amplifier and period circuit are provided in the instrument.

(3) Absolute Fission Counter Circuit (2 channels)

This unit consists of an ANL-A61DXXX linear pulse amplifier and an ANL-A138 pre-amplifier. The amplifier outputs are 20-volt pulses which drive an ANL-59D dual sealer at the control console, and 20-volt pulses to the Transient Integrated Power Circuit.

The input to the pre-amplifier is from a 2-in. diameter absolute fission counter.

(4) Transient Integrated Power Circuit (2 channels)

This unit is a Computer Measurements Corporation Model 6028A preset controller. It consists of 5 preset-type, decade scaling strips, and will provide an output (10 volts) to the Shutdown Chassis when a present total count has been reached. The input to the Transient Integrated Power Circuit is from the absolute fission counter circuit.

2. Rod Drive Control Systems

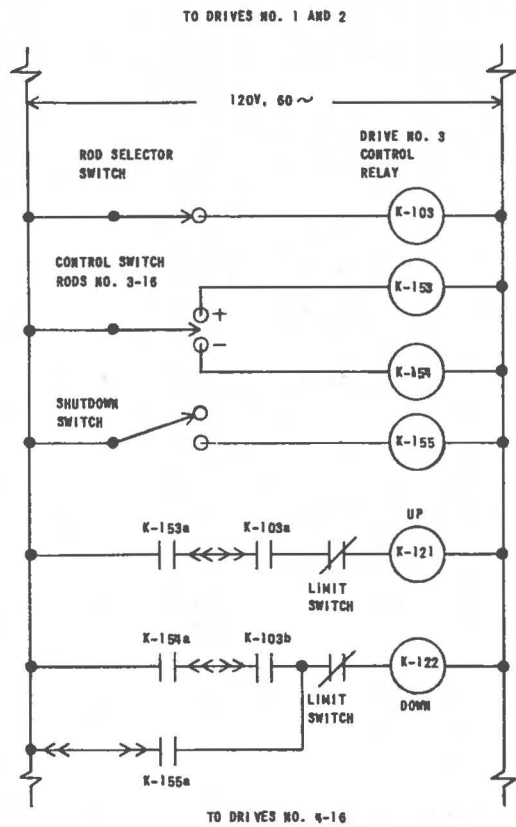
The instrumentation and related circuitry installed in TREAT is designed to accommodate 16 control rod drives (32 control rods). The four drives being used at present will be replaced by rod drives of a more advanced design as soon as performance tests on the prototype have been completed.

Two drives (No. 1 and No. 2) are used for fine reactivity control. Accordingly, both drives have selsyn position indicators (Bendix Mark 6, Model 4A, Type SHG), which are accurate to ± 0.002 in. Drive No. 1 is normally used for transients, and Drive No. 2 is used to effect reactor shutdown. The function of the respective drives can be reversed by a simple change in circuitry, as described later in this section.

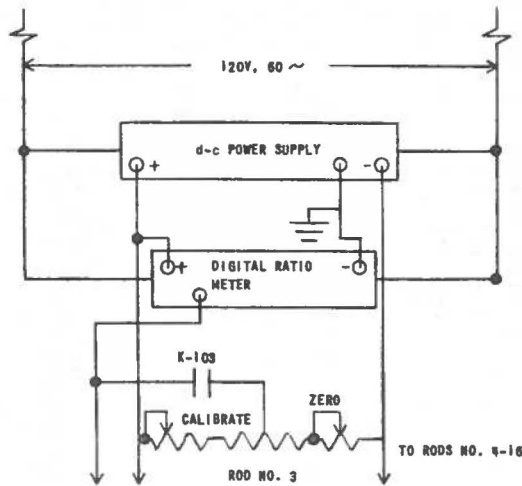
Drives No. 3 and 4, and the twelve additional drives to be installed, are equipped with 15-turn potentiometer position indicators (Beckman Helipot), which are read with a single digital ratio meter (Non-Linear Systems, Inc. Model 450R). The accuracy of this position indication is ± 0.02 in. Switching of the meter input from one potentiometer to the other is done by a contact on the "rod control relay" (K103, Fig. 43a). A section of the "rod selector switch" (Fig. 43d) is used to light a digital indicator corresponding to the rod (3-16) selected for control.

Three panel light indicators: "rod up," "rod down," and "scram latch engaged," are grouped on the control console for each rod drive. The "scram latch engaged" light is engraved to display the rod number; white lenses are used for the shutdown rods, and blue lenses are used for the transient rod drives.

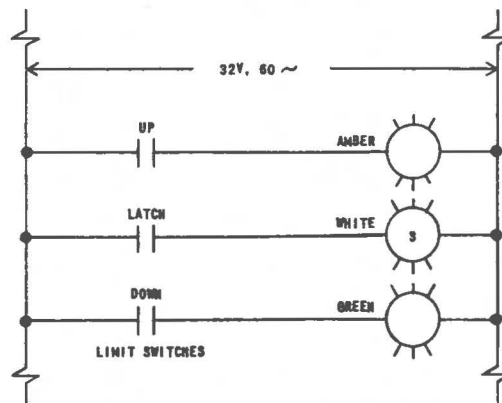
Separate motor control switches are provided at the console for drives No. 1 and No. 2 to facilitate positioning of the respective rods prior to a transient. The remaining drives (3-16) are controlled by a single motor control switch and a selector switch (Fig. 43a). This arrangement limits the amount of reactivity that can be added by the operator, and also saves considerable panel space. All shutdown rod drives (3-16) can be operated as a bank (in the down position only) by actuation of a "shutdown switch." This switch provides a means for rapid reactor shutdown without scrambling the drives and reduces the time required to return the drive latches to the bottom position after scram.



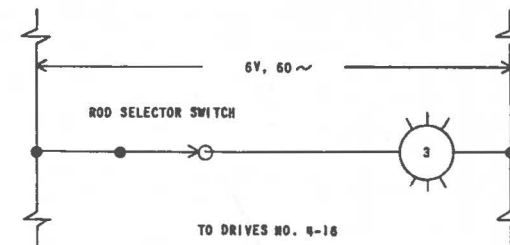
(a) MOTOR CONTROL FOR DRIVES NO. 3-16



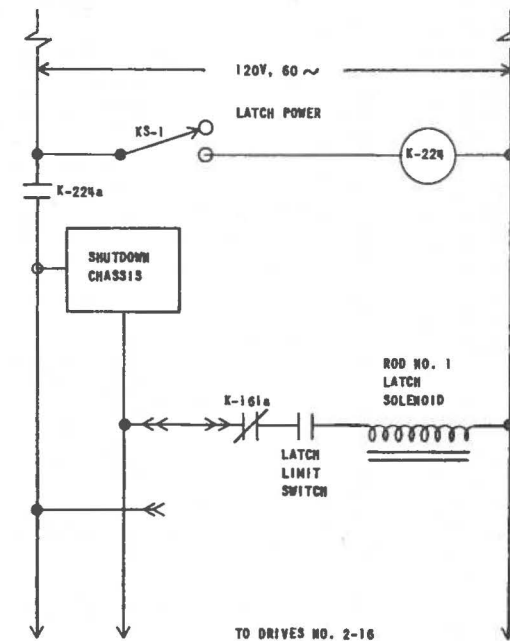
(b) POSITION INDICATOR - DRIVES NO. 3-16



(c) ROD POSITION LIGHTS - ALL DRIVES



(d) SELECTION LIGHT - DRIVES NO. 3-16



(e) SCRAM LATCH CONTROL

FIG. 43
TYPICAL CIRCUITRY FOR ROD DRIVE CONTROL AND POSITION INDICATION

Each switch on the control console operates a relay (or relays) in the Reactor Building which, in turn, performs the required switching functions. The use of these auxiliary relays reduces greatly the number and size of conductors required between the two buildings.

The control rod drives are designed for "fail safe" operation, i.e., scram action is produced by failure of power to the holding solenoid on the rod drive latch. In addition, a solenoid-operated scram latch safety bolt is installed on each transient drive to prevent an undesired scram in the event of a power failure (see page 47).

The function of each rod drive can be changed from "transient" to "shutdown" (or vice versa) by means of two jumper plugs installed on each drive. These plugs effect the following changes in the circuitry:

- (1) Interchange the leads between the motor starters K121 and K122, and control relay contacts K153a and K154a, to maintain the same relationship between the control switch position and reactivity addition.
- (2) Disconnect the power from the shutdown control relay contact K155a when changing from shutdown to transient, and connect the power when changing from transient to shutdown.
- (3) Disconnect scram latch solenoid from scram bus and connect to transient bus (or vice versa).
- (4) Connect scram latch safety bolt solenoid to safety bolt control circuit (or vice versa).
- (5) Connect "safety bolt in" and "safety bolt out" limit switch contacts to "transient safety bolt out" alarm and indicator light circuits (or vice versa).

3. Shutdown and Alarm System

The various operating parameters, fail-safe interlocks, and manual controls which can cause a reactor scram and/or an audible alarm are listed in Table V. In addition, audible alarms and warning lights are actuated inside and outside the reactor building when the latch power key switch (KS-1, Fig. 43e) is turned on. The warning lights continue to flash during reactor operation.

Table V

TREAT SCRAM INTERLOCKS AND ALARMS

| Condition | Reactor Scram | Panel light and Audible Alarm |
|---|------------------|-------------------------------------|
| Steady-state neutron level high | x | x |
| Steady-state period too short | x | x |
| Transient neutron level high | x | x |
| Transient period too short | x | x |
| Transient integrated power too high | x | x |
| Core temperature high | x | x |
| Power failure to transient timers | x | x |
| Control power failure | x | x |
| Low pressure in shutdown rod drive accumulators | | x |
| Lower pressure in shutdown rod drive accumulators | x | x |
| Manual scrams in control building (One each at steady-state console and transient control cabinet) | x | x |
| Manual scrams in reactor building (One each at top of reactor, main floor, and subpile room) | x | x |
| Loss of neutron detector high-voltage supply | | x |
| Reactor building radiation level high (Indicated by monitors for main floor, subreactor room, building air, exhaust filters, and stack effluent) | | x |
| Reactor coolant flow low | | x |
| High coolant air temperature at exhaust filters | | x |
| Transient drive safety bolts out | | x |

The audible alarm and alarm light system (Panelite Inc. Type 30) features a common horn, horn silence button, and reset and lamp test switches. There are individual indicator lights for each alarm; therefore silencing an alarm caused by one input does not prevent a subsequent signal from actuating the respective indicator.

All signals which cause reactor shutdown are connected to the Shutdown Chassis (ANL Model CD176; Fig. 43e). This multiple trip unit contains 13 transistorized amplifiers which accept inputs adjustable over a range from 0.1 to 10 volts, and seven contact-operated circuits for inputs that do not require level adjustment. The outputs from the chassis are contacts on Electromechanical Specialities Co. Type EMS relays connected in series. The contacts are rated at 20 amp at 110 volts ac inductive, with drop-out times of 3 milliseconds. The power for the scram

latch solenoids is carried by contacts on these relays. An additional set of contacts on each relay is used to illuminate the scram indicator light on the alarm panel.

A circuit is installed in the Shutdown Chassis to bypass the steady-state scrams during transient operation.

4. Transient Control System

The following functions are performed by the transient control system (Fig. 44):

- (1) Release transient rod drive safety bolts and pressurize transient rod drive air system (by operator).
- (2) Start program timer (by operator).
- (3) Bypass steady-state trip circuits (by program timer).
- (4) Start and stop cameras and recorders (by program timer).
- (5) Actuate drive latch to drop transient and shutdown control rods in accordance with preset time schedule (by rod timer or electronic timer).
- (6) Scram reactor at preset time (by program timer and electronic timer, if desired).

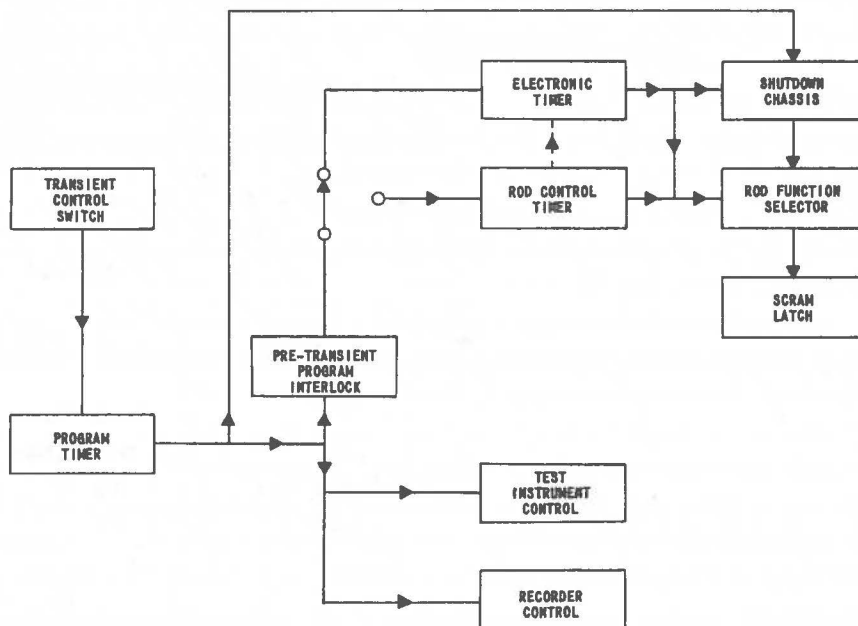


FIG. 44
SCHEMATIC OF TRANSIENT CONTROL SYSTEM

The Program Timer (see Figs. 44 and 45) is an Eagle Signal Co. Multiflex Mechanical Timer which has six contacts with opening and closing times adjustable over a range 0-60 sec. The Rod Timer is of the same type but with a range of 30 sec. It is used to control the programming of control rod drive scrams for transients longer than 10 sec.

The electronic timer (Computer Measurements Corporation Model 6028B) is used for accurate programming of transient and shutdown drives for transients up to 10 sec in duration. The electronic timer may also be used as an auxiliary to the rod timer for longer transients.

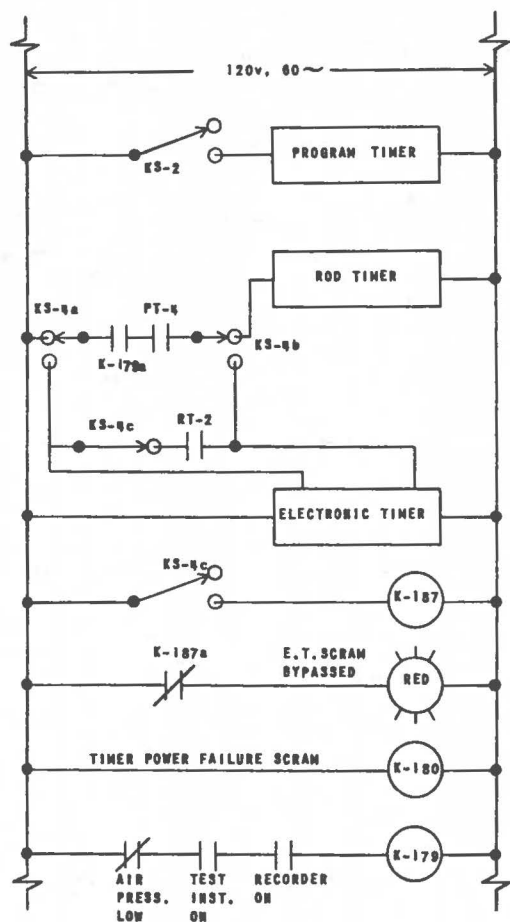
The Electronic Timer performs two switching functions: the first fixed at 0.001 sec, and the second variable from 0.001 to 9.99 sec, after the triggering signal. When the electronic timer is used as the primary rod control unit, the transient rods are operated by the fixed-time contact and scram is initiated by the variable time contact.

One set of contacts in the Program Timer is connected to initiate scram at a preset time and serves as a backup for the electronic and/or rod timers. Failure of power to any of the timers will result in reactor scram.

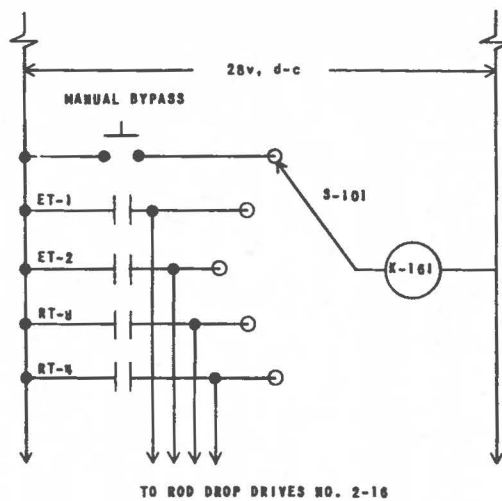
A relay (K-179, Fig. 45a) is installed to prevent starting of the Rod Timer or the Electronic Timer under the following conditions: (1) transient control rod drive air pressure is low; (2) Fast Recorder is inoperative; or (3) recording equipment (e.g., cameras) is inoperative. This relay has a time delay so that once started, the transient will not be terminated by any of the above conditions.

Transient operations are controlled independently from the transient programming and control cabinet. The cabinet is designed to provide flexibility in designating the function of individual control rod drives in a given experiment. The cabinet is locked except when transient experiments are being set up or in progress. However, the various indicator lights and control switches are visible through a glass panel in the cabinet door. These include:

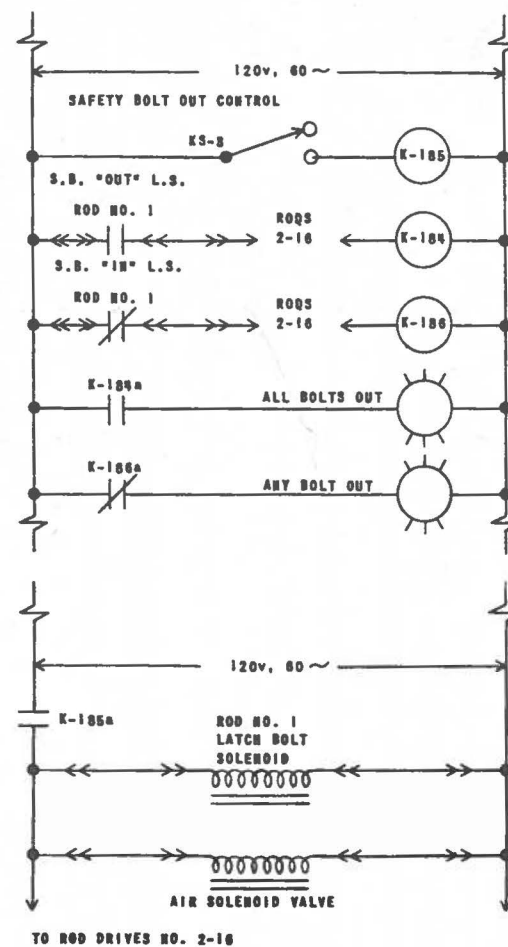
- (1) Safety bolt control switch (KS-3) which operates the transient control rod drive safety bolt solenoids, and transient air-control solenoid valve (Fig. 45c).
- (2) Program timer which starts switch (KS-2, Fig. 45a) which starts the transient.
- (3) Control selector key switch (KS-4, Fig. 45a) which selects either the rod timer or electronic timer as primary rod program control unit. When the rod timer is selected, contacts on the switch bypass the scram circuit on the electronic timer, and illuminate a warning light accordingly.



(a) TIMER CONTROL SYSTEM



(b) TIMER BUS SYSTEM



(c) ROD DRIVE SAFETY BOLT CONTROL

FIG. 45
TYPICAL CIRCUITRY FOR TRANSIENT CONTROL SYSTEM

- (4) Five-position selector switches (S-101, Fig. 45b) for each control rod drive scram latch. These switches connect the fast acting control relay (K-161, Fig. 45b and Fig. 43e) to any one of the four timing busses (ET-1, ET-2, RT-3, RT-4), or to the manual drop buttons on the control console.
- (5) Manual scram button.
- (6) Panel light which indicates that all safety bolts have been withdrawn, after closing switch KS-3 (Fig. 45c).

5. Radiation-monitoring System

The radiation-monitoring system consists of the following components:

- (1) A Jordan Electronics, Inc. Model "RAMS II" comprising a central power supply, and alarm and metering panel at the Control Building for detectors located in the subreactor room, on the main floor, and in the reactor coolant exhaust filters and exhaust stack. The detector in the exhaust stack is a dual range unit: 1 mr-1 r, and 1 r - 1000 r. The output of the stack detectors is recorded on a Brown Strip Chart Recorder, Model Y 153X17-V-II-III-30. The balance of the detector units have a range from 1 mr to 1 r. All detectors have remotely operated calibration sources.
- (2) The airborne activity in the Reactor Building is monitored with an Anton Model 23A cart mounted, continuous-sampling unit with integral recorder and alarm. The range of the detector is 0-27,000 counts/min. A remote alarm and alarm reset is installed in the Control Building.
- (3) High-level radiation electric signs are mounted at the top of the stairway leading to the subreactor room, and at the entrance to the exhaust filter room. The signs are illuminated by detectors located in the respective rooms.
- (4) An alarm is given on the Panelite unit annunciator panel in the Control Building when any one of the detectors registers a high level of activity.

Personnel monitoring equipment (Tracer Lab Model SU-3D) is installed in the Reactor Building.

6. Non-nuclear Instrumentation

The balance of the TREAT instrument and control system is comprised of the following components:

- (1) Coolant Air-flow Indicator - consisting of a Brown Model 293B2-D, low-range, bell-type transmitter, a Brown Model 204XI-F indicator, and an Ellison Draft Gage Co. straight stem-type pitot tube installed in one reactor outlet air duct. A second pitot tube which operates a Meriam Instrument Co. Model 40GE4 manometer is installed in the other outlet air duct and is used for calibration purposes.
- (2) Coolant Air Temperature-difference Recorder - is a Brown Model Y152X12-(W)-II-III-11-(V) circular chart recorder with Brown type-A resistance thermometers in the reactor inlet and outlet air ducts. The temperature range is from 0 to 100°C.
- (3) Twelve-point Temperature Recorder - unit consists of a Brown Model Y153X(67)-V12-II-III-(101)-(V) strip chart recorder, a remote stepping switch, a Pace Model BRJ14-24PP SPEC reference junction unit (150°F), and chromel-alumel thermocouples in fuel elements, reflector elements, permanent reflector, on the inside surface of the reactor shield, and in the coolant air outlet ducts. Two thermocouple patch panels are installed to facilitate connection of any of the many thermocouples to the reference junction and recorder. The number of wires required between the junction and the recorder is reduced from 24 to 5 by means of a remote stepping switch which is synchronized to the printing mechanism in the recorder.
- (4) Fast Recorder - is a Midwestern Instruments Model 606 light beam-type oscillograph with a capacity of 36 traces recording on direct writing-type paper. Paper speeds are adjustable from 0.07 to 173 in./sec. Galvanometers are available with natural frequencies to 8000 cps; however, 3000-cps galvanometers are being used, since these have adequate response plus larger deflection capabilities.
- (5) Fast Recorder Drive Amplifiers - are ANL Model A-145 transistor amplifiers with a maximum gain of 10 and a frequency response flat from 0 to 10,000 cps. The maximum output of these units is 150 ma into a 64-ohm load.

- (6) Thermocouple Amplifiers - are Video Instrument Co. Model 7212 amplifiers having a maximum gain of 1000 and a frequency response flat from 0 to 20,000 cps. These amplifiers are used to amplify signals from core thermocouples prior to transmission to the fast recorder driver amplifiers.
- (7) Wind Speed and Direction Recorder - is a Bendix Friez Model 120 wind speed and direction transmitter and a Model 141-7 recorder. The transmitter is mounted on a 10-ft mast on top the high bay of the reactor building.
- (8) Recording Barometer - is a Brown Model Y702X5-G-II-III-74 indicating and recording absolute pressure range of 20-30 in. Hg, absolute.
- (9) Ambient Air Thermometers - ordinary thermometers outside the reactor and control buildings.

7. Emergency Power

A 3.5-kw, gasoline engine driven, 115-volt, 60-cycle, ac generator provides emergency power for the following instruments:

- (1) Linear operating instrument
- (2) Radiation-monitoring system, with exception of building air monitor.
- (3) Twelve-point temperature recorder.



APPENDIX A

EVALUATION OF FUEL AND STRUCTURAL MATERIALSA. Outgassing of Graphite-Urania Fuel

A sample of fuel material was placed in a container having a free volume approximately equal to that of the reference fuel, outgassed for 24 hr at 900°C, and then sealed. The container was fitted with an electric heater, pressure transducer, and thermocouples.

The fuel was then irradiated in CP-5 for an integrated flux equivalent to 280 design transients (1000 Mw-sec) at an average temperature of 675°C. The result was a maximum pressure buildup of 53 mm Hg.

In view of the severity of the test conditions (peak temperature for a design transient is only 400°C), it is concluded that fuel outgassing will not pose a problem for a period of several years on a schedule of two 1000-Mw-sec transients per week.

B. Dimensional Changes of Graphite-Urania Fuel

Two fuel samples were encapsulated and irradiated in CP-5 for an integrated flux equivalent to 363 design transients at an average temperature of 290°C. Post-irradiation examination indicated a dimensional change of less than 0.033% in all of the three mutually perpendicular directions measured. On the basis of these studies it is concluded that the dimensional change of the fuel is negligible for the expected life of the reactor.

C. Increased Thermal Resistivity of Graphite-Urania Fuel

During the preceding irradiation study, the thermal resistivity of the fuel increased only 7% (as measured by increased temperature drop between the center and edge of the sample).

D. Corrosion of Zircaloy Can

The corrosion rate of Zircaloy-3 is <1 mil/year in air at 400°C (the hot spot fuel temperature in a 1000-Mw-sec transient). Hence, the life expectancy of the 25-mil Zircaloy fuel cans is many years based on design transients (1000 Mw-sec) and steady-state operation at 100 kw. The latter mode of operation results in peak fuel temperatures well below 400°C.

Above 400°C, the corrosion rate increases rapidly, and is about 0.9 mil/day at 700°C. In addition, the accelerated corrosion promotes growth of the metal. One Zircaloy fuel can exposed for two days in air at

700°C exhibited longitudinal and transverse growths of $\frac{7}{8}$ in. and $\frac{1}{16}$ in., respectively.

E. Reaction of Zircaloy with Graphite

Several experiments were performed to determine the extent of reaction between Zircaloy and graphite at elevated temperatures. In one test, a segment of fuel can containing a graphite block was placed in a bomb, evacuated, and heated to 900°C. No embrittlement or deleterious effect on the Zircaloy was noted, other than a slight discoloring. In another test, small discs of Zircaloy were placed in contact with graphite pellets in an evacuated bomb and held at 800°C for 60 days. Metallographic examinations showed no evidence of reaction at the Zircaloy-graphite interface. Based on these results, it is concluded that Zircaloy-graphite reactions do not constitute a danger to the integrity of the fuel cans up to temperatures where oxidation will damage them severely.

F. Oxidation of Graphite

Oxidation of the fuel element graphite reflector pieces is possible in the event the reactor becomes severely overheated. However, as shown in Table VI, the oxidation rate in air at 300°C is very low.

Table VI

OXIDATION RATES FOR GRAPHITE IN AIR

| <u>Temp,</u> <u>°C</u> | <u>Weight Loss,</u> <u>%</u> | <u>Time</u> | <u>Reference</u> |
|---------------------------|---------------------------------|-------------|------------------|
| 300 | 0.47 | 1000 days | 7 |
| 400 | 40 | 1000 days | 8 |
| 500 | 1 | 6-200 hr | 9 |
| 600 | 1 | 0.75-7 hr | 9 |
| 700 | 1 | 0.2-0.6 hr | 9 |

⁷L. P. Bupp, Trip Report: AEC Technical Cooperation Program on Graphite Gas Reactions, WASH-478-A (July 21, 1954).

⁸L. P. Bupp and S. S. Jones, The Pile Gas Problem, HW-20787 (June 1, 1951).

⁹The Production and Properties of Graphite for Reactors, National Carbon Co. (New York), 1955.

APPENDIX B

HEAT TRANSFER

The uranium oxide-graphite matrix acts as a heat sink during a transient; therefore, heat transfer calculations are primarily concerned with: (1) the rapidity of heat transfer from the uranium oxide particles to the graphite moderator; (2) the gross heat-absorbing capability of the fuel blocks; and (3) rate of heat transfer across the heat barrier between the fuel blocks and the axial graphite reflector blocks. The overall rate of heat removal from the core by the air coolant is not crucial, since it merely influences the core-operating temperature at a given steady-state power level, and the length of the post-transient cooling period.

Table VII is a summary of the design transient and steady-state temperatures for the reactor.

Table VII

REACTOR THERMAL DATATransient (nominal 5 x 5 x 4-foot core; 225 elements):

| | |
|---|--|
| Design energy release | 1000 Mw-sec |
| Average fuel temperature at termination of transient | 523°F |
| Maximum fuel temperature (hot spot) at termination of transient | 775°F |
| Time to cool hot spot to 150°F after transient | 1.5 hr |
| Air outlet temperature | Limited to 250°F by coolant bypass valve |

Steady-state (180 elements):

| | |
|--------------------------------------|-------------------------------------|
| Design power | 100 Kw |
| Zircaloy can hot spot temperature | 380°F |
| Fuel hot spot temperature | 510°F |
| Bulk air temperature rise (6500 cfm) | 68°F |
| Average heat flux | 1940 Btu/(hr)(ft ²)(°F) |
| Maximum heat flux | 2940 Btu/(hr)(ft ²)(°F) |
| Coolant velocity (6500 cfm) | 80 ft/sec |

A. Heat Transfer from Oxide Fuel Particles

The equation of Hetrick¹⁰ gives the time lag between the temperature of a uranium oxide particle and the average temperature of the surrounding graphite call in terms of geometrical arrangement, thermal properties of both materials, gas gaps between oxide and graphite, and period of exponential power rise. No allowance is made for heat released directly in the moderator due to escape of fission product fragments from the oxide particle; hence, for small particle sizes, the time lag is probably overestimated.

The time lag* for the TREAT fuel was calculated to be about 0.9 msec for operating conditions more severe than anticipated, i.e., with the reactor on a 5-millisecond period, a 44-micron oxide fuel particle (-325 mesh), and a 2-micron gas gap around the particle. This time lag is pessimistic because the actual average particle diameter for material passing 325 mesh is about 16-20 microns. The time lag was found to be essentially independent of uranium concentration below 1.0 wt-% uranium dioxide.

The effect of increased thermal resistivity of the fuel on the time lag was also studied. The time lag increases to 1.8 msec with a 67% increase in thermal resistivity. However, such a large increase in thermal resistivity is not expected because of the anticipated low burnup and annealing of neutron damage at reactor operating temperatures (see Appendix A). It is concluded that at peak temperature-limited operating conditions (period ~35 msec), there is negligible time lag in transfer of heat to the moderator. Under the most severe conditions examined (5-msec, 67% increase in thermal resistivity), the probable time lag (1.8 msec) will produce a maximum 43% increase in the integrated power of a transient due to the delay in operation of temperature coefficient.

B. Transient Heating and Cooling

The standard TREAT fuel element contains a 4-ft center section of uranium oxide-bearing graphite blocks canned in Zircaloy. Two aluminum cans containing the reflector graphite pieces are riveted to the top and bottom of the fuel section. To protect the aluminum cans and graphite reflector blocks from excessive heat resulting from possible transients greater than 1000-Mw-sec, a heat barrier is provided at both ends of the Zircaloy can. The barrier is a Zircaloy sheet stamping which essentially provides a dead space between the fuel blocks and the end of the evacuated can. Transient heat transfer calculations were performed for two cases: (1) without coolant

¹⁰D. L. Hetrick, The Effect of Fuel Particle Size on the Transient Behavior of a Homogeneous Graphite Reactor, NAA-SR-210 (December 1, 1952).

*The time lag is defined as the displacement in time between the time-temperature curve for the oxide particle, and the time-temperature curve for its surrounding moderator.

flow to determine the effectiveness of the barrier in protecting the aluminum and graphite, should it not be possible or desirable to turn on reactor coolant air immediately after a transient; and (2) with coolant flow to obtain cooling rates and fuel temperature profiles as a function of time.

1. Method

By applying the numerical method of Dusenberre¹¹ to an axial cylindrical segment of the core around a single coolant channel (Fig. 46), and writing heat balances for the 24 fuel plus reflector segments, a series of equations of the following form were obtained:

$$t_n(\theta + \Delta\theta) = \alpha_n t_n(\theta) + \beta_n t_{n+1}(\theta) + \gamma_n t_{n-1}(\theta) + \delta_n [C_{n-1}(\theta) + C_n(\theta)] \quad (1)$$

where

$$t_n(\theta) = \text{average temperature of segment } n \text{ at time } \theta$$

$$C_n(\theta) = \text{average temperature of coolant in channel adjacent to segment } n \text{ at time } \theta$$

$$\Delta\theta = \text{time interval}$$

$$\alpha_n, \beta_n, \gamma_n, \delta_n = \text{constants for segment } n.$$

Heat balances for the corresponding 24 segments of coolant channel yielded equations of the form

$$C_n(\theta) = A_n t_n(\theta) + (1 - A_n) C_{n-1}(\theta) \quad (2)$$

where A_n is a constant for segment n . The constants $\alpha_n, \beta_n, \gamma_n, \delta_n$, and A_n are functions of heat capacities and thermal resistances of fuel and coolant were calculated by hand. Equations (1) and (2) were programmed for the IBM-704 computer to calculate time-dependent temperatures, given an initial temperature profile.

2. Initial Temperature Distribution

The initial temperature distribution was obtained by assuming the energy input in question is released in the graphite-urania fuel of the nominal 5 ft by 5 ft by 4 ft core (225 elements). Measured enthalpy data for the graphite-urania fuel were used to obtain the peak core temperature rise. A maximum-to-average radial power distribution of 1.36, and an axial ratio of 1.19 (1.62 overall) were used to determine the peak integrated power. A

¹¹W. H. McAdams, Heat Transmission, McGraw-Hill Book Co., Inc., New York, (1954), 3rd ed., p. 44.

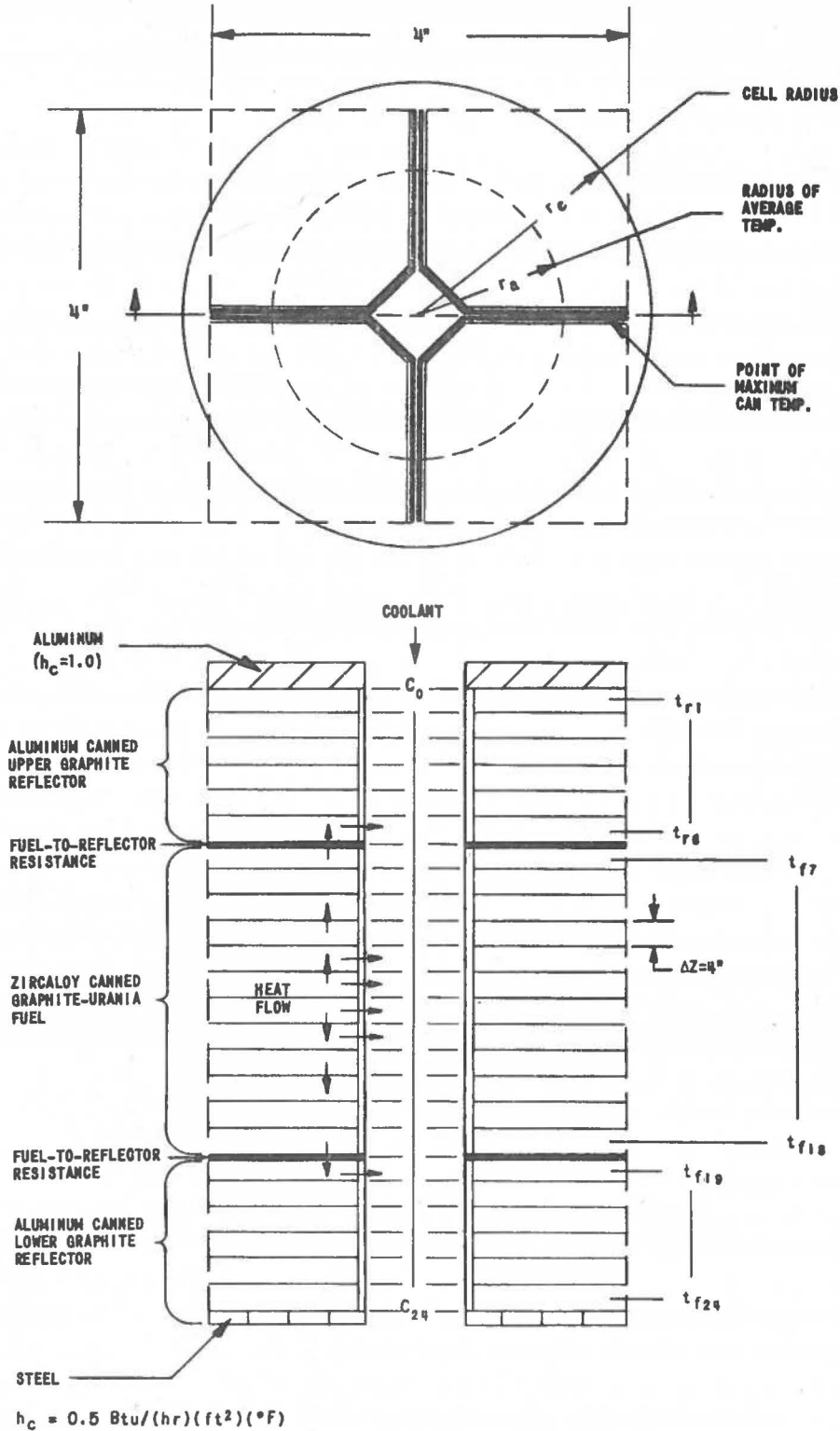


FIG. 46
 MODEL OF FUEL CELL USED FOR
 TRANSIENT TEMPERATURE
 CALCULATIONS.

chopped cosine was assumed to calculate the initial axial profile. It was further assumed that radial heat conduction between elements, and heat generation in the reflector (axial and radial) was negligible.

3. Thermal Resistances

In the fuel element there is a nominal gap of 0.055 in. between the can and fuel blocks before evacuation of the cans. It is difficult to determine the heat transfer across this gap due to the combined effects of conduction in a gas at reduced pressure, radiant heat transfer, and possible points of direct contact between the can and fuel blocks. In the absence of data, a conservative estimate of this resistance was made by assuming it to be equal to the conduction of an air gap at 1 atm pressure. The total radial resistance is then the sum of the following terms:

$$(1) \text{ Air film, } hD/k = 0.020 (\text{Re})^{0.8} \quad , \quad (3)$$

where

h = heat transfer coefficient, $\text{Btu}/(\text{hr})(\text{ft}^2)(^\circ\text{F})$

D = equivalent channel diameter, ft

k = thermal conductivity of air, $\text{Btu}/(\text{hr})(\text{ft})(^\circ\text{F})$

Re = Reynolds Number;

(2) Metal can wall;

(3) Air gap (discussed above);

(4) Fuel from inner wall of can to point of average temperature in the fuel.

The resistances were then lumped together so that Eq. (1) could be written in terms of the difference between the average graphite segment temperature and the coolant temperature. The lump radial resistance is written as

$$R = \Delta t/q \quad , \quad (4)$$

where

R = thermal resistance per foot of coolant channel, $(^\circ\text{F})(\text{hr})(\text{ft})/\text{Btu}$

q = heat transfer rate, Btu/hr per foot of coolant channel

Δt = temperature difference between coolant and fuel, $^\circ\text{F}$.

For purposes of calculation, the thermal resistance of the axial heat barrier at the end of the fuel can was assumed to be equivalent to a layer of asbestos $\frac{1}{4}$ in. thick. Experimental data obtained from an electrically heated model of a segment of the reactor core indicated that the asbestos layer and the Zircaloy spacer (actually used) offer about the same thermal resistance over the temperature range studied (up to 500°F). This experiment also verified that the values of radial (fuel to coolant) resistances were conservative.

4. Results

A calculated axial temperature profile at the core center after a 1000-Mw-sec transient is plotted in Fig. 47. The core is assumed to be initially at a uniform temperature of 100°F. The calculated peak fuel temperature is 775°F. Included for comparison are measured axial temperature plots in the central fuel element and one off-center element immediately following a 445-Mw-sec (1.9% $\Delta k/k$) transient (core loading = 163 elements). The peak fuel temperature attained in the transient was 506°F. The asymmetric shape of the measured profiles is typical of all transients, and is in agreement with flux traverse data.

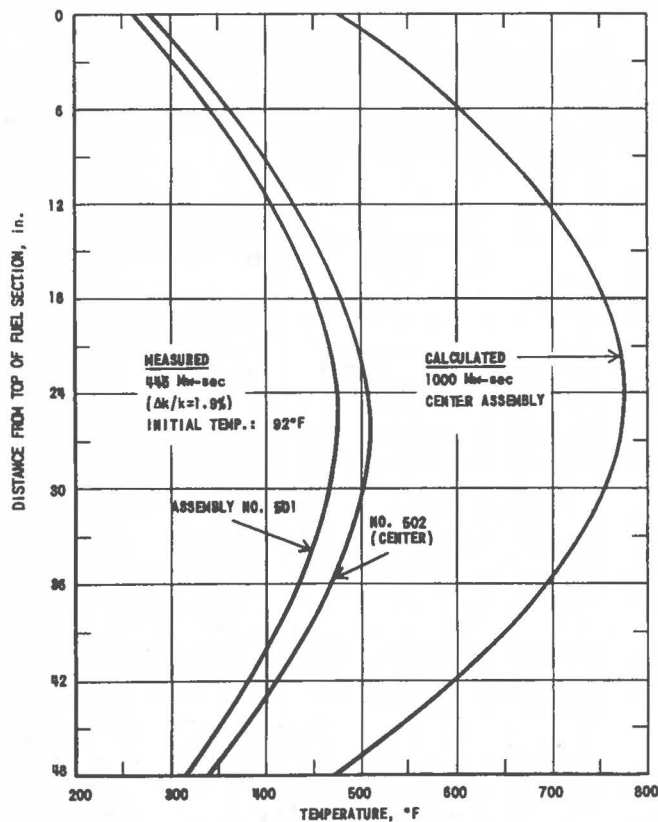
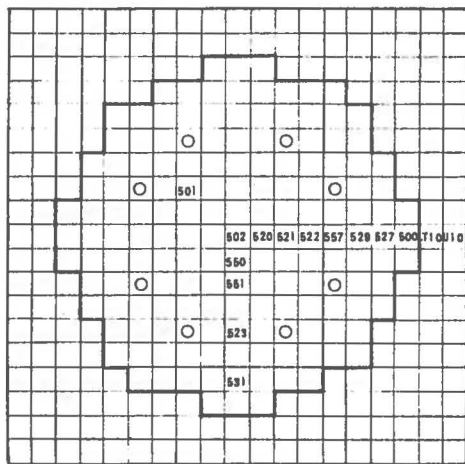
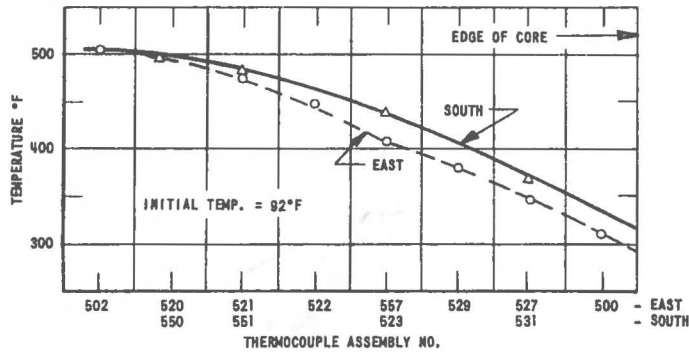


FIG. 47
CALCULATED AND MEASURED AXIAL TEMPERATURE PROFILES
IN FUEL IMMEDIATELY FOLLOWING TRANSIENTS.

Radial temperature profiles measured after the 445-Mw-sec transient are plotted in Fig. 48. The depression in the east profile was caused by control rods which were not fully withdrawn from the top of the core.

A maximum/average power ratio of 1.67 was calculated from temperature profiles taken from several other transients with core loadings of 160 assemblies. This ratio compares favorably with the value based on flux traverse data.

lated from temperature profiles taken from several other transients with core loadings of 160 assemblies. This ratio compares favorably with the value based on flux traverse data.



CORE LATTICE - 163 ASSEMBLIES

FIG. 48
MEASURED RADIAL TEMPERATURE PROFILES IMMEDIATELY
FOLLOWING A 445 Mw-sec TRANSIENT ($\Delta k/k = 1.0\%$)

A series of calculations was performed to determine the degree of protection afforded the aluminum cans by the thermal barrier of both ends of the Zircaloy can. The initial calculation considered the extreme conditions: an energy input of 2500 Mw-sec with no immediate flow of coolant air. This energy input is considered to be limiting, since corrosion of the Zircaloy fuel cans would be intolerably rapid at the peak fuel temperature (1450°F) corresponding to such a transient.

The results, plotted in Fig. 49, show that despite the absence of coolant air flow for almost 4 hr, the reflector temperatures are still well below the range that would promote damage of the aluminum cans, or oxidation of the graphite. The effects of convection cooling were neglected in the calculations;

therefore the cooling rates for the fuel section would be slightly higher than shown in Fig. 49.

Calculations were also made for energy inputs up to 2500 Mw-sec with coolant flow. In all cases, the peak temperature in the lower reflector was less than 400°F during the post-transient cooling period. The calculated peak air temperature at the exit of a center coolant channel was 490°F for a 2500-Mw-sec energy input. While the mixed mean temperature would be lower (depending on the core size and number of coolant channels), it would still exceed the maximum permissible operating temperature (250°F) of the exhaust filters. The coolant bypass line was installed to provide a means of subcooling the effluent air accordingly, should it become necessary to cool an overheated reactor.

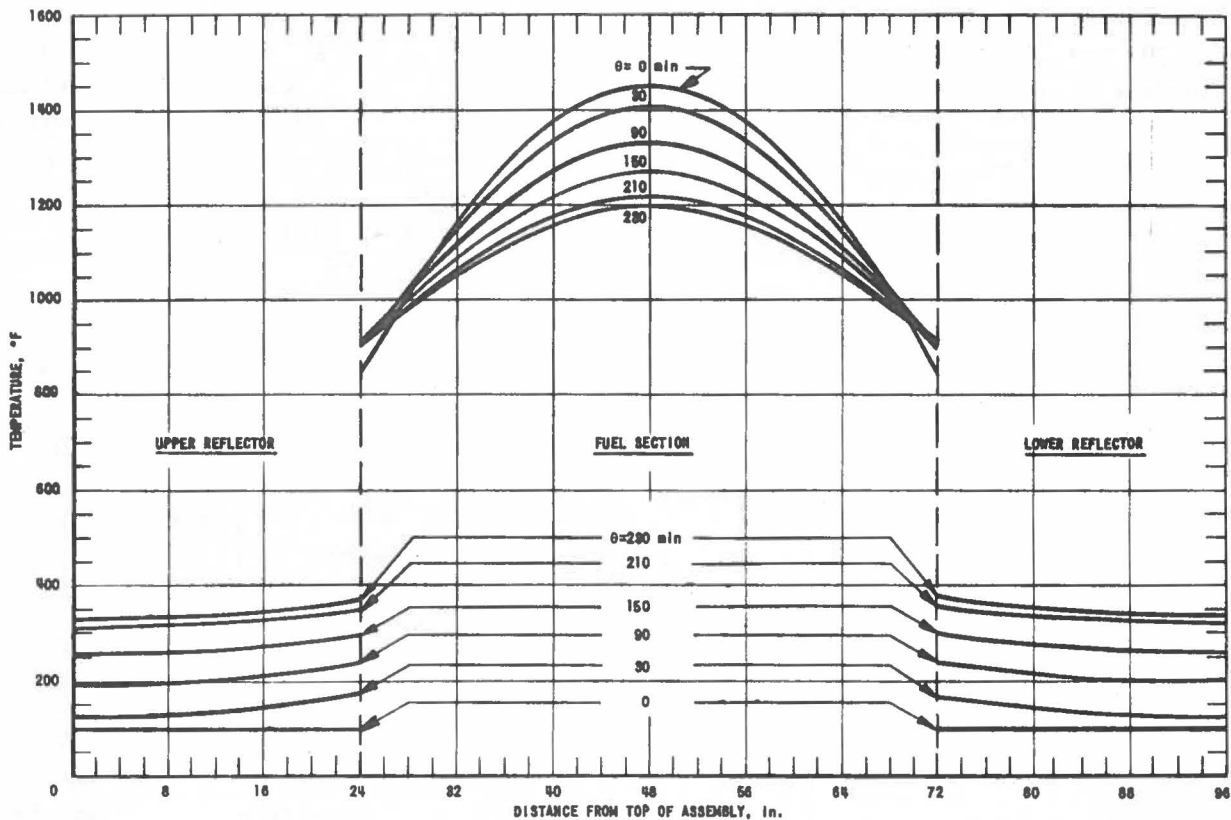


FIG. 49
CALCULATED AXIAL TEMPERATURE PROFILES IN CENTER FUEL ASSEMBLY AS A FUNCTION OF TIME AFTER A 2600 Mw-sec TRANSIENT WITH NO COOLANT FLOW.

Figures 50 and 51 show typical axial and radial temperature profiles measured during post-transient cooling from a peak temperature of 506°F (energy input = 445 Mw-sec). The effect of convection cooling can be seen in the profiles of Fig. 50 before the cooling air was turned on. The radial temperature profiles indicate (as would be expected) that radial conduction in the core is very slow during cooling.

Analysis of all transients performed in the reactor (as of this writing) indicates negligible heat generation in the axial and radial reflectors. The large permanent radial reflector is unaffected by temperature changes in the core.

C. Steady-state Cooling

Figure 52 shows the calculated temperature profiles for a central coolant channel during reactor operation at a steady-state power level of 100 kw. The coolant temperature rise was calculated from the known air flow rate and radial power distribution. Zircaloy can temperatures and fuel temperatures were then computed from the coolant profile by means

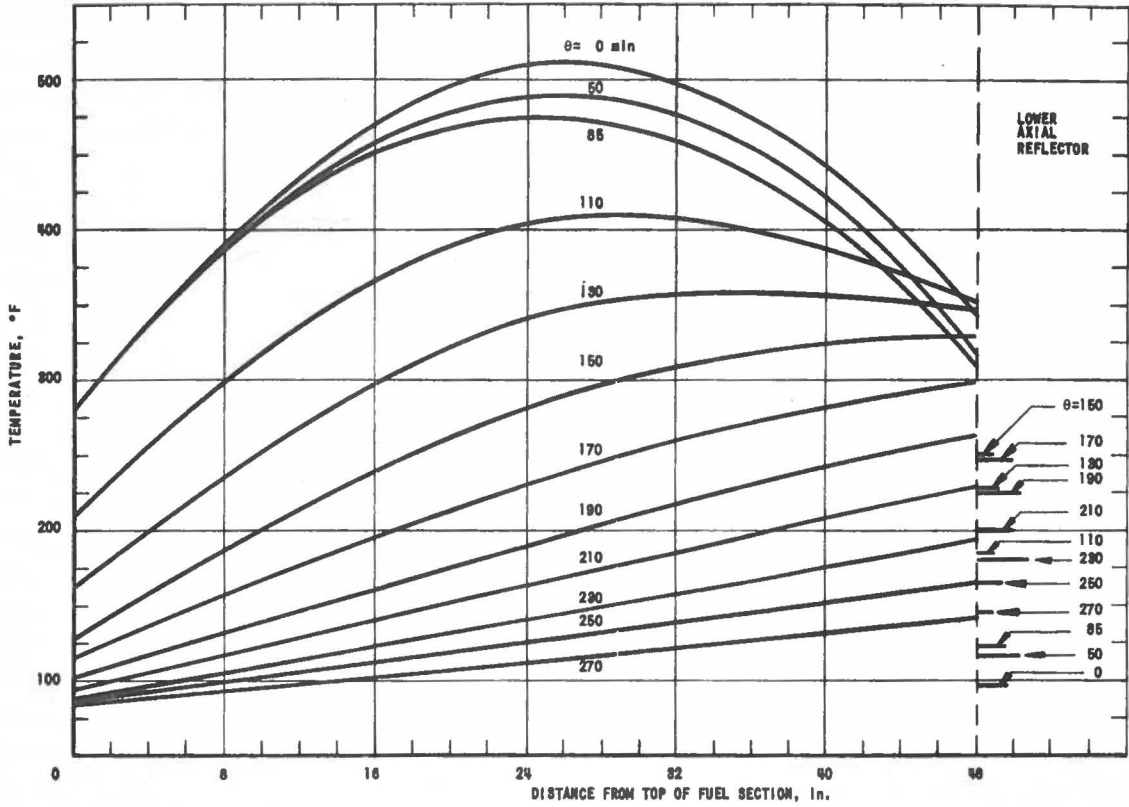


FIG. 50
MEASURED COOLING CURVES FOR CENTER FUEL ASSEMBLY AFTER A 446-Mw-sec TRANSIENT ($\Delta k/k = 1.9\%$). AIR COOLANT TURNED ON AT $\theta = 87$ min (70% FLOW).

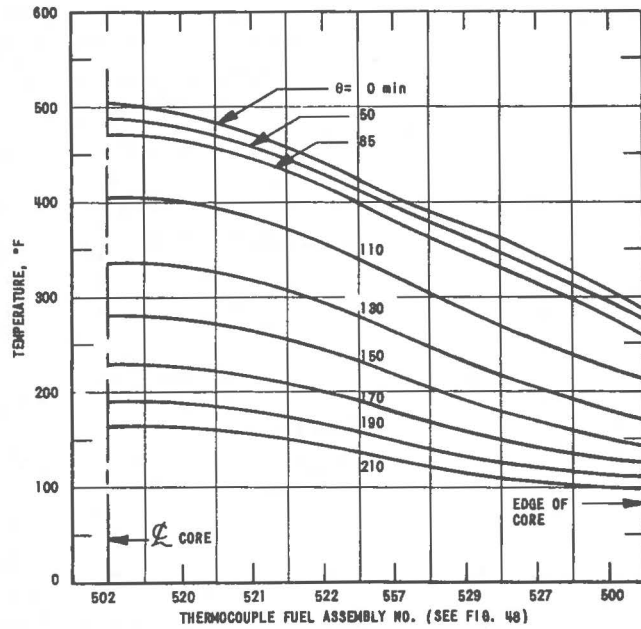


FIG. 51
MEASURED RADIAL TEMPERATURE PROFILES IN FUEL AS A FUNCTION OF TIME AFTER A 446 Mw-sec TRANSIENT ($\Delta k/k = 1.9\%$). AIR COOLANT TURNED AT $\theta = 87$ min (70% FLOW).

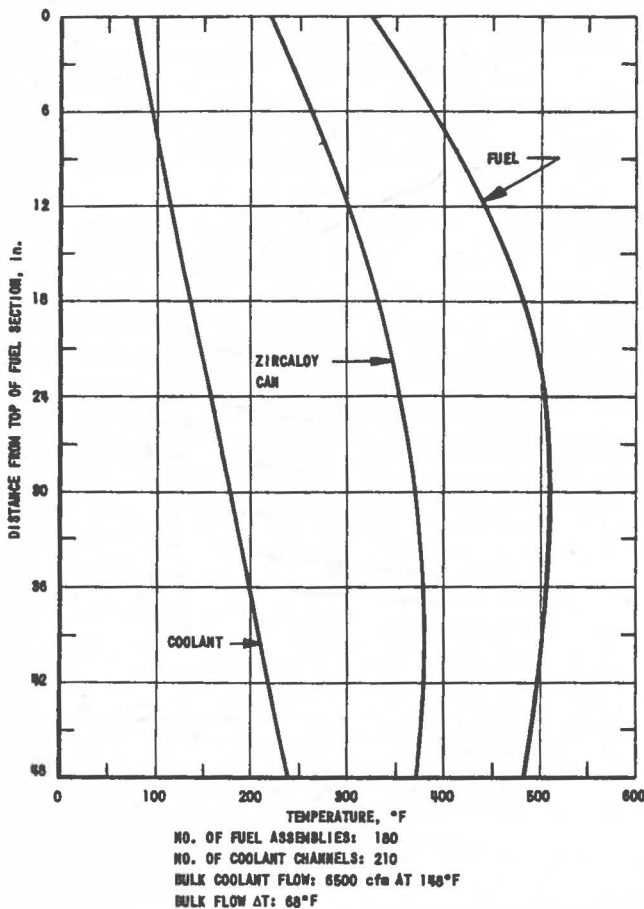


FIG. 52
 CALCULATED AXIAL TEMPERATURE PROFILES IN CENTRAL
 COOLANT CHANNEL AT 100 kw.

of using calculated heat fluxes and fuel-to-coolant thermal resistances. The thermal resistances were divided into two groups: (1) resistance from coolant to Zircaloy can (air film); and (2) resistance from cladding to fuel (can wall + air gap + fuel).

The number of coolant channels removing heat in the core will vary with the core loading. Accordingly, for a given power and coolant flow rate, the curves in Fig. 52 will shift to the right as the loading is decreased, and to the left as the loading is increased.

Figures 53 and 54 show the axial and radial temperature profiles measured at a power level of 50 kw, with 50% coolant flow and a loading of 157 fuel assemblies. The radial temperatures were measured at the horizontal midplane of the core. The axial profile at the core center (Fig. 53) shows a peak fuel temperature of 470°F. Figure 53 also

shows the effectiveness of the heat barrier in maintaining the temperature of the lower reflector well below that of the fuel hot spot. Figure 54 lends support to the assumption in the calculations (see page 89) that radial conduction of heat from the core to the temporary reflector is negligible.

D. Reactor Cooling with Viewing Slot

The TREAT core is comprised of slotted assemblies which permit visual access to experiments installed in the center of the core. The slots extend through the air gap between the core and radial reflector. As a consequence, some of the bulk coolant air flow to the upper portion of the slotted assemblies will be bypassed through the lateral opening. Accordingly, thermocouples are installed in the upper sections of two slotted assemblies to monitor the temperatures in these areas.

Figures 55 and 56 show the radial and axial temperature profiles measured at a power level of 100 kw with 84% coolant flow in a core with a

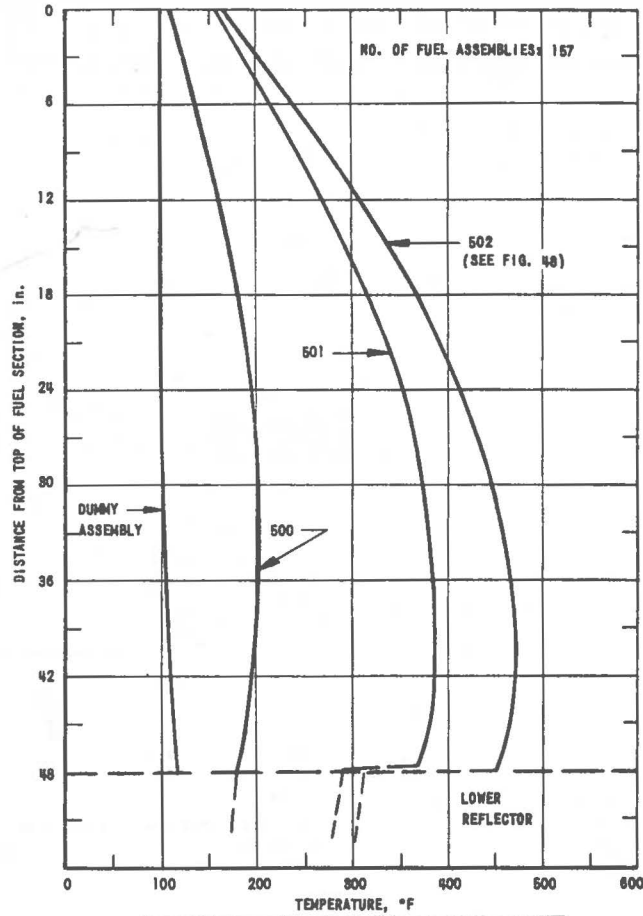


FIG. 53
MEASURED AXIAL TEMPERATURE PROFILES IN FUEL
AT 50 kw WITH 80% COOLANT FLOW.

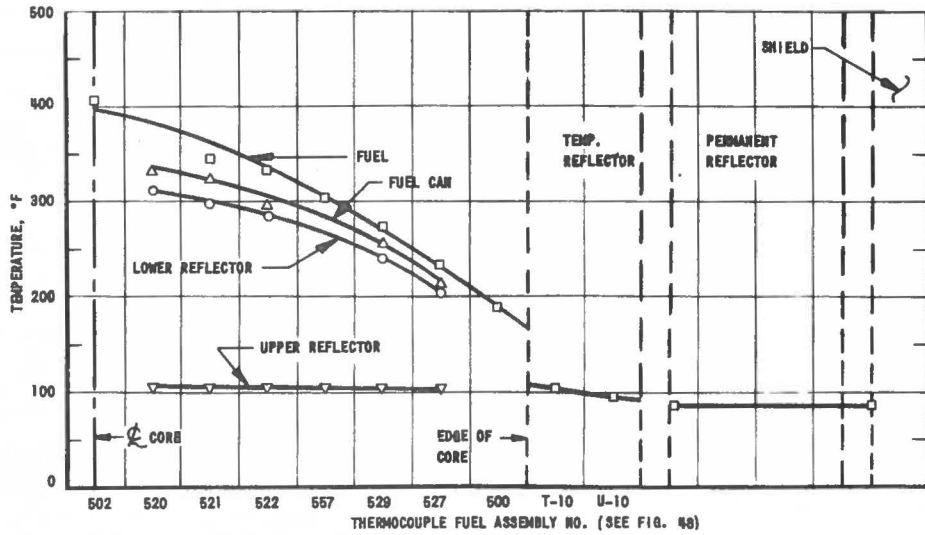


FIG. 54
MEASURED RADIAL TEMPERATURE PROFILES AT 50 kw
WITH 157 FUEL ASSEMBLIES AND 80% COOLANT FLOW.

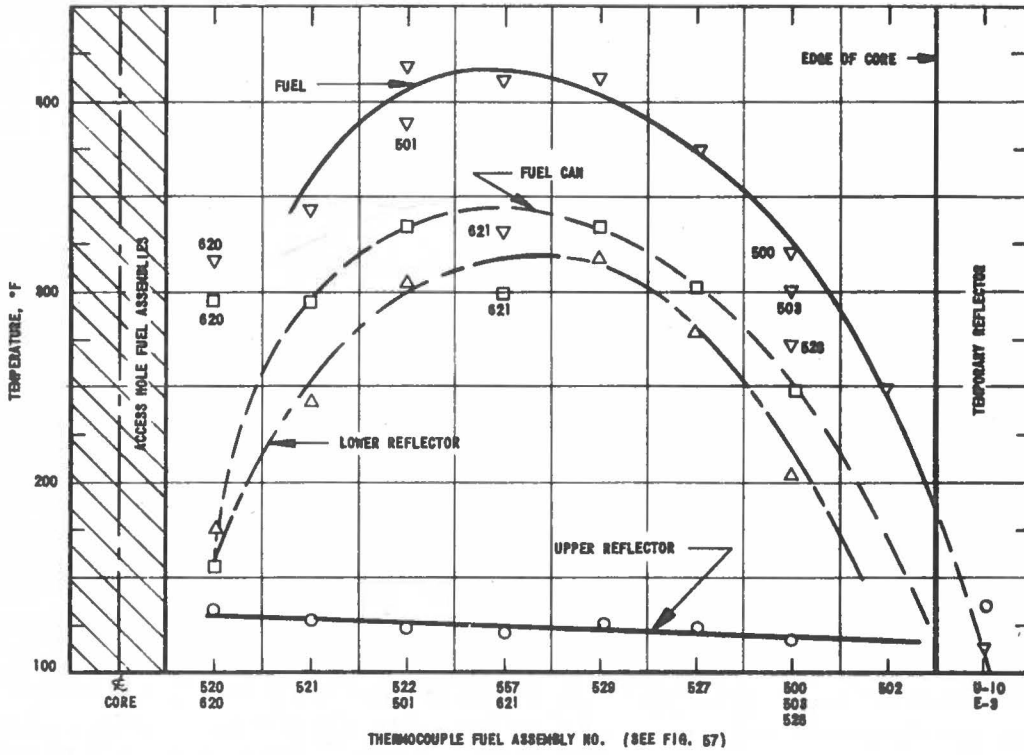


FIG. 55
 RADIAL TEMPERATURE PROFILES AT 100 kW WITH 84% COOLANT FLOW AND VIEWING SLOT THROUGH CORE CENTER.

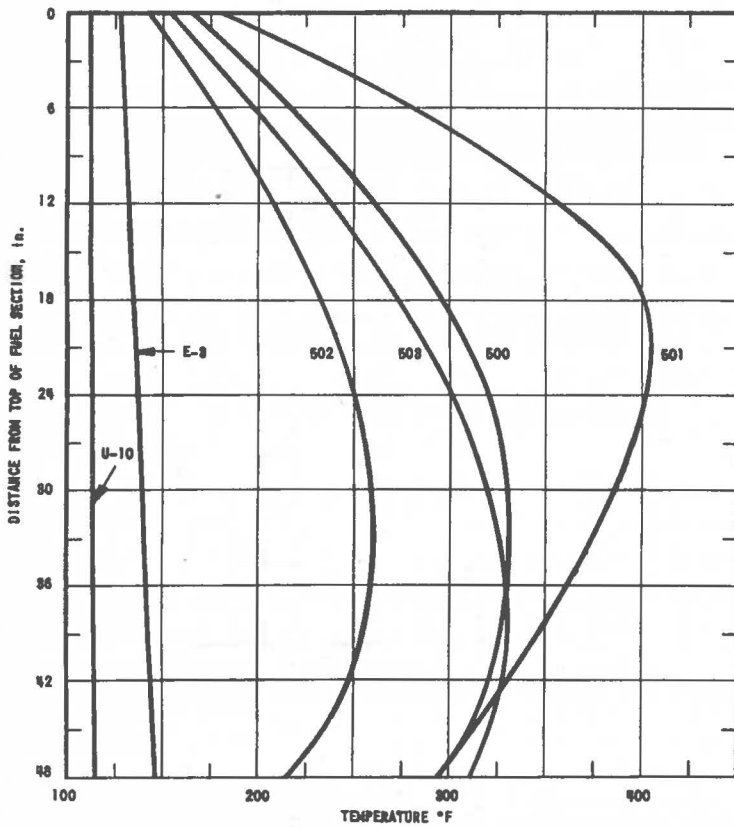


FIG. 56
 MEASURED AXIAL TEMPERATURE PROFILES IN FUEL AT 100 kW WITH 84% COOLANT FLOW AND VIEWING SLOT EXTENDING THROUGH CORE. (SEE FIG. 57).

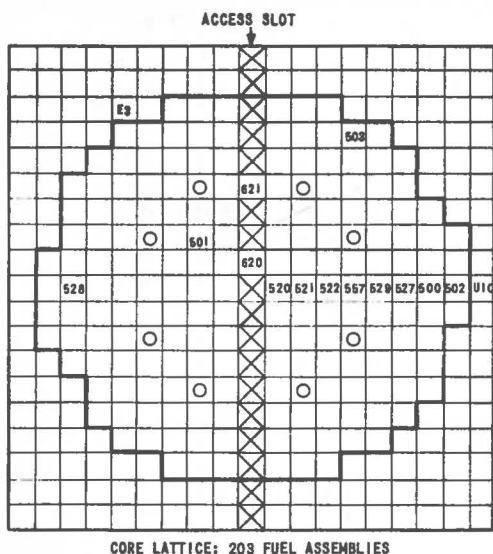


FIG. 57
PLAN VIEW OF CORE LOADING AND
LOCATION OF THERMOCUPLE FUEL
ASSEMBLIES USED TO MEASURE
TEMPERATURE PROFILES IN FIGS.
55 AND 56.

viewing slot extending through the core (north to south). The core loading is shown schematically in Fig. 57.

The radial fuel temperatures in the upper sections of the slotted assemblies are well below peak fuel temperatures elsewhere in the core. One explanation for this is that the reduction in coolant flow is compensated by the flux depression effected by the slot.

The axial temperature profiles illustrate the disturbance of normal coolant and heat flows in the core region close to the slot. The peak temperature in assembly No. 501 is shifted toward the upper end, whereas typical profiles are observed for elements farther removed from the slotted region. The peak temperature is still within tolerable limits; therefore the slot imposes no restriction on reactor operation at 100 kw.

E. Thermal Properties of Fuel

The results of thermal conductivity measurements on the graphite-urania fuel specimens are shown in Fig. 58. Curve A was plotted during step-wise electric heating of a fuel sample in a helium atmosphere from 150°F to 1950°F. The sample was held at 1950°F for 36 hr. Curve B was obtained during subsequent step-wise cooling.

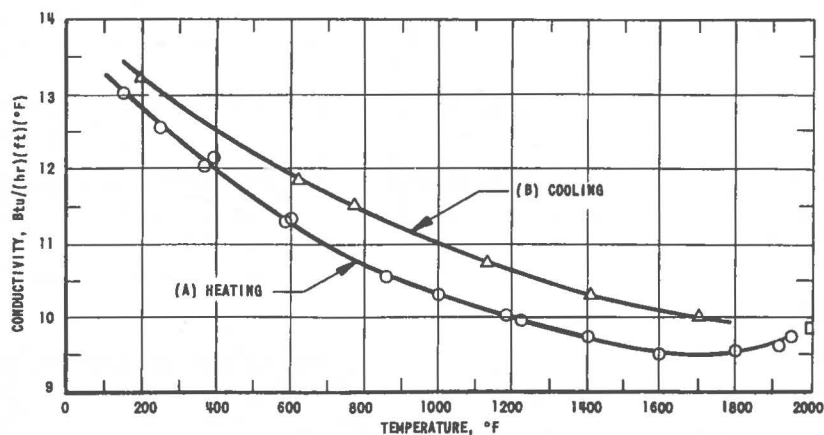


FIG. 58
MEASURED THERMAL CONDUCTIVITY OF SPECIMEN GRAPHITE-URANIA
FUEL DURING STEPWISE ELECTRIC HEATING IN HELIUM ATMOSPHERE.

Curve A is more representative of the fuel material in the reactor since the baking temperature of the fuel during fabrication (1650°F) is considerably below 1950°F. As would be expected, the thermal conductivity of the fuel is more nearly that of carbon rather than of graphite since the baking temperature is well below the graphitization range.

Figure 59 shows the measured enthalpy of the fuel material as a function of temperature. A 4th-order polynomial fit of the enthalpy curve was obtained by machine computation (IBM-704). This function was then differentiated to obtain the equation for heat capacity as a function of temperature:

$$C_p = 0.1614 + 0.0332 \times 10^{-2}T - 0.0651 \times 10^{-6}T^2 - 0.2384 \times 10^{-10}T^3 .$$

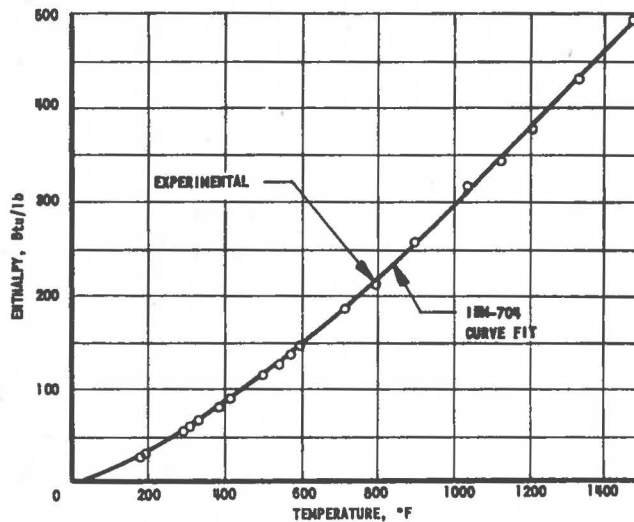


FIG. 59
ENTHALPY OF GRAPHITE-URANIA FUEL
(BASE TEMPERATURE = 32°F)

The results are plotted in Fig. 60.

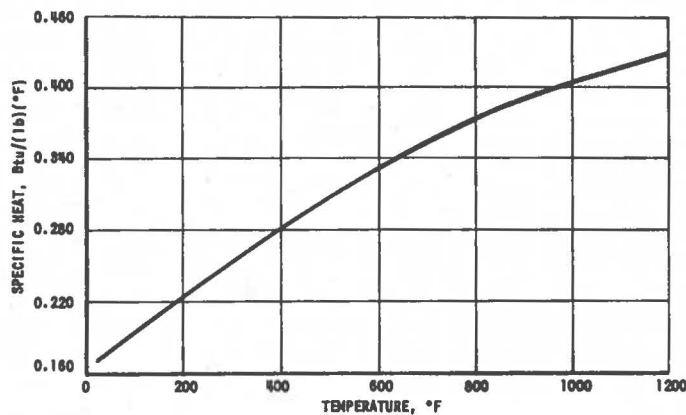


FIG. 60
HEAT CAPACITY OF GRAPHITE-URANIA FUEL

Other pertinent heat transfer and coolant flow constants for the reactor core are listed in Table VIII.

Table VIII

HEAT TRANSFER AND COOLANT FLOW CONSTANTS

Fuel Elements

| | |
|--------------------------------|--|
| Density | 1.72 gm/cm ³ (107 lb/ft ³) |
| Volume of fuel/assembly | 0.390 ft ³ |
| Weight of fuel/assembly | 41.7 lb |
| Thermal resistance* | |
| Fuel to coolant | 0.50 (°F)(hr)(ft)/(Btu) |
| Axial reflector to coolant | 0.50 (°F)(hr)(ft)/(Btu) |
| Zircaloy spacer (heat barrier) | 1.20 (°F)(hr)(ft)/(Btu) |

Coolant Channels

| | |
|--|--|
| Equivalent diameter | 0.0665 ft |
| Cross-sectional area | 0.00368 ft ² |
| Area per linear foot | 0.240 ft ² |
| Number of coolant channels removing heat | $(\sqrt{\text{Total Assemblies}} + 1)^2$ |

*Values are best estimates for temperatures up to 500°F, obtained from a trial-and-error fit of computer calculation to the curves of Fig. 50.

APPENDIX C

CONTROL ROD DRIVE CALCULATIONSA. Acceleration

From Newton's Law,

$$F = ma = mv_p \frac{dv_p}{dx} \quad (1)$$

where

F = force, lb

m = mass of moving component, (lb)(sec²)/ft

a = acceleration, ft/sec²

x = distance traveled, ft

v_p = velocity of moving components, ft/sec.

The force on the piston due to the compressed gas is given by

$$F = P_x A_d \quad (2)$$

where

A_d = piston area, in.²

P_x = pressure due to isentropic adiabatic expansion of the gas, lb/in.², at x distance of piston travel, ft.

The term P_x can be expressed by the equation

$$P_x = P_0 / [1 + (x/L_a)]^\gamma \quad (3)$$

where

P_0 = initial pressure, lb/in.²

L_a = length of accumulator, ft

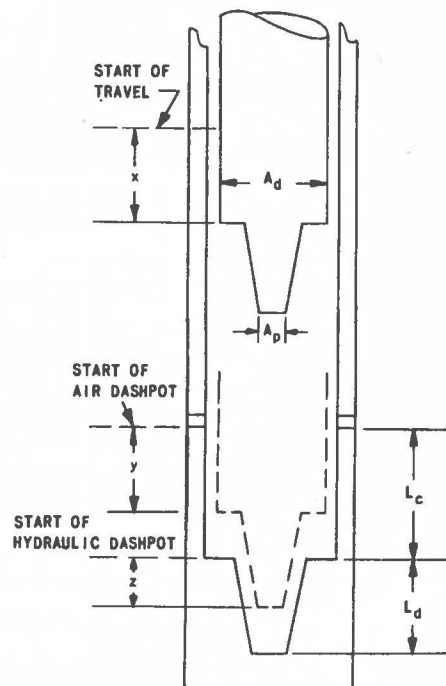
γ = ratio of molal heat capacities
(air)

$$= C_p / C_v = 1.4$$

Neglecting friction losses and assuming that the air back pressure at the front of the piston is atmospheric, the velocity at distance x is obtained by combining Eqs. (1), (2), and (3):

$$mv_p \frac{dv_p}{dx} = A_d \left[P_0 \frac{1}{[1 + (x/L_a)]^\gamma} - P_a \right] \quad (4)$$

and integrating:



$$\int_{v_0}^{v_x} v_p dv_p = \frac{A_d}{m} \left[\int_0^x P_0 \frac{1}{[1 + (x/L_a)]^\gamma} - \int_0^x P_a \right] dx \quad (5)$$

Thus, for $v_0 = 0$,

$$v_x = \sqrt{\frac{2A_d}{m} \left[\frac{P_0 L_a^\gamma (L_a + x)^{1-\gamma}}{1-\gamma} - \frac{P_0 L_a}{1-\gamma} - P_a x \right]} \quad (6)$$

For downward movement, gravitational acceleration is added.

Equation (6) was used to calculate the velocity as a function of distance traveled of a pneumatic accelerator for TREAT. The following values were substituted for the terms in the equation:

$$\begin{aligned} A_d &= 10.2 \text{ in.}^2 \\ m &= 0.518 \text{ (lb)(sec}^2\text{)/in.} \\ P_0 &= 350 \text{ psi} \\ P_a &= \text{atmospheric pressure} \\ L_a &= 40 \text{ in.} \\ \gamma &= 1.4 \end{aligned}$$

The results are plotted in Fig. 61.

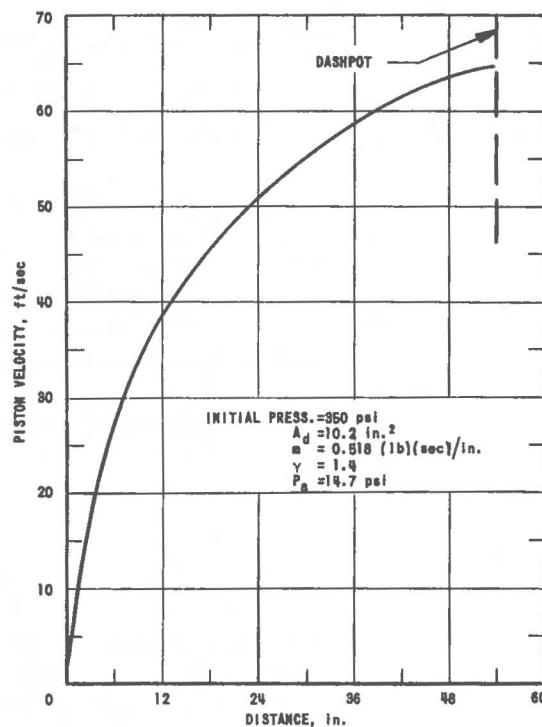


FIG. 61
VELOCITY OF PISTON VS. DISTANCE TRAVELLED
FOR PNEUMATIC ACCELERATOR.

Figure 62 shows the experimental data in terms of distance vs time for various starting pressures. The data were taken by means of photo-electric cells and a Sanborn recorder. The time can be obtained by numerical or graphical integration of the equation

$$t = \int (1/v_p) dx \quad (7)$$

Numerical integration of the calculated curve is in reasonable agreement with the corresponding experimental curve on Fig. 62, indicating relatively small friction losses in the scram mechanism.

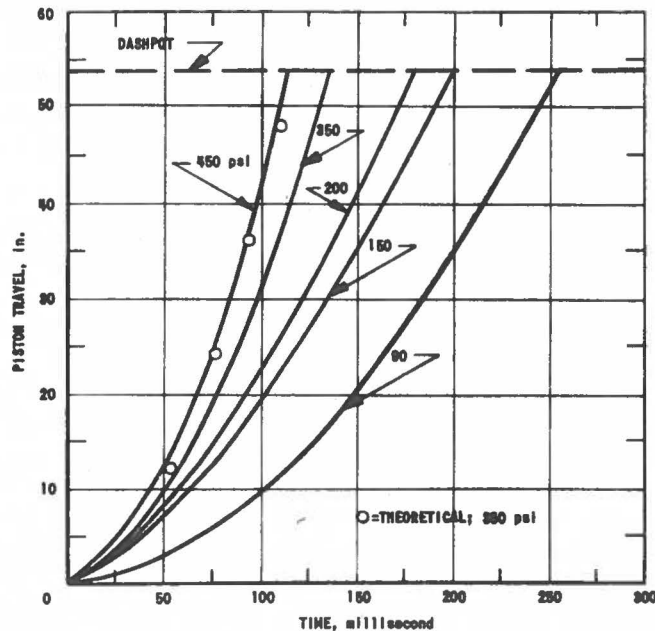


FIG. 62
PERFORMANCE OF PROTOTYPE ACCELERATOR
AT VARIOUS INITIAL PRESSURES.

B. Deceleration

1. Air Chamber

Analogous to Eq. (3), the pressure of the confined gas (P_y) varies with distance as follows:

$$P_y = P_a \left[\frac{1}{1 - (y/L_c)^\gamma} \right] \quad (8)$$

where

P_a = initial atmospheric pressure in air chamber, psi
 y = distance of piston travel into air chamber, ft
 L_c = total length of air chamber, ft.

Assuming that the air pressure of the accumulator is relieved, the expression for the retarding force is obtained by combining Eqs. (8) and (1):

$$mv_p \frac{dv_p}{dy} = -A_c P_a \left[\frac{L_c^\gamma}{(L_c - y)^\gamma} - 1 \right] \quad (9)$$

where A_c is the cross-sectional area of the air chamber (in.²). By integrating.

$$\int_{v_1}^{v_y} v_p dv_p = -\frac{A_c P_a}{m} \int_0^y \left[\frac{L_c}{(L_c - y)^\gamma} - 1 \right] dy \quad (10)$$

and

$$\begin{aligned} v_y^2 - v_1^2 &= -\frac{2A_c P_a}{m} \left\{ L_c^\gamma \left[\frac{(L_c - y)^{1-\gamma}}{\gamma-1} - \frac{L_c^{1-\gamma}}{\gamma-1} \right] - y \right\} \\ &= -\frac{2A_c P_a}{m} \left\{ \frac{L_c^\gamma}{\gamma-1} [(L_c - y)^{1-\gamma} - L_c^{1-\gamma}] - y \right\} \quad (11) \end{aligned}$$

the velocity at distance y is given by the equation

$$v_y = \sqrt{v_1^2 - \frac{2A_c P_a}{m} \left\{ \frac{L_c^\gamma}{\gamma-1} [(L_c - y)^{1-\gamma} - L_c^{1-\gamma}] - y \right\}} \quad (12)$$

Figure 63 shows plots of piston velocity vs distance into the air chamber for various initial piston velocities. The curves indicate that the air chamber is efficient only for the very last part of the compression; hence the hydraulic dashpot was added.

2. Hydraulic Dashpot

The hydraulic dashpot was designed to dissipate energy by forcing fluid to flow in an annular duct. By Darcy's formula

$$h_f = f \frac{L_d v_f^2}{(D)(2g)} \quad (13)$$

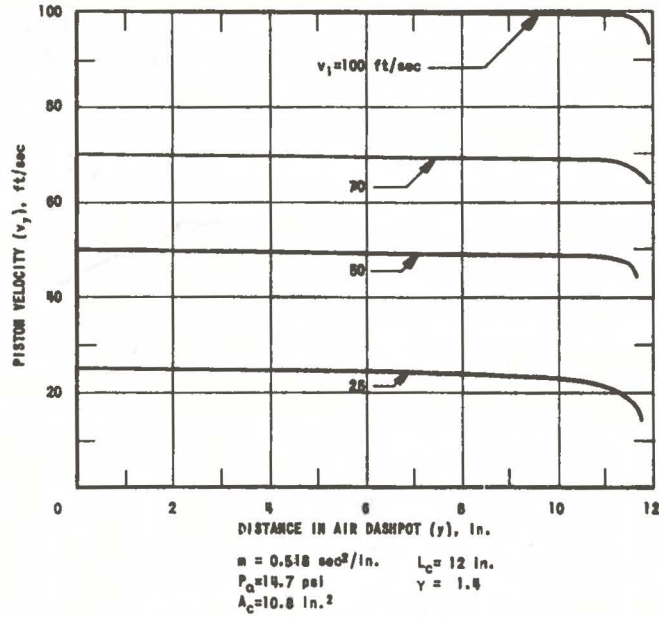


FIG. 63
 CALCULATED PISTON VELOCITY VS DISTANCE
 TRAVELED IN AIR DASHPOT FOR VARIOUS INITIAL
 VELOCITIES.

where

- h_f = hydraulic head, ft
 D = hydraulic diameter, ft
 v_f = velocity of fluid, ft/sec
 g = gravitational constant, $(\text{lb}_{\text{mass}})(\text{ft})/(\text{lb}_{\text{force}})(\text{sec}^2)$
 f = friction factor
 L_d = length of hydraulic dashpot, ft.

The area of the annulus is given by

$$A_a = (D_p + b)b\pi \quad (14)$$

and the area of the piston is

$$A_p = \left(\frac{1}{2} D_p\right)^2 \pi \quad (15)$$

where

- D_p = diameter of piston, in.
 b = radial clearance, in.

The velocity of the fluid is given by

$$v_f = (A_p/A_a)v_p \quad , \quad (16)$$

where

$$v_p = \text{velocity of piston.}$$

Combining Eqs. (14), (15), and (16),

$$v_f = \frac{v_p D_p^2 \pi}{4(D_p b + b^2)\pi}$$

and neglecting b^2 , since b is a small quantity,

$$v_f = v_p D_p / 4b \quad . \quad (17)$$

For small values of b , the hydraulic radius is given by

$$r_n = \frac{(D_p + b)\pi b}{\pi(2D_p + 2b)} = \frac{b}{2} \quad . \quad (18)$$

Then

$$D = 4r_h = 2b \quad . \quad (19)$$

Substituting into Eq. (13)

$$h_f = fL_d v_p^2 D_p^2 / 64gb^3 \quad (20)$$

and

$$\Delta p = h_f \rho \quad , \quad (21)$$

where

$$\rho = \text{density of fluid, lb/ft}^3.$$

The shear resistance is given by

$$\tau = (\Delta p)A_a \quad . \quad (22)$$

Finally, the incremental kinetic energy dissipated is

$$dKE = \tau dz \quad , \quad (23)$$

where

z = distance of piston travel into dashpot.

Making the necessary substitutions,

$$dKE = f \frac{\rho \pi D_p^3 v_p^2 z dz}{64 g b^2} \quad (24)$$

The Darcy friction factor (f) is eliminated from Eq. (24) by use of the familiar Poiseuille relationship for laminar flow:

$$f = 64/Re \quad , \quad (25)$$

where

$$\begin{aligned} Re &= \text{Reynolds Number} \\ &= D v \rho / \mu \end{aligned} \quad .$$

Combining Eqs. (17) and (25):

$$f = 128 \mu / v_p D_p \rho \quad . \quad (26)$$

Substituting Eq. (26) into Eq. (24),

$$dKE = \frac{2 \mu \pi D_p^2 v_p^2 z dz}{g b^2} = \tau dz \quad . \quad (27)$$

The expression for change of dashpot plunger velocity with distance traveled into the dashpot is obtained by combining Eqs. (27) and (1):

$$\frac{dv_p}{dz} = - \frac{2 \mu \pi D_p^2 z}{W b^2} \quad , \quad (28)$$

where

W = weight of moving components, lb

Substituting for a tapered dashpot,

$$b = c - \frac{cz}{L_d} \quad , \quad (29)$$

where

c = maximum radial clearance

L_d = length of dashpot with piston fully inserted

yields

$$\frac{dv_p}{dz} = - \frac{2\mu\pi D_p^2 L_d^2 z}{W(L_d c - cz)^2} \quad (30)$$

Integrating,

$$\int_{v_0}^{v_z} dv_p = - \frac{2\mu\pi D_p^2 L_d^2}{Wc^2} \int_0^z \frac{zdz}{(L_d - z)^2}$$

and

$$v_z = v_0 - \frac{2\mu\pi D_p^2 L_d^2}{Wc^2} \left(\ln \frac{L_d - z}{L_d} + \frac{L_d}{L_d - z} - 1 \right) \quad (31)$$

where

v_z = velocity of moving component at distance z

v_0 = velocity of moving component when plunger enters dashpot.

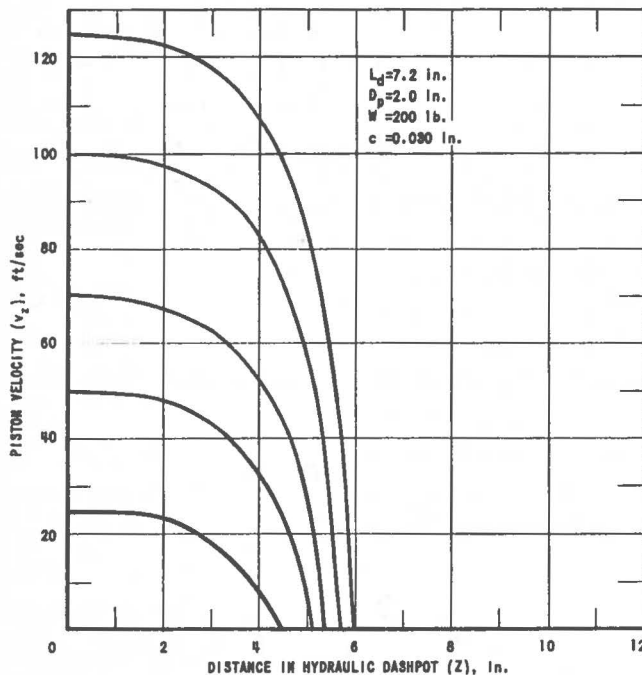


FIG. 64
CALCULATED PISTON VELOCITY VS DISTANCE
TRAVELED IN HYDRAULIC DASHPOT. ASSUMED
VISCOSITY OF DIL: 1182 cp AT 10,000 psi.

Figure 64 is a plot of Eq. (31) for various initial velocities. It is difficult to obtain an accurate estimate for the dashpot fluid viscosity (μ) because of the high and changing pressure in the dashpot. Furthermore, the flow occurs in a very narrow annulus; hence shearing of the oil films contributes appreciably to the fluid friction.

According to McAdams,¹² the theoretical fluid flow equations are applicable for flow in annuli having length: width ratios as small as 0.050. For the dashpot under consideration, this ratio is 0.0024; hence the friction losses are greater than predicted by the friction factor used in deriving Eq. (31). For these reasons, the curves of Fig. 64 are to be considered as lower limits for the dashpot performance.

¹²W. H. McAdams, Heat Transmission, McGraw-Hill Book Co., Inc., New York (1954), 3rd ed., p. 150.

For purposes of comparison, an alternate derivation of the dashpot distance-velocity relationship was made, assuming a constant friction factor. Combining Eqs. (24) and (1), and integrating gave

$$v_z = v_0 / \exp \left[\frac{f \pi \rho D_p^3 L_d^2}{64 W c^2} \left(\ln \frac{L_d - z}{L_d} + \frac{L_d}{L_d - z} - 1 \right) \right] \quad (32)$$

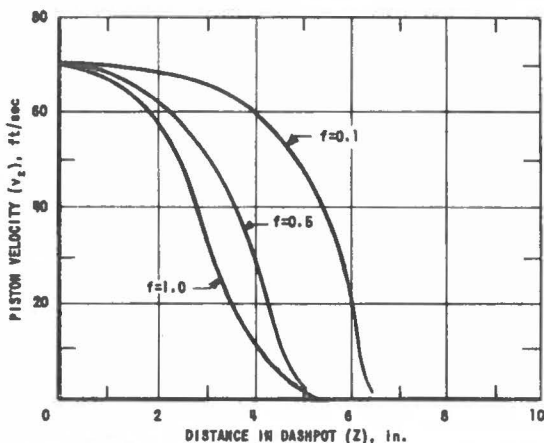


FIG. 65
PISTON VELOCITY VS DISTANCE
TRAVELED IN HYDRAULIC DASHPOT
FOR SEVERAL VALUES OF FRICTION
COEFFICIENT.

Figure 65 is a plot of Eq. (32) with an initial velocity (v_0) of 70 ft/sec for various values of the Darcy friction factor (f). The curve for $f = 0.5$ most nearly coincides with the curve derived from the experimental data. Thus, the high value of f (about a factor of 10 above a reasonable value) necessary to fit the equation to the data supports the breakdown of the usual empirical relationships for this dashpot, as discussed above.

C. Mechanical Strength of Control Rods

The control rods were studied with regard to buckling and dynamic stresses when rapidly accelerated or decelerated. The control rods as slender

columns tend to buckle under a dynamic load (approximately) according to the equation

$$l_{cr} = \sqrt[3]{\frac{\pi^2 E I g}{(122)^2 q a}} \quad (33)$$

where

- l_{cr} = critical length (distance between support points), in.
- E = modulus of elasticity, psi
- I = moment of inertia, in.⁴
- q = weight of rod per unit length, lb/in.
- a = acceleration (deceleration in this case), in./sec².

Figure 66 is a plot of Eq. (33) for 1.750-in. diameter control rods with wall thicknesses of $\frac{1}{8}$ in. and $\frac{1}{4}$ in., respectively. The curves indicate little effects due to difference between the two wall thicknesses and the advisability of supporting the control rods at 60-in. intervals.

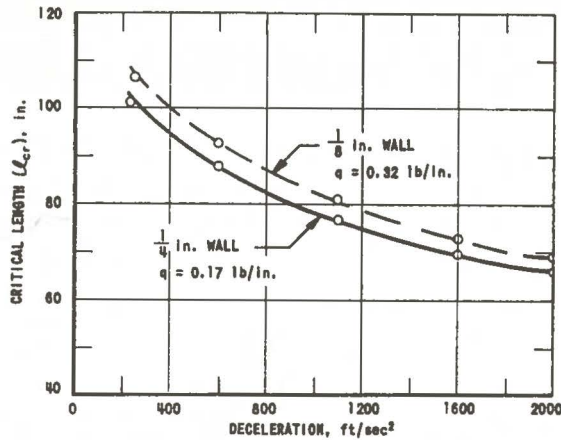


FIG. 66
CRITICAL LENGTH OF TUBULAR CONTROL ROD AS A
FUNCTION OF WALL THICKNESS AND DECELERATION.

The impact stress induced in a control rod as a result of a sudden stop from a given velocity is given by the approximate equation

$$\sigma_i = v_i \sqrt{\frac{WE}{gA\ell}} \quad (34)$$

where

- σ_i = impact stress, lb/in.²
- v_i = impact velocity, ft/sec
- W = weight of tube, lb
- A = cross-sectional area of tube, in.²
- ℓ = length of tube, in.
- E = modulus of elasticity, psi
- g = gravitational constant.

Figure 67 is a plot of Eq. (34) for 1.750-in. diameter control rods with wall thicknesses of $\frac{1}{8}$ in. and $\frac{1}{4}$ in., respectively. The large stresses produced even at moderate impact velocities indicate the need of eliminating impact in the dashpot. Because of the reduced weight, the stress in a $\frac{1}{8}$ -in. wall tube is not significantly greater than that produced in a $\frac{1}{4}$ -in. wall tube.

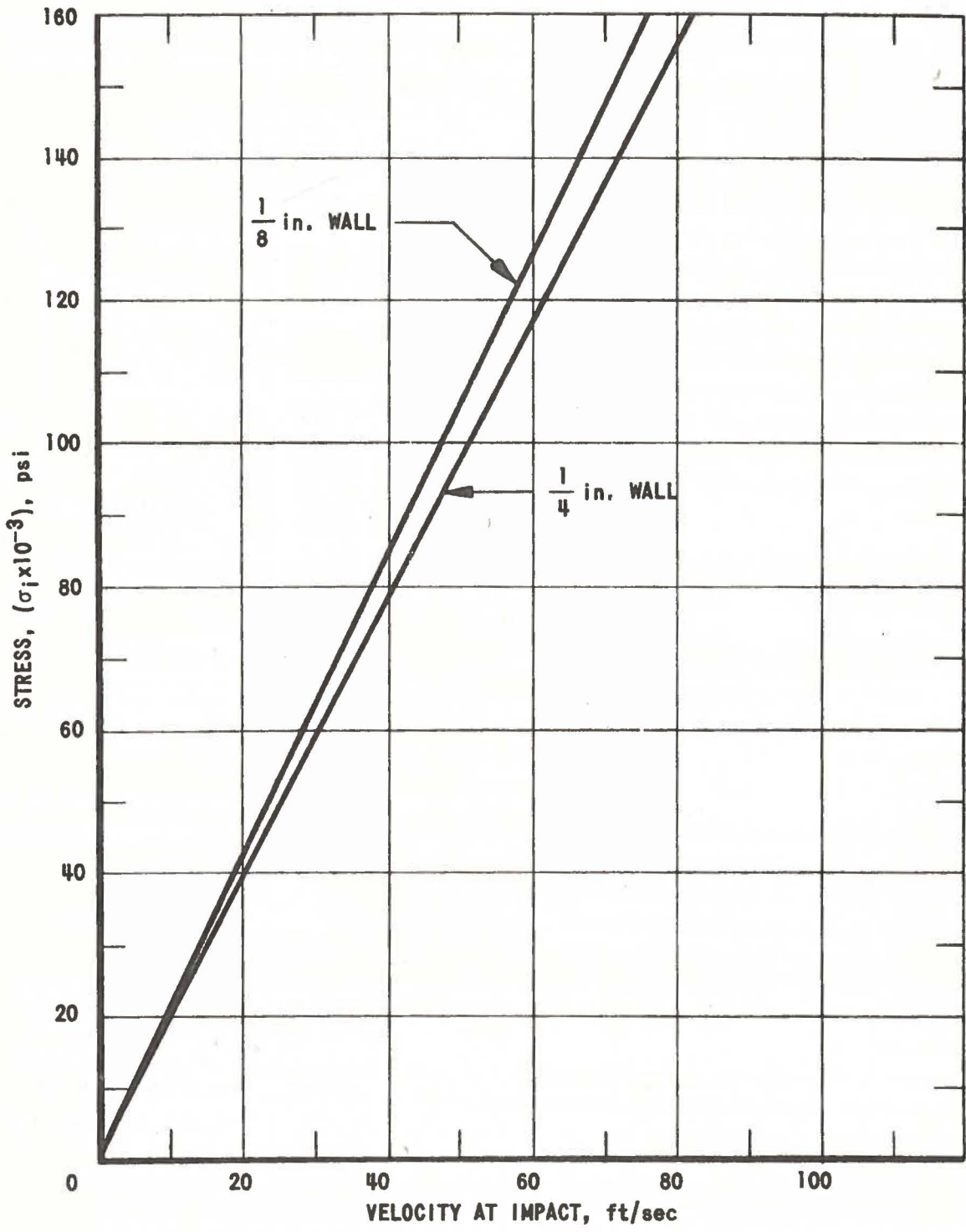


FIG. 67
INDUCED STRESS VS IMPACT VELOCITY
FOR TUBULAR CONTROL RODS (1.750 in.
O.D.)

APPENDIX D

SHIELD DESIGN CALCULATIONSA. Basis for Design

The following operational limits of the reactor were used as a basis for the shield design:

- (1) Operation at a maximum steady-state power level of 100 kw for a period not to exceed 100 hr.
- (2) During steady-state operation up to 100 kw, personnel access will be limited to the main floor around the reactor, the top of the reactor, and the sodium-equipment room. Personnel will not be permitted to enter the sub-reactor room while the reactor is operating.
- (3) Transients will not exceed 1000 Mw-sec of integrated power.
- (4) Transient operation of the reactor will be controlled from a remote location. All personnel will be evacuated from the Reactor Building prior to the onset of transient operations.
- (5) Personnel access to the top of the reactor for fueling operations, etc., will not be permitted for several hours after transients and after sustained periods of operation at 100 kw.

B. Calculations

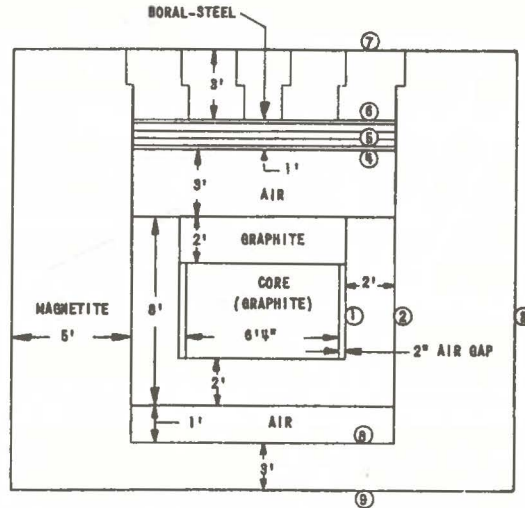
The shielding thicknesses were calculated by means of fast neutron removal theory and thermal neutron diffusion theory. Both methods are described extensively in the literature, and are only summarized here as follows:

1. Geometry

Figure 68 shows the geometrical configuration and material compositions selected for purposes of calculation.

2. Assumptions

- (a) The core effectively has the attenuation characteristics of pure graphite.
- (b) The core is spherical with a volume equal to that of the actual parallelepiped core.



NOTE: ENCIRCLED NUMERALS CORRESPOND TO LOCATIONS LISTED IN TABLE I.

FIG. 68
MODEL USED FOR SHIELD DESIGN
CALCULATIONS.

(c) Slab geometry is assumed for the reflector and shield to simplify calculations.

(d) Activation of Zircaloy and aluminum is negligible.

(e) Bulk shield is magnetite concrete ($\rho = 220 \text{ lb/ft}^3$).

3. Formulae

a. Fast Neutron Fluxes

The fast neutron fluxes at the edge of the core were calculated by the equation¹³

$$\phi_f = \frac{S_v}{2\mu_s} \left[1 - \frac{1}{2\mu_s R_0} + \left\{ \exp(-2\mu_s R_0) \right\} / 2\mu_s R_0 \right] \quad (1)$$

Outside the core,

$$\phi_f = \frac{2}{3} S_v R_0 \left[E_1(b_2) - E_1(b_2 \sec \theta) \right] \quad (2)$$

¹³T. Rockwell (ed.), Reactor Shielding Design Manual, TID-7004 (March 1956), p. 368

where

- S_V = volume source term in core, fast neutrons/(cm³)(sec)
 R_0 = equivalent core radius, cm
 $b_2 = \sum \mu_i t_i + \mu_s z$
 μ_i, μ_s = fast removal cross sections in the i'th region, and in the source, respectively, cm⁻¹
 t_i = thickness of i'th region, cm⁻¹
 z = effective self-attenuation distance,¹⁴ cm
 $\theta = \arctan [R_0 / \sum t_i + z]$
 E_1 = exponential integral¹⁵

b. Thermal Neutron Fluxes

The thermal neutron flux at the edge of the core was assumed to be 80% of the fast flux.

The thermal neutron flux outside the core was calculated by means of the equation¹⁶

$$\phi_{th} = A_i e^{\kappa_i x_i} + B_i e^{-\kappa_i x_i} + C_i e^{-\sigma_i x_i}, \quad (3)$$

where

- A_i, B_i = constants for the i'th region found by applying boundary conditions for the thermal flux at $x = 0$ and $x = \infty$
 κ_i = $1/\text{diffusion length}$ for i'th region, cm⁻¹
 x_i = thickness of i'th region, cm
 σ_i = logarithmic slope of fast flux in i'th region, cm⁻¹

$$= \ln \left[\frac{\phi_f(\text{inner boundary})}{\phi_f(\text{outer boundary})} \right] / x_i$$

 $C_i = [\phi_f(\text{inner boundary}) \sigma_i] / D_i (\kappa_i^2 - \sigma_i^2)$
 D_i = thermal neutron diffusion constant, cm

c. Gamma-ray Fluxes

The primary gammas from the reactor core were calculated by means of the equation¹⁷

¹⁴Ibid., p. 369.

¹⁵Ibid., p. 372.

¹⁶M. Grotenhuis, Lecture Notes on Reactor Shielding, ANL-6000 (March 1959), p. 100.

¹⁷Linear buildup; A. D. Rossin (ANL), personal communication.

$$\phi_{\gamma} = \frac{Q}{2} \frac{R_0}{R_0 + R} \exp(-\sigma_a a + \sigma_r t) \quad , \quad (4)$$

where

R_0 = core radius, cm

R = distance from core to point considered, cm

σ_a, σ_r = macroscopic gamma-absorption cross sections for shield and reflector, respectively, cm^{-1}

a = thickness of shield to point considered, cm

t = thickness of reflector, cm

$$Q = \frac{Q_{\gamma}}{\sigma_s} \left[2 - \frac{2}{\alpha} (1 - e^{-\alpha}) - \frac{1 - e^{-\alpha}(1 + \alpha)}{\alpha} \right]$$

Q_{γ} = volume source term for gammas in core; sum of decay product gammas by Way's formula and fission gammas, gammas/ $(\text{cm}^3)(\text{sec})$

σ_s = macroscopic gamma-absorption cross section for source, cm^{-1}

$$\alpha = 2\sigma_s R_0.$$

The secondary gammas from the reflector were calculated by means of the equation

$$\begin{aligned} \phi_{\gamma} = \frac{Q_{\gamma}}{2k} \left\{ e^{kt} E_1(\sigma_a a + \sigma_n t) \quad E_1(\sigma_a a) \right. \\ \left. + \frac{k}{k - \sigma_n} e^{-\sigma_a a} \left[e^{(k - \sigma_n)t} - 1 \right] \right. \\ \left. + e^{\nu \sigma_a a} \left[E_1(\sigma_a a [1 - \nu]) \right. \right. \\ \left. \left. - E_1([\sigma_n t + \sigma_a a][1 - \nu]) \right] \right\} \quad (5) \end{aligned}$$

for $\nu < 1$, where

E_1 = exponential integral

k = logarithmic slope of source term (thermal flux)

$$= \ln \left[\frac{\phi_{th}(\text{inner boundary of reflector})}{\phi_{th}(\text{outer boundary of reflector})} \right] / t$$

t = reflector thickness, cm

σ_a, σ_n = macroscopic gamma-ray cross section of shield and reflector, respectively, cm^{-1}

a = thickness of shield to point considered, cm

$$\nu = k/\sigma_n$$

Q_γ = volume source term for gammas in reflector
 = Q_{th} (outer boundary of reflector) Σ_a , where Σ_a is the macroscopic thermal neutron-absorption cross section of the reflector, cm^{-1} .

The secondary gammas from the shielding were calculated by means of the equation

$$\phi_\gamma = \frac{Q_\gamma}{2k} \left\{ e^{ka} E_1(\sigma_a a) - \ln(1 - \nu) - E_1[\sigma_a a(1 - \nu)] \right. \\ \left. + \frac{k}{k - \sigma_a} \left[e^{(k - \sigma_a)a} - 1 \right] \right\} \quad (6)$$

for $\nu < 1$, where

E_1 = exponential integral

k = logarithmic slope of thermal neutron flux in shield, cm^{-1}

$$= \ln \left[\frac{\phi_{th}(\text{inner boundary of shield})}{\phi_{th}(\text{outer boundary of shield})} \right] / t$$

t = shield thickness, cm

a = distance from inner boundary of shield to point considered, cm

σ_a = macroscopic gamma absorption cross section of the shield, cm^{-1}

$\nu = k/\sigma_a$

Q_γ = volume source term for thermal flux in the shield, gammas/
 (cm^3)(sec)

= ϕ_{th} (at point considered) Σ_a , where Σ_a is the macroscopic thermal neutron absorption cross section of the shield, cm^{-1} .

The gamma-ray source after shutdown was calculated by means of the equation¹⁸

$$Q_\gamma = \Sigma_a \phi_{th} (1 - e^{-\lambda T}) e^{-\lambda t} \quad (7)$$

where

Σ_a = thermal neutron-absorption cross section of source material

ϕ_{th} = thermal neutron flux at point considered

λ = radioactive decay constant of foil material, cm^{-1}

T = time of operation, sec

t = time after shutdown, sec.

¹⁸S. Glasstone and M. C. Edlund, The Elements of Nuclear Reactor Theory, D. Van Nostrand Co., Inc., New York (1957). p. 53.

Table IX

CONSTANTS USED IN SHIELDING CALCULATIONS

| <u>Material:</u> | <u>Graphite</u> | <u>Magnetite</u> | <u>Iron</u> | <u>Manganese</u> | <u>Silicon</u> | <u>Boron</u> |
|---|-----------------|------------------|-----------------------|-----------------------|-----------------------|--------------|
| Fast Neutron-removal Cross Section, cm^{-1} | 0.674 | 0.125 | 0.169 | 0.162 | - | - |
| Thermal Neutron-absorption Cross Section, cm^{-1} | 0.000362 | - | 0.065 | 1.0 | 0.0386 | 110.0 |
| Thermal Neutron-absorption Cross Section, barns | 0.0045 | - | 0.80 | 12.6 | 0.80 | 772 |
| Thermal Neutron Diffusion Constant D, cm | 0.922 | 0.418 | 0.362 | - | - | - |
| Reciprocal Diffusion Length, cm^{-1} | 0.0192 | 0.377 | 0.725 | - | - | - |
| 1-Mev Gamma-absorption Coeffi- cient, cm^{-1} | 0.096 | 0.217 | 0.468 | - | - | - |
| 2-Mev Gamma-absorption Coeffi- cient, cm^{-1} | 0.064 | 0.145 | 0.312 | - | - | - |
| 4-Mev Gamma-absorption Coeffi- cient, cm^{-1} | - | 0.127 | 0.250 | - | - | - |
| Decay Constant, sec^{-1} | - | - | 1.79×10^{-7} | 7.44×10^{-5} | 10.4×10^{-5} | - |

As a further check, the gamma-ray fluxes in the top and bottom shields were calculated by assuming a constant thermal flux value across a section of the shield. The equations for a slab with constant volume source were then applied. The shielding constants used are summarized in Table IX.

3. Results

Table X lists the calculated fast, thermal, and gamma-ray fluxes at various locations (see Fig. 68) for operation at 100 kw.

Table X

CALCULATED NEUTRON AND GAMMA-RAY FLUXES

| <u>Location</u> | <u>Neutron Flux,</u> <u>n/(cm²)(sec)</u> | | <u>Gamma-ray Flux,</u> <u>photons/(cm²)(sec)</u> |
|-----------------|--|----------------------|--|
| | <u>Fast</u> | <u>Thermal</u> | |
| 1 | 1.8×10^{10} | 1.5×10^{10} | - |
| 2 | 3.7×10^7 | 2.6×10^{10} | - |
| 3 | <1 | <1 | <1 |
| 4 | 3.7×10^7 | 9.3×10^9 | - |
| 5 | 3.7×10^7 | 2.6×10^5 | - |
| 6 | 9.7×10^4 | 2.2 | $1.8 \times 10^{3*}$ |
| 7 | <1 | 1.2 | 13 |
| 8 | 3.7×10^7 | 9.3×10^9 | - |
| 9 | 7.4×10^3 | - | - |

*Two hours after shutdown from 100-hr operation at 100 kw.

The required thickness of the thermal column shield door was found to be 30 in. of magnetite concrete with a sheet of boral ($\frac{1}{4}$ in. thick) on the inside face.

There will be no significant argon-41 activity at the reactor exhaust stack either immediately after a transient or during steady-state operation at 100 kw with minimum coolant flow.

Scattering and leakage of neutrons through the coolant inlet ducts and the horizontal access slots do not make for reliable calculations. This was recognized during the design stage, and consequently additional local shielding was provided in these areas. Removable shielding (magnetite concrete, 20 in. thick) was installed behind the optical camera equipment. Pipe cartridges (1 ft long) filled with fine lead shot were inserted in the thermal

column thimbles. The inlet coolant ducts were fitted with lead louvers (2 in. thick) and a sheet of boral ($\frac{1}{4}$ in. thick) on the high radiation side. The removable instrument line adapter for the south central top shield block was also filled with fine lead shot.

Table XI lists the neutron and gamma-ray levels during 100-kw operation after installation of this additional shielding. The high thermal flux levels at the side edges of the thermal column door are attributed to inconsistencies in the walls of the thermal column extending toward the reactor core. Additional temporary shielding will be installed in this area.

Table XI

RADIATION LEVELS AROUND REACTOR SHIELD AFTER
INSTALLATION OF ADDITIONAL SHIELDING

| Location | Fast Neutrons, n rep | Thermal Neutrons, n/(cm ²)(sec) | Gammas, mr/hr |
|--|----------------------------|---|------------------|
| General background at 10 ft from reactor on main floor | negligible | 50-1,500 | 5-8 |
| Camera access holes | | | |
| North (Gamma Camera Installed) | 115 | 4,000 | 50 |
| South } Camera assembly and removable } | negligible | 200 | 7 |
| West } backup shield blocks in place } | | | |
| Thermal column shield door (East face) | | | |
| Around edges, with additional 2 in. of lead on south edge: | negligible | 400 | 150 |
| With 2 in. of lead and strip of boral sheet on north edge: | negligible | 2,000 | 50 |
| Top of shield | | | |
| Intake filter ducts | negligible | 700 | 11-18 |
| Maximum level through concrete shield ($1\frac{1}{2}$ ft concrete)* | negligible | 500 | 220 |
| Average level through concrete | negligible | 100-300 | 8-14 |
| Subreactor room entrance | <5 | 4,000 | 150 |
| Exhaust filters with coolant flow | - | - | <1 |

*Half-thickness of center top shield block is to provide space for installation of test loop return line above rotating shield plug.

APPENDIX E

COOLANT SYSTEM PRESSURE DROP AND FLOW DISTRIBUTION

Reactor power at steady state is measured by a heat balance on the coolant. The coolant temperature change Δt is monitored by resistance thermometers in the inlet and the outlet air ducts and recorded at the control console. The coolant flow rate is measured by pitot tubes in the exhaust ducts, and indicated at the control panel (Brown Square Root Low Pressure Electric Flow Meter) as a percentage of full flow (85% flow meter reading at 80°F and 25 in. Hg pressure = 6,000 cfm). Using the control panel Δt and flow meter readings, reactor power is given by

$$\text{Power (kw)} = 0.1184 (\Delta t)R \sqrt{\frac{P}{273 + t}}$$

where

R = flow meter reading, %
 P = barometer reading, in. Hg
 t = temperature, °C.

Owing to the very great thermal inertia of the reactor, runs of several hours or longer are required to achieve a true steady-state temperature equilibrium between fuel assemblies and coolant.

The measured pressure drop and flow distribution data are summarized in Table XII and XIII, respectively.

Table XII

PRESSURE DROPS IN TREAT COOLING SYSTEM

(Air Flow = 6,000 cfm at 85°F and 25 in. Hg)

| Location | ΔP , in. H ₂ O |
|--|--------------------------------------|
| Across reactor (includes intake air filters and ~10 ft of exhaust duct) | 6.8 |
| Reactor to control valve | 0.5 |
| Across control valve | 28.4 |
| Across exhaust filters (clean) | 1.2 |
| Exhaust stack | 0.5 |

Table XIII

COOLANT FLOW DISTRIBUTION

| <u>Conditions</u> | <u>Flow rate, cfm at 80°F and 25 in. Hg</u> | | | |
|---------------------------------|---|-------------|------------------|-----------------|
| | <u>Total*</u> | <u>Core</u> | <u>Reflector</u> | <u>Bypass**</u> |
| Both turbocompressors operating | | | | |
| Bypass valve closed | 4670 | 4210 | 450 | 0 |
| Bypass valve opened | 4670 | 2920 | 260 | 1490 |
| One turbocompressor operating | | | | |
| Bypass valve closed | 2270 | 2270 | negligible | 0 |
| Bypass valve opened | 2270 | 1485 | negligible | 785 |

*Total flow rates are not maximum; flow controller was set below maximum during these measurements.

**Reactor intake dampers and bypass fully open.

APPENDIX F

INITIAL FUEL LOADING AND STARTUPA. Control Rod Drive Tests

The eight control rod fuel assemblies (less control rods) were inserted into the inner ring of control rod thimbles and locked in place. Two rings of dummy fuel assemblies, and a 44-in. square jig were clamped in position with the core clamping bars. The jig was used to hold and align each of the control rod fuel assemblies. The eight control rods were inserted in each control rod assembly and attached to their respective drives. With the control rod assemblies thus held in alignment, the check out tests on the rod drives were carried out.

B. Instruments

The instruments used for the initial loading to critical comprised four BF_3 proportional counters operating dual scalers and log count rate and period meters. Three counters were located next to the permanent reflector in the reactor shield at the northeast and southwest corners, and at the south face of the reactor. The fourth counter was installed in the permanent reflector next to the reflector fuel elements at the west face.

C. Neutron Source

For the initial loading the source fuel element was placed at the center of the core. A plutonium-beryllium source (10^6 n/sec) was used for startup. After initial criticality, a stronger (1.5×10^7 n/sec) polonium-beryllium source was substituted and the source element was moved from the core center to position S-3.

D. Initial Fuel-loading Procedure

The jig used for control rod alignment was removed and dummy fuel assemblies were installed in all but 25 core positions at the core center. This central region was loaded with the source element at the center and with standard fuel assemblies surrounding it. This starting configuration is shown in Fig. 69. Thereafter the dummy assemblies were replaced with fuel, working out from the nucleus of 25 as symmetrically as possible. Count rates with the control rods in and with rods out were taken after incremental fuel additions. Criticality was attained with 146 assemblies in the configuration shown in Fig. 70. Subsequent measurements with the source element moved from the reactor center established the minimum critical loading as 141 assemblies.

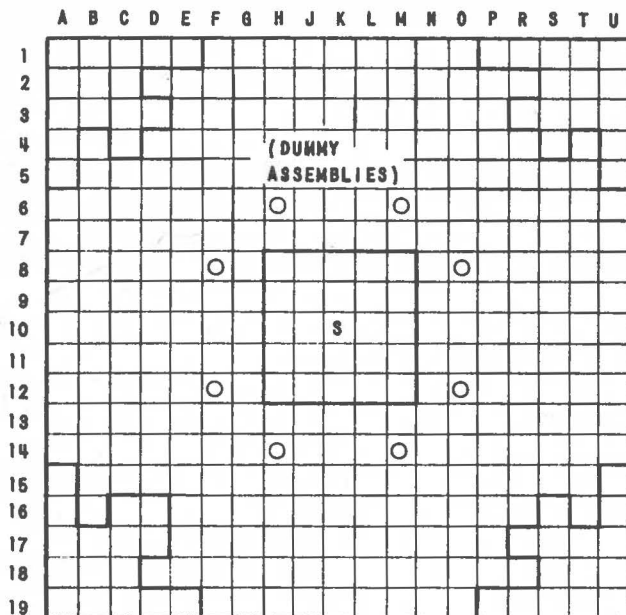


FIG. 69
 START OF LOADING TO FIRST
 CRITICAL (24 STANDARD FUEL
 ASSEMBLIES).

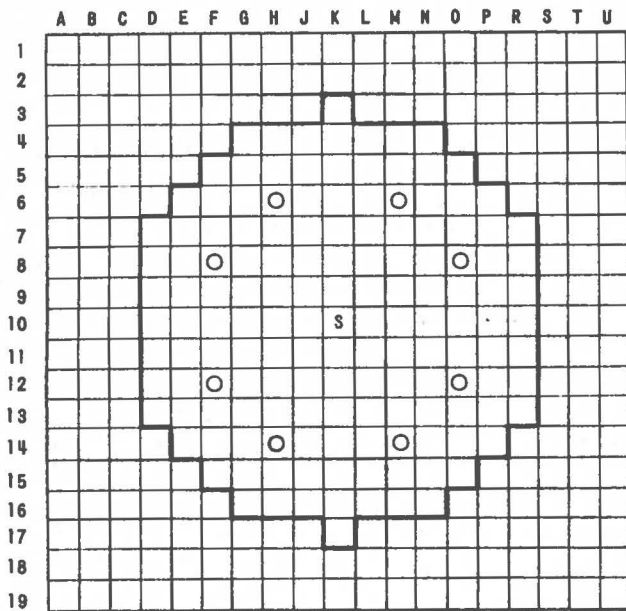


FIG. 70
 FIRST CRITICAL LOADING OF 138
 STANDARD FUEL ASSEMBLIES AND
 8 CONTROL ROD FUEL ASSEMBLIES.